IDENTIFICATION OF NOVEL REGULATORY GENES IN ACETAMINOPHEN INDUCED HEPATOCYTE TOXICITY BY A GENOME-WIDE CRISPR/CAS9 SCREEN

A THESIS IN

Cell Biology and Biophysics

and Bioinformatics

Presented to the Faculty of the University
of Missouri-Kansas City in partial fulfillment of
the requirements for the degree

DOCTOR OF PHILOSOPHY

By

KATHERINE ANNE SHORTT

B.S, Indiana University, Bloomington, 2011

M.S, University of Missouri, Kansas City, 2014

Kansas City, Missouri

2018

IDENTIFICATION OF NOVEL REGULATORY GENES IN ACETAMINOPHEN INDUCED HEPATOCYTE TOXICITY BY A GENOME-WIDE CRISPR/CAS9 SCREEN

Katherine Anne Shortt, Candidate for the Doctor of Philosophy degree,

University of Missouri-Kansas City, 2018

ABSTRACT

Acetaminophen (APAP) is a commonly used analgesic responsible for over 56,000 overdose-related emergency room visits annually. A long asymptomatic period and limited treatment options result in a high rate of liver failure, generally resulting in either organ transplant or mortality. The underlying molecular mechanisms of injury are not well understood and effective therapy is limited. Identification of previously unknown genetic risk factors would provide new mechanistic insights and new therapeutic targets for APAP induced hepatocyte toxicity or liver injury.

This study used a genome-wide CRISPR/Cas9 screen to evaluate genes that are protective against or cause susceptibility to APAP-induced liver injury. HuH7 human hepatocellular carcinoma cells containing CRISPR/Cas9 gene knockouts were treated with 15mM APAP for 30 minutes to 4 days. A gene expression profile was developed based on the 1) top screening hits, 2) overlap with gene expression data of APAP overdosed human patients, and 3) biological interpretation including assessment of known and suspected

APAP-associated genes and their therapeutic potential, predicted affected biological pathways, and functionally validated candidate genes.

This screen is the first genome-wide CRISPR/Cas9 knockout screen of APAP-induced hepatocyte toxicity. The top hits from this screen included numerous genes previously not linked to liver injury. We further demonstrated the implementation of intermediate time points for the identification of early and late response genes. A negative selection screen identified genes involved in fundamental processes, including NAAA, ATG2B, and MYOZ3. A positive selection screen identified numerous genes potentially involved in pathogenic processes, including LZTR1, PGM5, and EEF1D. A top essential pathway at 24 hours of APAP treatment was *Regulation of Skeletal Muscle Contraction*. We additionally identified 6 genes, 3 novel and 3 known, that have drug-gene interactions favorable for re-purposing existing therapies to treat APAP-induced hepatotoxicity. Collectively, this line of research has illustrated the power of a genome-wide CRISPR/Cas9 screen to systematically identify novel genes involved in APAP induced hepatocyte toxicity and to provide potential new targets to develop novel therapeutic modalities.

APPROVAL PAGE

The faculty listed below, appointed by the Dean of the School of Graduate Studies, have examined a thesis titled "Identification of Novel Regulatory Genes in Acetaminophen Induced Hepatocyte Toxicity by a Genome-Wide CRISPR/Cas9 Screen", presented by Katherine Anne Shortt, candidate for the Doctor of Philosophy degree, and certify that in their opinion it is worthy of acceptance.

Supervisory Committee

Shui Qing Ye, M.D, Ph.D., Chair
Division of Cell Biology and Biophysics, School of Biological Sciences
Department of Biomedical and Health Informatics, School of Medicine

Mary Gerkovich, Ph.D.
Department of Biomedical and Health Informatics, School of Medicine

Daniel P. Heruth, Ph.D.
Department of Pediatrics, School of Medicine

Saul Honigberg, Ph.D.
Division of Cell Biology and Biophysics, School of Biological Sciences

Gerald J. Wyckoff, Ph.D.
Division of Molecular Biology and Biochemistry, School of Biological Sciences

CONTENTS

ABSTRACT iii

LIST OF ILLUSTRATIONS x

LIST OF TABLES xi

GLOSSARY xii

ACKNOWLEDGMENTS xiv

Chapter

1. INTRODUCTION 1

2. REVIEW OF THE LITERATURE 4

Candidate gene approaches for biomarker discovery in APAP-induced hepatotoxicity 4

"Omics" approaches for biomarker discovery in APAP-induced hepatotoxicity 7

Gene editing approaches for biomarker discovery in other diseases 10

Novel approach to APAP-induced hepatotoxicity biomarker discovery 11

3. RESEARCH QUESTION 13

4. METHODS 15

Research design 15

sgRNA library amplification 15

Cell culture 16

Lentivirus production and concentration 17

Acetaminophen kill curve 18

In vitro hepatocellular carcinoma transduction using the GeCKOv2 sgRNA library....18
CRISPR/Cas9 acetaminophen screen and sample collection....19
CRISPR/Cas9 screen amplicon sequencing....19
CRISPR/Cas9 Screen deconvolution and analysis....20
Pathway analysis....21
Statistical analysis of gene expression datasets from the Gene Expression Analysis of overlapping data from Gene Expression Omnibus....21
Human APAP induced liver injury data....21
Mouse APAP induced liver injury data....23
Analysis of acetaminophen-associates SNPs in the literature....24
Drug-gene interaction analysis....25
Functional validations in primary mouse hepatocytes....25
Semi-quantitative PCR....27
Western Blotting....27
Plasmids....28
5. RESULTS AND DISCUSSION PART 1: CRISPR/CAS9 SCREEN....29
Development of screening strategy and preparation of cell lines....29
CRISPR/Cas9 knock-out screen and deconvolution....29
Discussion....39
6. RESULTS AND DISCUSSION PART 2: OUR SCREEN IN THE CONTEXT OF OTHER ACETAMINOPHEN DATA SETS....42

Overlapping analysis of our screen top hits with other gene expression acetaminophen datasets....42
Analysis of RNA-sequence from mice with acetaminophen-induced acute liver injury....42
Analysis of microarray of human liver biopsies from normal and acetaminophen-induced acute liver failure patients....43
Analysis of microarray of human blood from normal and acetaminophen-dosed participants....45
Identification of candidate genes from overlapping gene sets....48
Discussion....49
7. RESULTS AND DISCUSSION PART 3: ACETAMINOPHEN-ASSOCIATED SINGLE NUCLEOTIDE POLYMORPHISMS IN THE LITERATURE....52
Acetaminophen-associated single nucleotide polymorphisms in the literature....52
Functional in silico analyses of SNPs associated with acetaminophen-induced hepatotoxicity....54
Discussion....58
8. RESULTS AND DISCUSSION PART 4: VALIDATIONS OF TOP CANDIDATE GENES....61
Validation of screening strategy....61
Drug-gene interactions of candidate genes....62
Functional validations of candidate genes....64
Discussion....67
9. CONCLUSIONS AND FUTURE DIRECTIONS....71

Conclusions....71

Future directions....72

Appendix

A. SUPPLEMENTARY FIGURES....74

B. SUPPLEMENTARY TABLES....79

REFERENCE LIST....154

VITA....166

ILLUSTRATIONS

Figure Page

1. Genome-scale positive and negative screening using CRISPR/Cas9 31
2. Positive and negative screening reveal top gene and pathway candidates after 4 days of APAP treatment.....32
3. Highly ranked genes and pathways after 24 hours of APAP treatment.....34
4. Identification of gene hits across the APAP time course in the CRISPR/Cas9 screen 37
5. Overlapping analysis of significant CRISPR/Cas9 screen hits with mouse ALI (GSE110787) and human ALF gene expression data (GSE74000) 44
6. Overlapping analysis of significant CRISPR/Cas9 screen hits with human ALI gene expression data (GSE70784) 47
7. Validation experiments in primary mouse hepatocytes 66

TABLES

Table Page

1. The top 100 genes for various APAP treatment times were queried in pubmatrix to determine novelty 35
2. Top canonical pathways predicted by Ingenuity Pathway Analysis.....56
3. Top diseases and disorders predicted by Ingenuity Pathway Analysis.....57
4. Top candidate genes with known drug effects annotated by the DRUG Gene Interaction Database.....63

GLOSSARY

ALI: Acute Liver Injury.

ALF: Acute Liver Failure.

Allele: One of a number of alternate nucleotides of a specific locus on a strand of DNA.

Amino acid: Organic acids that form the building blocks of proteins. Each of the 20 amino acids are coded by a 3 nucleotide DNA sequence.

Cas9: DNA endonuclease guided by RNA. It is involved in CRISPR adaptive immunity in prokaryotes.

CRISPR: Clustered Regularly Interspaced Palindromic Repeats

Deoxyribonucleic Acid (DNA): Nucleic acids that encode genetic instructions of all living organisms.

DILI: Drug-Induced Liver Injury.

Exon: DNA sequence that remains in the mature RNA of a gene after introns are removed.

Genome: The total genetic material of an organism.

Genome-wide association study (GWAS): An approach that involves comprehensively scanning markers across the complete sets of DNA, or genomes, of many people to find genetic variations associated with a particular disease.

Genotype: The set of alleles that an organism possesses for a given genetic locus. Normally a genotype contains 2 alleles due to the presence of 2 chromosomes.

Hepatocellular carcinoma: A primary malignancy of the liver and the most common type of liver cancer in adults, and occurs commonly in people with liver disease

Hepatocyte: The primary cell type in the liver.

Hepatotoxicity: Chemically-induced liver injury.

Intron: DNA sequence in a gene but is not transcribed into the mature RNA.

Linkage disequilibrium: When alleles for two genetic loci are not distributed randomly the loci are in linkage disequilibrium.

Major allele: For a genomic position the allele that occurs most frequently in a population is the major allele.

Mendelian disease: Diseases that have simple genetic inheritance patterns and are caused by a small number of genes.

Minor allele: For a genomic position an allele that occurs in a population less frequently than a different allele at the same position is called a minor allele.

Next generation sequencing (NGS): Current high throughput genetic sequencing technology that produces the order of nucleotides within a DNA molecule.

Nonsynonymous mutation: A genetic variant that causes a change in amino acid coding.

Single nucleotide polymorphism (SNP): Genetic variant that occurs at one nucleotide (base pair). Different alleles are observed at one position across a population.

Synonymous mutation: A genetic variant in a protein coding region that causes no change in amino acid coding.

ACKNOWLEDGMENTS

I would like to express my gratitude to my PhD committee for their guidance; the Ye lab for their support and excellent technical assistance; the students, staff and faculty of School of Biological Sciences and Department of Biomedical and Health Informatics in the School of Medicine, UMKC, for their tutelage, time, and advice in the completion of this project. Thanks to my friends and family for constantly encouraging and supporting me. I couldn't have gotten here without all of you!

This thesis was adapted with permission from the manuscripts Shortt *et. al.* (2018, under review) and Heruth *et. al.* (2018, under review).

FUNDING

Funding was provided in part by the start-up fund, William R Brown/Missouri State Endowment, The Children's Mercy Hospital, UMKC (Ye, SQ), a School of Graduate Studies Research Grant of UMKC School of Graduate Studies (Shortt, K), five UMKC GAF Awards of UMKC Women's Council (Shortt, K), and a Sarah Morrison Student Research Award of UMKC School of Medicine (Singh, S).

CHAPTER 1

INTRODUCTION

Acetaminophen (APAP) is a widely used medication and is responsible for ~50% of acute liver failure (ALF) cases in the United States (US) and Great Britain[1-2]. APAP is the top risk factor for acute liver injury (ALI) and ALF in the US and Great Britain and in the top 3 in China[3]. The recommended maximum daily dose of APAP is 4g for adults, with a single dose of just 7.5-10g causing acute toxicity[4]. Ultimately, 36% of cases of APAP induced ALF survive if no liver transplant occurs, and patients who receive a liver transplant have a 75% survival rate.

At a therapeutic dosage about 90% of APAP is metabolized to glucoronate and sulfate conjugates by uridine 5'-diphoso-glucuronosyltransferases and sulfotransferases. Five to ten percent of APAP is processed in the liver by cytochrome-P450 enzymes (CYPs) to produce a highly toxic metabolite N-acetyl-p-benzo-quinone imine (NAPQI)[5-7]. Glutathione is conjugated with NAPQI by Glutathione-s-transferases (GST) to convert NAPQI to a non-toxic substrate. This mechanism, however, fails in cases of acute and chronic APAP overdose resulting in oxidant stress-induced liver injury[8]. When the enzymes responsible for glucuronidaiton (UDP-glucuronosyltransferases, e.g. UGT1A1, UGT1A6, UGT1A9, UGT287, UGT2815) and sulfation (sulfotransferases, e.g. SULT1A1, SULT1A3, SULT1A4, SULT1E1, SULT2A1) are saturated, APAP is metabolized by oxidation via the microsomal cytochrome P450 pathway into *N*-acetyl-*p*-benzoquinone imine (NAPQI) [9-10].

The cytochrome P450 (CYP) enzymes, including CYP1A2, CYP2A6, CYP2D6, CYP2E1, and CYP3A4, convert acetaminophen into the highly reactive NAPQI metabolite [11-15]. At toxic acetaminophen levels, CYP3A4 presented with the highest relative capacity for acetaminophen bioactivation to NAPQI by oxidation, followed by CYP2E1, CYP2D6, and CYP1A2 [16]. At therapeutic acetaminophen levels, CYP3A4 again had the highest rate of conversion to NAPQI while the other CYP enzymes possessed significantly lower capacity for bioactivation [16].

NAPQI, a strong oxidizer that is toxic to liver tissue, is reduced (inactivated) by conjugation with glutathione by glutathione S-transferases (GST), a family of enzymes (e.g. GSTT1, GSTP1) that detoxifies many hepatic drugs [17]. The toxicity of NAPQI is associated with its ability to bind to cysteine residues in proteins to form NAPQI-protein adducts [18]. At therapeutic doses, the small amount of NAPQI-protein adducts produced are removed effectively by autophagy [19-20]. High levels of NAPQI deplete glutathione and accumulate in hepatocytes where excess NAPQI binds to cysteine residues on cellular and mitochondrial proteins, causing an immune response and necrosis, leading to ALI and ALF[18, 21-22].

The current model of acetaminophen-induced hepatic necrosis links the NAPQI-protein adducts with amplified cascades of reactive oxygen and nitrogen species (ROS/RNS) resulting in the swift loss of hepatic cells and liver function [23-24]. This model has been studied extensively [25-29], and the ROS/RNS induce increased mitochondrial permeability resulting in impaired mitochondrial function and necrotic cell death [30-31]. Subsequently, necrotic hepatocytes release damage associated molecular patterns

(DAMPs) resulting in an immune response mediated by various cytokines and innate immune cells [32-34].

The etiology of APAP-induced ALF is complex and is not fully understood, particularly for cases that present more than 8 hours post-ingestion[5]. These cases are extremely troublesome from a clinical perspective, because the liver injury can be asymptomatic for 24-48 hours[4]. When the canonical APAP clearance pathways including metabolism via CYPs are overwhelmed or low-functioning, redundant or accessory pathways may help to preserve function[35]. Current treatments of APAP-induced ALF focus on clearing excess APAP and replenishing glutathione and are only effective during a very short window of time post-overdose. Furthermore, there is evidence that APAP overdose may cause cell death by multiple mechanisms[36]. There is a demonstrated need for improved modalities of risk assessment, diagnosis, and therapeutics.

CHAPTER 2

REVIEW OF THE LITERATURE

Candidate gene approaches for biomarker discovery in APAP-induced hepatotoxicity

Although acetaminophen is a dose-dependent hepatotoxin, elevated alanine aminotransferase (ALT) serum levels were measured in some healthy adults following a 7 to 14 day administration of the maximum daily dose of 4 g per day [37-38]. Additional case studies, although rare, have reported the development of ALI even at therapeutic doses [39-40]. These findings confirm that some healthy individuals experience mild to severe liver injury in response to therapeutic doses of acetaminophen suggesting that genetic components are involved in acetaminophen metabolism. Thus, several groups have proposed that NAPQI toxicity can be enhanced by alterations in the metabolism of acetaminophen due to genetic polymorphisms in the corresponding enzymes [29, 41-42].

Since hepatic injury can occur at sub-therapeutic doses in some individuals genetic disposition may play a significant role in an individual susceptibility to APAP induced hepatotoxicity[29, 41-43]. Genetic variations, including single nucleotide polymorphisms (SNPs), can predict population and inter-individual differences in APAP degradation and hepatotoxicity [44-45]. Currently several genome wide association studies (GWAS) in humans have identified pharmacogenetic SNPs associated with drug induced liver injury, including APAP-induced injury [46-47]. Polymorphisms have been identified that alter the activity of the SULT, UGT, and CYP enzymes, all of that play important roles in APAP metabolism

[29, 41, 46], however very few SNPs have been experimentally confirmed to be associated directly with acetaminophen-induced hepatotoxicity [48-50].

Of the APAP-associated polymorphisms that have been identified, a number have resulted from candidate gene-based approaches. Homozygous carriers of the rs2031920 variant T allele presented with a two-fold increase in the elimination rate of acetaminophen compared to CC and CT individuals in a study by Ueshima *et. al.*[48], that correlated with increased promoter activity due to the homozygous minor genotype [51] and higher hepatic levels of CYP2E1 [52]. CYP2E1 is an isoform of Cytochrome P450, which is responsible for metabolizing APAP to NAPQI.

Court *et al*. identified three 3' UTR SNPs (rs8330, rs10929303, rs1042640) in the *UGT1A* gene that is associated with increased glucuronidation activity (more specifically it is a UDP glucouronosyl transferase) following acetaminophen exposure [49]. The UGT1A rs8330 MAF (G) was significantly lower in the unintentional acetaminophen hepatotoxicity group (16%) compared with the other ALF subgroups (22%), with an OR = 0.53 (0.30-0.94; P = 0.027) [50]. This finding was consistent with a protective effect of the variant rs8330 G allele through enhancement of acetaminophen glucuronidation and detoxification, as demonstrated by a series of *in vitro* mechanistic studies by Court *et al.* [49]. rs8330 increased glucuronidation activity due to altered splicing of the primary UGT1A transcript resulting in the preferential retention of exon 5A versus exon 5B. Translation of UGT1A mRNA containing exon 5B produces a truncated UGT1A protein, termed isoform 2 variant, which lacks enzymatic activity and further represses enzymatic activity through hetero-dimerization with the wild type isoform [49]. Like rs776746, the rs8330 MAF varies among ethnic populations.

The *CYP3A5* splice donor variant (rs776746) associated with acetaminophen-induced hepatotoxicity. The minor A allele (also known as *CYP3A5*1*) encodes a functional Cytochrome P450 Family 3 Subfamily A Member 5 protein, while a non-functional protein is produced from *CYP3A5* genes containing the major G allele (rs776746; *CYP3A5*3*) [53]. The *CYP3A5*1* A allele was observed more frequently in intentional acetaminophen-overdose cases compared to all other acute liver failure patients [50]. The heterozygous GA genotype was an "at risk" genotype with an OR = 2.3 (1.1-4.9; P = 0.034) [50]. The homozygous AA genotype was not observed in this cohort. Subsequently, the *CYP3A5* diplotypes have been correlated with phenotypes for the metabolism of drugs, like tacrolimus: **1/*1*, extensive metabolizer; **1/*3*, intermediate metabolizer; **3/*3*, poor metabolizer [54-55]. However, the rs776746 MAF does not correlate with the incidence of acetaminophen-induced hepatotoxicity across different non-Caucasian ethnic groups [45, 56-58].

The *CD44* rs1467558 TT minor allele genotype was over represented in the unintentional hepatotoxicity group with an OR = 4.0 (1.0-17.2; P = 0.045) [50], suggesting that rs1467558 TT is an "at risk" genotype. This observation was supported by previous studies that revealed that rs1467558 associated with elevated serum alanine aminotransferase (ALT) levels [37-38]. *In silico* mechanistic structural analysis predicted that rs1467558 can alter many of the complex, alternative *CD44* transcripts, including a potentially damaging amino acid change from threonine to isoleucine [38]. Interestingly, *CD44* is not an acetaminophen metabolizing enzyme, but rather a cell surface receptor involved in cell-cell interactions, cell adhesion, and cell migration in inflamed tissue [59]. The rs1467558 MAF of 21% in the Caucasian unintentional hepatotoxicity cohort is higher

than in each of the ethnic populations determined by the 1000 Genomes Project: African (1%), American (11%), Asian (0%), European (19%), and Southern Asian (3%) [60].

The rs1902023 missense polymorphism in *UGT2B15* (termed *UGT2B15*2*) was associated with lower acetaminophen glucuronide-to-acetaminophen concentration ratios in urine [61] and blood [62]. Court *et al.* demonstrated that *UGT2B15*2* associated with increased plasma concentrations of NAPQI-protein adducts and that the plasma concentrations of the protein adducts negatively correlated with acetaminophen glucuronidation [63]. Thus carriers of rs1902023 are slower metabolizers of acetaminophen glucuronidation resulting in increased availability of acetaminophen for oxidative metabolism to NAPQI and subsequent liver damage.

"omics" approaches for biomarker discovery in APAP-induced hepatotoxicity

Genomic approaches to biomarker discovery have had a small amount of success in identifying candidate polymorphisms and genes. To test the hypothesis that genetic polymorphisms downstream of NAPQI formation contribute to hepatotoxicity, Moyer *et. al.*.tested 176 lymphoblastoid cell lines (HVP-LC) established from healthy donors for association of genetic polymorphisms downstream of NAPQI formation with hepatotoxicity [43]. Initially, Moyer et al. examined the association of 716 SNPs, located in 31 GSH pathway genes, with NAPQI-IC_{50}. Only 45 SNPs had significant P values (<0.05), 24 of which were located in the multidrug resistance ATP-binding cassette, sub-family C (CFTR/MRP), member 3 (*ABCC3*) and member 4 (*ABCC4*) genes. Expression of *Abcc3* and *Abcc4* in mice upon acetaminophen-induced hepatotoxicity have been shown to be

dependent upon the transcription factor, Nrf2 [64]. Nrf2 has been shown to play a protective role in acetaminophen-induced hepatotoxicity as *Nrf2*$^{-/-}$ knockout mice were more susceptible to acetaminophen-induced liver damage compared to their wild type *Nrf2*+/+ controls [65]. The remaining significant SNPs were located in glutamate cysteine ligase (*GCLC*), glutathione peroxidase (*GPX2*, *GPX3*, *GPX4* and *GPX7*), glutathione synthetase (*GSS*), and glutathione transferase (*GSTA2*, *GSTA3* and *GSTP1*).

When Moyer *et. al.* applied a genome-wide approach ninety-six SNPs ($P < 1\times10^{-4}$) associated with NAPQI-IC_{50}. Interestingly, 15 of the top 20 significant SNPs mapped to intergenic regions. Ten of these 15 intergenic SNPs clustered in a region of chromosome 3, between the *C3orf38* and *EPHA3* genes. Functional analysis of rs2880961, that lies 317 kb downstream of *C3orf38*, demonstrated binding of transcription factors (TF), including NF-κB, HSF1, and HSF2, although significant differences in NF-κB, HSF1, and HSF2TF binding were not detected by chromatin immunoprecipitation (ChIP) assays between wild-type and variant SNPs [43]. However, this does not preclude differential binding of other TFs. The top 10 intragenic SNPs are canonical splicing variants located in the introns of genes involved in gene regulation (*LMX1A*), signal transduction (*ETKN2*, *KCNJ3*, *MCPT1*), immune response (*IL23R*, *UBASH3A*), extra-cellular matrix (*SPAG16*, *LAMA4*), and the detoxification of aldehydes generated by lipid peroxidation (*ALDH1A3*). To identify potential *cis* effects of SNPs on gene expression, Moyer et al. measured mRNA expression to identify 17 genes associated significantly with NAPQI IC_{50} with $P < 0.0001$, however none of these 17 genes overlapped with genes containing SNPs, suggesting that the SNPs may have a *trans* effect on the expression of these genes [43].

Two studies by Harrill et al. [38, 66] identified potential susceptibility targets using a panel of 36 inbred mouse strains to model genetic diversity. Haplotype-associated mapping and targeted sequencing revealed that polymorphisms in *Ly86*, *Cd44*, *Cd59a*, and *Capn8* correlated with increased ALT levels. To determine if the orthologous human genes were also associated with acetaminophen-induced liver injury, genomic DNA from two independent cohorts, UNC [38] and Purdue Pharma [37], were sequenced. Although Harrill *et al.* did not detect SNP associations within *LY86* and *CD59*, rs3749166 in *CAPN10* (the human orthologue of mouse *Capn8*) (P = 0.045) and rs1467558 in *CD44* (P = 0.002) were associated with elevated ALT levels in both cohorts [38]. To validate these findings further, liver damage was measured in C57BL/6J Cd44 knock-out mice administered acetaminophen. Cd44 knock-out mice presented with greater liver injury (61%±7% mean liver necrosis ± SE) compared to wild-type controls (40%±4%) following a 24 hour dose of acetaminophen (300 mg/kg). These results indicate a role for CD44 in modulation of susceptibility to acetaminophen hepatotoxicity, as supported by Court *et al*. [50]. Further gene expression profiling identified 26 genes that associated significantly with liver damage. Similar with the Moyer *et al*. study, these genes did not overlap with the hepatotoxicity SNPs identified in their mouse panel. This observation supports the hypothesis that in addition to affecting protein-coding regions, SNPs may disrupt non-coding regulatory regions. An alternative explanation is that the 26 genes function either upstream or downstream of the SNP modified genes.

Transcriptomic studies measure the changes in gene expression post-drug treatment using RNA sequencing or gene expression profiling, however the genes identified may not be causal. Although a major limitation of these studies is the absence of control populations

that ingested a similar dose of acetaminophen but did not develop ALF, the results are compelling. The association of these polymorphisms with acetaminophen-induced hepatotoxicity, along with their population variations, should be investigated further. To overcome the challenges of the candidate gene approach in human populations with ALF resulting from acetaminophen toxicity, additional studies have employed alternative approaches, such as GWAS, to identify SNPs that may serve as biomarkers for acetaminophen susceptibility. Further analysis of the candidate polymorphisms and genes identified by these methods will better elucidate their role as well as their diagnostic and therapeutic utility.

Gene-editing approaches for biomarker discovery in other diseases

Effective, reproducible screening methods for identification of disease-associated genes have long been sought. Microarray and omics approaches have widely been used to identify genes acting in APAP-induced injury[43, 67-71]. These studies measure the changes in gene expression post-drug treatment using RNA sequencing or gene expression profiling, however the genes identified may not be causal. Previous screens of various diseases were accomplished using gene knockdown by RNA interference (RNAi), resulting in incomplete gene knockout and limiting the applications of the method[72-74]. Gene-trap mutagenesis made genome-wide insertional mutagenesis studies possible, however it is only possible in haploid cell types, making it infeasible to study drug effects in diverse organ systems or *in vivo*[75]. Zinc finger nucleases (ZFNs) and transcription activator-like

effector nucleases (TALENs) produce double-stranded breaks, however it is difficult to target multiple targets simultaneously with these methods[76-80].

CRISPR/Cas9 pooled lentiviral libraries provide stable, genome-wide gene knockout alternative that makes possible direct assessment of gene function that previous methods have not achieved[80-81]. In addition to the CRISPR/Cas9 pooled gene knockout libraries, genome-wide CRISPR/Cas9 SAM (Synergistic Activation Mediator) and CRISPRi (CRISPR interference) sgRNA libraries enable robust, multi-approach CRISPR screens for human, mouse, and other model organisms[82-86]. Similarly to RNAi screens, in a CRISPR/Cas9 knockout library a positive screen identifies enriched gene knockouts after drug treatment. These genes potentially increase susceptibility to the treatment condition. A negative screen identifies depleted gene knockouts after drug treatment. These genes are potentially essential to survival of the treatment condition. The genome-wide CRISPR/Cas9 knockout screen has successfully identified genes contributing to a large variety of mechanisms, including essential genes and genes that conferred loss of resistance to vemurafenib in a melanoma model[82, 87].

Novel approach to APAP-induced hepatotoxicity biomarker discovery

Genome wide association studies (GWAS) provide a powerful tool to scan for SNPs that associate with a disease phenotype, such as hepatotoxicity. Unfortunately, large scale GWAS and transcriptomic studies for acetaminophen-induced hepatotoxicity have not been performed in humans due to the lack of control populations consisting of individuals who ingested the same elevated doses of acetaminophen but did not develop

ALI. These “controls” are typically not captured since the need to pursue medical attention after their “overdose” is limited.

This study builds on the existing CRISPR/Cas9 screening technology and applies it to a novel study of APAP-induced hepatotoxicity. We performed a genome-scale CRISPR/Cas9 screen of APAP toxicity (30 minutes-4 days) using the GeCKOv2 sgRNA library. We identified groups of genes and biological pathways that are protective against APAP and other genes that increase susceptibility to injury. An understanding of genes that act in protecting from or enhancing injury at different times can better inform better candidate gene discovery and elucidate the molecular pathways acting in response to APAP. By cross-referencing these data with existing gene expression data on APAP overdose in humans and mice, we validated findings from our screen and connected the effect of CRISPR/Cas9 gene knockout on drug metabolism with the effect of drug on gene expression. From these data we hypothesized the role of novel genes and validate the functional effect of knockdown of select candidate genes. These findings inform changes in the diagnostic and therapeutic modalities employed at the patient level, with the ultimate goal of improving outcomes of APAP-induced ALF.

CHAPTER 3

RESEARCH QUESTION

The purpose of this study is to discover new candidate genes for acetaminophen - induced risk assessment, diagnosis, and treatment. The identification and validation of new biomarkers hold promise for mechanistic insights and novel therapeutic targets.

We hypothesize that the mechanism of acetaminophen toxicity is more complex than is currently known, and expect to find novel genes associated with acetaminophen induced ALF. Our short-term goal is to identify new and robust candidate genes in APAP induced ALF. Our long-term goal is to expand and establish new genetic markers to better understand the physiology of the disease as well as direct the development of diagnostic, prognostic and therapeutic tools to address acetaminophen induced ALI and ALF. These aims advance our understanding of the molecular mechanisms underlying the pathogenesis of ALI/ALF and provide novel insights into effective prevention and treatment of acetaminophen induced liver injury.

Aim 1: CRISPR/Cas9 gene knockout screen of Acetaminophen-induced hepatotoxicity

Specific aim 1 was to identify novel genes associated with acetaminophen toxicity using a genome-wide CRISPR/Cas9 screen of acetaminophen-induced hepatotoxicity in a hepatocellular carcinoma cell line. We identified genes that are protective against

acetaminophen toxicity as well as genes that increase susceptibility to acetaminophen. The results of specific aim 1 are discussed in chapter 5.

Aim 2: Overlapping analysis of post-Acetaminophen treated gene-expression data with our CRISPR/Cas9 screen top hits

Specific aim 2 cross-evaluated the CRISPR/Cas9 screen gene list (+/- APAP) from specific aim 1 by a meta-analysis of 2 human microarray datasets (ALF and overdose) and 1 mouse RNA-seq dataset (+/- APAP). This analysis identified an overlapping and robust list of genes that are differentially expressed in APAP overdose and in APAP-induced ALF. The results of specific aim 2 are discussed in chapter 6.

Aim 3: Exploration of candidate genes identified from the CRISPR/Cas9 screen and the literature

Specific aim 3 analyzed the annotation and functional role of SNPs that are associated with APAP-induced hepatotoxicity in the literature. We additionally assessed overlap of genes containing SNPs with genes identified from our CRISPR/Cas9 screen strategy. We also explored top candidate genes identified from our screening strategy as well as from the literature. We validated selected genes, and began to investigate in-depth the molecular mechanisms underlying the roles of these genes and potential therapeutic targets in acetaminophen induced acute liver injury or acute liver failure. The results of specific aim 3 are discussed in chapters 7 and 8.

CHAPTER 4

METHODOLGY

Research design

This study uses a novel genome-wide CRISPR/Cas9 knockout screening strategy to quantify the effect of specific, targeted gene knockouts on cellular survival of acetaminophen for a range of exposure times. Top enriched and depleted gene knockouts and pathways are assessed and placed in the context of other gene expression datasets representing acute overdose and chronic acetaminophen exposure. Selected candidate genes were knocked down in primary hepatocytes to validate screen findings.

sgRNA library amplification

The genome-wide CRISPR/Cas9 gene knockdown screen was accomplished using HuH7 human hepatoma cells and the GeCKOv2 gene knockout library[82, 88-90]. The human GeCKOv2 sgRNA library halves A and B contain 122,411 targeting sgRNA and 1,000 non-targeting control sgRNA, of that 119,461 are unique sgRNAs (117,481 targeting sgRNAs). Library halves A and B were amplified in Endura competent cells (Lucigen cat. 60242-1, Middleton, WI) and isolated using the Purelink HiPure plasmid midi prep kit (Invitrogen k210005, Carlsbad, CA) as previously described[82, 89].

Cell culture

HEK293FT cells (Thermo Fisher cat. R70007, Waltham, MA) were maintained in high-glucose DMEM (Thermo Fisher cat. 11965118) supplemented with 100 U/ml penicillin and streptomycin (Thermo Fisher cat. 15140122), non-essential amino acids (Thermo Fisher cat. 11140050), 2mM L-glutamine (Thermo Fisher cat. 25030081), 1mM sodium pyruvate (Thermo Fisher cat. 11360070), and 10% fetal bovine serum (Atlanta Biologicals cat. S11150, Atlanta, GA). Cells were detached with trypsin-EDTA (Thermo Fisher cat. 25200056).

HuH7 was obtained from the Japanese Collection of Research Bioresources Cell Bank[91]. The HuH7 human hepatocellular carcinoma cell line (JCRB cat. 0403, Osaka, Japan) was chosen as a model for APAP toxicity studies because it is more robust than primary hepatocytes, allowing efficient lentiviral transduction, transfection, and genome editing with CRISPR/Cas9[92-96].

Cells were maintained in DMEM (Thermo Fisher cat. 111885092) supplemented with 100 U/ml penicillin and streptomycin (Thermo Fisher cat. 15140122), non-essential amino acids (Thermo Fisher cat. 11140050), and 10% fetal bovine serum (Atlanta Biologicals cat. S11150) as previously described, with the addition of 2mM L-glutamine (Thermo Fisher cat. 25030081) and 1mM sodium pyruvate (Thermo Fisher cat. 11360070)[97]. Cells were detached with trypsin-EDTA (Thermo Fisher cat. 25200056). All incubations were performed at 37°C and 5% CO_2.

Lentivirus production and concentration

T-150 TPP flasks (18 T-150 flasks for the library, MidSci cat. TP0151, Valley Park, MO) of HEK293T cells were seeded at ~40% confluence the day before transfection in DMEM. One hour prior to transfection, media was removed and 18mL of pre-warmed reduced serum OptiMEM media (Thermo Fisher cat. 31985070) was added to each flask. Transfection was performed using Lipofectamine 2000 (Thermo Fisher cat. 11668019) and Plus reagent (Thermo Fisher cat. 11514015). For each flask, 200µl of Plus reagent was diluted in 3 ml OptiMEM with 20µg of lentiCRISPR plasmid library, 10µg of pVSVg, and 15µg of psPAX2. 100µl of Lipofectamine 2000 was diluted in 3ml OptiMEM and, after 5 min, it was added to the mixture of DNA and Plus reagent. The complete mixture was incubated for 20 min before being added to cells. After 6 h, the media was changed to 24ml D10 supplemented with 1% BSA (Sigma cat. A8412-100ML, St. Louis, MO). After 84h, the media was removed and centrifuged at 1,000 rpm at 4°C for 5 min to pellet cell debris. The supernatant was filtered through a 0.45 um low protein binding membrane (EMD Millipore Steriflip cat. SE1MO03MO0 or stericup cat. SCHVU05RE, Billerica, MA). To achieve concentration of the GeCKO v2 pooled library, the virus was ultracentrifuged (Beckman-Coulter, Brea, CA) at 32,800 rpm for 1h at 4°C and then re-suspended overnight at 4°C in D10 supplemented with 1% BSA. Aliquots were stored at –80°C. Lentiviruses were titrated by qRT-PCR (Clontech Lenti-X™ qRT-PCR Titration Kit cat. 631235, Mountain View, CA).

Acetaminophen kill curve

The APAP concentration used for the screen was determined by measuring cell proliferation of HuH7 stably transduced with Cas9 and Guide-Puro (empty vector) in the presence of 0-20mM APAP (Sigma cat. A7085. St. Louis, MO) daily for 7 days. HuH7 were seeded at 20,000 cells/96-well (MidSci cat. TP92696, Valley Park, MO) prior to APAP treatment. Titration of APAP concentrations ranging from 5mM-20mM was accomplished by measuring cell count at 24 hour intervals for seven days by trypan blue counting (Sigma cat. T8154-100ML, St. Louis, MO). Percent of cell death was determined as an average of the APAP-treated cell count divided (do you mean subtracted?, only dead cells stain, right? I can't see why you would divide) by untreated cell count (N=3). For the screen, 15mM APAP was chosen because there was 5% survival (95% cell death) at 3 days selection when APAP-treated cells were compared with untreated cells and 1% survival (99% cell death) at day 4 selection when APAP-treated cells were compared with untreated cells, based on the strategy of Wang *et. al*.[86].

***In vitro* hepatocellular carcinoma transduction using the GeCKOv2 sgRNA library**

HuH7 cells were detached using 0.25% Trypsin-EDTA (Thermo Fisher cat. 25200056) and seeded the day prior to transduction at 6E6 cells per T-150 TPP flask (MidSci cat. TP0151, Valley Park, MO). The flasks were then transduced for 48h in culture media + 8µg/ml polybrene (Thermo Fisher cat. 107689-10G) + Cas9 lentivirus at an MOI <0.1. HuH7 underwent monoclonal selection by 1ug/ml blasticidin (Thermo Fisher cat.

A1113903) before Cas9 expression was confirmed by western blot. HuH7-Cas9 was transfected with the GeCKOv2 packaged lentiviral library as described above at 0.5 MOI. The pooled, transduced cells were selected with 1.5µg/ml puromycin (Invitrogen cat. Ant-pr-1) for 3 days alongside cells transduced with the empty vector lentiGuidePuro, positive fluorescent control pLJM1-EGFP. pLJM1-EGFP fluorescence was verified 48h post-transduction.

CRISPR/Cas9 acetaminophen screen and sample collection

After 8 days of transduction a T0 sample was collected (N=2) and the remaining library-transduced cells were treated with 15mM APAP for 30 minutes up to 4 days (2 biological replicates for T0, 24 hour, and 4 day samples). Samples that underwent 4 days of APAP treatment were outgrown for 21 days prior to collection. Genomic DNA was isolated from samples of a minimum of $2x10^7$ cells using the Blood and Cell Culture Midi Kit (Qiagen cat. 13343, Valencia, CA), resulting in a minimum of 136µg DNA per sample. DNA was quantified using the Qubit high-sensitivity DNA quantification assay (Thermo Fisher cat. Q32851) and Take3 microspot plate reader (BioTek Epoch, Winooski, VT).

CRISPR/Cas9 Screen amplicon sequencing

DNA amplification, library preparation, and sequencing were conducted using standard protocols. 3.33µg of the isolated genomic DNA was used to amplify the bar-coded amplicons in 39 Herculase II DNA polymerase (Agilent cat. 600679, Santa Clara, CA)

reactions per sample (primers described in supplementary table 1). 5µl amplicon or 1µl diluted plasmid library was used as template in 13 50µl Herculase II DNA polymerase reactions per sample to attach pooled variable-length spacers and Illumina indexes (primers described in supplementary table 1). 24 cycles were used to amplify DNA in the first and second PCR. The amplicon fragments after PCR 2 have the following sequence (354-362bp library with variable 20bp sgRNA sequence in the middle) (SF1). DNA was pooled by sample and purified using the Nucleospin Gel and PCR Clean-up kit (Clontech cat. 740609.250, Mountain View, CA). DNA was quantified using a Qubit high-sensitivity DNA quantification assay (Thermo Fisher cat. Q32851) and Take3 microspot plate reader (BioTek). DNA quality was analyzed by Experion CHIP assay (BioRad cat. 7007-163, Hercules, CA). Clusters were generated on the flow cell using the HiSeq Rapid Duo CBot Sample Loading Kit (Illumina CT- cat. 403-2001, San Diego, CA). A single-read rapid run of 75 cycles was performed on a HiSeq 1500 (Illumina cat. GD-402-4002) using the HiSeq Rapid SBS kit (Illumina cat. FC-402-4022) with 10% PhiX.

CRISPR/Cas9 screen deconvolution and analysis

The sequence reads were demultiplexed and converted to fastQ with BCL2FastQ v2.17 (Illumina) and trimmed in cutadapt 1.7.1 (with Python 2.7.6) to include only the 20bp sgRNAusing the 5' sequence GTGGAAAGGACGAAACACCG and the 3' sequence GTTTTAGAGCTAGA [98]. Trimmed reads were aligned to the index in Bowtie2 v2.1 with a 1bp mismatch allowance[99]. Read counts were normalized to the median with T0 as control and analyzed using sgRNA and gene-level RRA (Robust Rank Aggregation) in

MaGeCK v0.5.6[100]. In comparisons between 2 time points the biological replicates were handled as independent replicates and in the pooled T0 vs. 30min-24h and 30min-4d the replicates were combined. Gene-level analysis was validated using Maximum Likelihood Estimate (MLE) in MaGeCK v0.5.6. Genes with fewer than 3 sgRNA were not included in the gene-level analysis but were included in the Gene Set Enrichment Analysis (GSEA) pathway analysis implemented in MaGeCK v0.5.6[101]. Scatter plots and heat maps were generated in R. Venn-diagrams were generated using http://bioinformatics.psb.ugent.be/webtools/Venn/. CRISPR/Cas9 screen data were submitted to the Gene Expression Omnibus (GSE112463, https://www.ncbi.nlm.nih.gov/geo/).

Pathway analysis

Analysis of pathway-level effects of APAP treatment in the 24h and 4d samples individually vs. T0 was accomplished using GSEA in Mageck v0.5.6 using the MsigDB "Kegg gene sets" and "all GO gene sets". Ingenuity Pathway Analysis of 24h vs. T0 (genes with $p<0.05$) and 4d vs. T0 (genes with $p<0.05$) was also used to predict pathway-level effects of APAP treatment.

Analysis of overlapping data from the Gene Expression Omnibus

Human APAP-induced liver injury. We then analyzed samples from 2 publically available human datasets of acetaminophen overdose from the Gene Expression Omnibus,

GSE74000 and GSE70784[67, 102]. Gene candidates identified using the genome-wide CRISPR/Cas9 screen were cross-referenced with gens that were significantly correlated with APAP overdose from 2 human microarray datasets identified in the Gene Expression Omnibus (https://www.ncbi.nlm.nih.gov/geo/). These datasets were analyzed in GEO2R using the microarray data normalized and deposited by the original authors.

Of the available gene expression datasets assessing the effect of APAP, these were selected because they address hepatotoxicity at a range of stages. These datasets were analyzed in GEO2R using the microarray data normalized and deposited by the original authors. GSE70784 contains gene-expression data from blood in patients receiving a daily dose of APAP or placebo. These data compare patients at a higher risk of injury (responders) to non-responders and placebo after 1 day and 8 days of dosing. Genes with differential expression in blood, especially early after dosing, are ideal diagnostic biomarkers. GSE7400 contains gene expression data from liver biopsies from healthy patients and patients APAP-induced-ALF. These data address differential gene expression in end-stage disease, and better inform the biological mechanisms active in APAP-induced ALF.

In GEO2R, microarray data from 12 APAP responder blood samples were compared to 32 non-responders and 10 placebo controls on 1 day and 8 days of APAP treatment. Subjects were treated with 4g APAP or placebo for 7 days and were followed for 14 days. Responders were classified as patients with ALT (alanine aminotransferase). >2 times the upper limit of normal during days 4-9 after the start of APAP dosing. Background correction and normalization was completed by the depositing authors. Data

was log 2 transformed prior to analysis and the unadjusted p-values were used for comparison with the CRISPR screen.

Microarray data from 3 APAP-induced ALF liver samples were compared to 2 healthy liver samples were obtained from the GEO dataset GSE74000 and compared using GEO2R. Background correction, median polish summarization, and quantile normalization were completed by the depositing authors. Data was log 2 transformed prior to analysis and the FDR-adjusted p-values were used for comparison with the CRISPR screen. Heat maps were generated in R. Box plots were generated in GEO2R.

Mouse APAP-induced liver injury. RNA-seq data from mice previously published by our lab (GSE110787, Zhang *et al.* Am J Pathol. In press, 2018) evaluating the effect of APAP overdose on RNA expression changes in the liver was 7 male 11 week old C57BL/6 mice, 4 saline treated control mice and 3 mice 24h after 200mg/kg APAP (Sigma cat. A7085, St. Louis, MO) exposure via intraperitoneal injection, underwent RNA-sequencing on an Illumina HiSeq1500. RNA was isolated from liver using the MirVana miRNA isolation kit (Thermo Fisher cat. AM1561, Waltham, MA).

Samples were prepared using the TruSeq Stranded Total RNA Sample Preparation Kit (Illumina cat. RS-122-2201, San Diego, CA) and clusters were generated using the TruSeq Paired-End Cluster Kit v3-cBot-HS (Illumina cat. PE-401-3001, San Diego, CA). Paired –end sequencing (2x101 cycles) was completed using the TruSeq SBS kit v3-HS (Illumina cat. FC-401-3001, San Diego, CA). The raw base calling (.bcl) files were converted to demultiplexed compressed FASTQ files using Illumina's bcl2fastq v2.17 software. TopHat 2.0.9 was used to map RNA-seq reads against the mouse reference

genome (mm10) using default parameters[103-104]. Transcript assembly, abundance estimation, and comparison of expression were conducted with Cufflinks v2.2.1 and reported in Fragments Per Kilobase of exon per Million fragments mapped (FPKM)[104]. Cuffdiff, a part of the CuffLinks package, was used to calculate statistical significance changes of gene expression between treated and untreated mice[105]. Box plot and heat maps were generated in R.

This RNA-seq study of APAP-induced ALI identified genes that were differentially expressed in a genetically and drug dosage controlled environment after liver injury has occurred, but prior to ALF. These data better illustrate the changes in gene expression due to the drug overdose absent of the variation that is unavoidable in human studies.

Analysis of acetaminophen-associates SNPs in the literature

In this analysis we evaluate the 147 genetic polymorphisms that have been identified as associated with either protection against or susceptibility to APAP-induced hepatotoxicity and then provides functional interpretation of the biological relevance of these SNPs. The 147 SNPs analyzed in this analysis were identified from studies by Ueshima *et. al.*, Court *et. al.*, Harrill *et. al.*, and Moyer *et. al*.[38, 43, 48-50, 63, 66]. Ueshima et al. described a *CYP2E1* promoter SNP (rs2031920) that associated with altered acetaminophen metabolism[48].

To determine the potential biological processes and regulatory relationships for the SNPs discussed in previous studies of APAP and APAP metabolite-induced toxicity [38, 43, 48, 50], we reanalyzed the 147 SNPs. Variant annotations were obtained from RefSeq,

GENCODE, and Ensembl[106-108]. Annotations of noncoding polymorphisms were assessed with HaploReg v4.1 [109]. Ingenuity Pathway Analysis (Qiagen) was used to predict functional consequences and PubMatrix was used to assess novelty of the gene associations with APAP-induced ALF[110]. Genome Wide Annotation of VAriants (GWAVA) was used to score the functional relevance of the 147 SNPs[111].

Drug-gene interaction analysis

Genes in the top 10 of a CRISPR/Cas9 knockout screen list and overlapping a gene expression dataset ($p<0.05$), in a CRISPR/Cas9 knockout screen list ($p<0.05$) and involved in NAD metabolism, or in a CRISPR/Cas9 knockout screen list ($p<0.05$) and containing or nearest neighbor to APAP-associated SNPs were compared against the Drug Gene Interaction Database (http://www.dgidb.org/) to assess known drug interactions and potential re-purposing of existing drugs[112].

Functional validations in primary mouse hepatocytes:

Cryopreserved hepatocytes (Lonza cat. MBCP01, Allendale, NJ) from 8-week old male C57/Bl6 mice were thawed in thawing media (Lonza. Cat. MCRT50) and immediately seeded at a density of 15,000 cells/96-well and 250,000 cells/12-well in Williams E media with thawing and plating supplement (Thermo cat. A1217601, cat. CM3000, respectively). After 4 hours the cells were transfected using the standard Polyplus INTERFERin protocol for 4 hours (VWR cat. 89129-930, Radnor PA) and 25nM TYE-

563 fluorescent control (IDT cat. 51-01-20-19) or SmartPool scrambled siRNA or (Nampt, Lztr1, and Naaa) siRNA (Dharmacon, Lafayette, CO) or 50-100nM SmartPool siRNA (Pgm5, Dharmacon) in Williams E media with thawing and plating supplement (serum-free, Thermo cat. A1217601, cat. CM4000, respectively). 20 hours after transfection TYE-563 positive fluorescent controls were imaged and cells were treated with +/-7.5mM APAP for 3 hours beginning 22 hours post-transfection. Cell viability was measured by ATP luminescence read at 0.25 seconds with n=6 and the high and low values removed for a final n=4 (Promega CellTiter-Glo cat. G7571, Madison, WI) using a TriStar LB 941 Multimode Microplate Reader (Berthold Technologies, Bad Wildbad, Germany). For each siRNA transfection, APAP-treated wells were normalized to untreated wells. Statistical significance was determined by a 2 sample 2-tailed Student's t-test assuming equal variance ($p<0.05$). Gene expression was validated by sqPCR.

Semi-quantitative PCR

RNA was isolated using the MirVana miRNA isolation kit (Thermo Fisher cat. AM1561, Waltham, MA) and quantified using the Epoch Take3 (BioTek, Winooski, VT). cDNA was amplified from 500ng mRNA by SuperScript IV (Thermo Fisher cat. 18091200, Waltham, MA). 2µl CDNA was used as sqPCR template using Platinum Taq polymerase (Thermo Fisher cat. 10966-026, Waltham, MA) (primers are listed under sqPCR in supplementary table 1). A 2.5% agarose gel was run @100V to visualize knockdown of *Lztr1*, *Nampt*, and *Pgm5* with *ActB* used as a loading control.

Western blotting

HuH7 cell lysates were collected on ice in RIPA buffer and isolated by centrifugation at 13,000 RPM for 10 minutes at 4°C. Protein was quantified by Pierce BCA (Thermo Fisher cat. 23225, Waltham, MA). 30µg protein (western) was boiled with sample buffer prior to loading on a polyacrylamide gel. Cas9 antibody diluted 1:2,000 in TBS-T+3% milk (EMD Millipore cat. MAC133, Billerica, MA), vinculin antibody diluted 1:1,000 in TBS-T+5% milk (Enzo cat. BML-VG6110, Farmingdale, NY). Goat anti-rabbit HRP antibody 1:10,000 in TBS-T + 5% milk (Vector Biolabs cat. PI-1000, Malvern, PA) and horse anti-mouse HRP antibody in TBS-T + 5% milk (vector Biolabs cat. P1-2000, Malvern, PA) were used to visualize westerns.

Plasmids

The lenti Guide_puro backbone, lenti Cas9_blast, and the Human GeCKOv2 CRISPR knockout pooled library were originally from Feng Zhang's lab (Addgene pooled library #1000000048, #1000000049, plasmid #52962, 52963, respectively)[89]. psPAX2 was originally from Didier Trono's lab (Addgene plasmid # 12260) and pCMV-VSV-G was originally from Bob Weinberg's lab (Addgene plasmid # 8454) [113]. pLJM1-EGFP was originally from David Sabatini's lab (Addgene plasmid # 19319)[114].

CHAPTER 5

RESULTS PART 1

Development of screening strategy and preparation of cell lines

HuH7-Cas9 was monoclonally selected and expression of Cas9 was confirmed by western blot (figure 1 a). To determine the optimal dosage of APAP, HuH7-Cas9 cell count and viability were assessed daily (N=3) in the presence of 0-20mM APAP in growth media (figure 1 b). A screening strategy was developed based on the rate of cell death in 15mM APAP to assess the effect of the gene knockouts on cellular survival and proliferation with APAP treatment (figure 1 c).

CRISPR/Cas9 knock-out screen and deconvolution

HuH7-Cas9 cells ($1.62x10^8$ total) were transduced with the lentiviral sgRNA library at an MOI of 0.5 resulting in >630x total library coverage at the time of transduction. The first replicate contains plasmid and samples collected at 0h, 30min, 3h, 6h, 12h, 24h, and 4d (end) of APAP treatment. The second replicate contains samples collected at 0, 24h, and 4d of APAP treatment. A minimum of $2x10^7$ cells were collected per sample, resulting in 160x library coverage per sample as template for the 1st PCR. The average library coverage of aligned reads calculated from amount of isolated DNA per sample was 205x and 284x, respectively for replicates 1 and 2. On average, 70% of the sequence reads

aligned to the reference sgRNA library resulting in 230.9x average library coverage per replicate (supplementary table 2).

After 4 days of APAP treatment and 21 days outgrowth, the endpoint sample is significantly different from the plasmid library or T0 ($p<10^{-10}$) by comparison via Wilcoxon Rank-Sum test and there is a noticeable increase in variation of read counts after 4 days of drug treatment (figure 1 D-E, supplementary table 3). Scatter plots of the read counts between the untreated and 24h samples and the untreated and 4d samples show an increase in differential sgRNA count between 24h and 4d of drug treatment (supplementary figure 2 A-B).

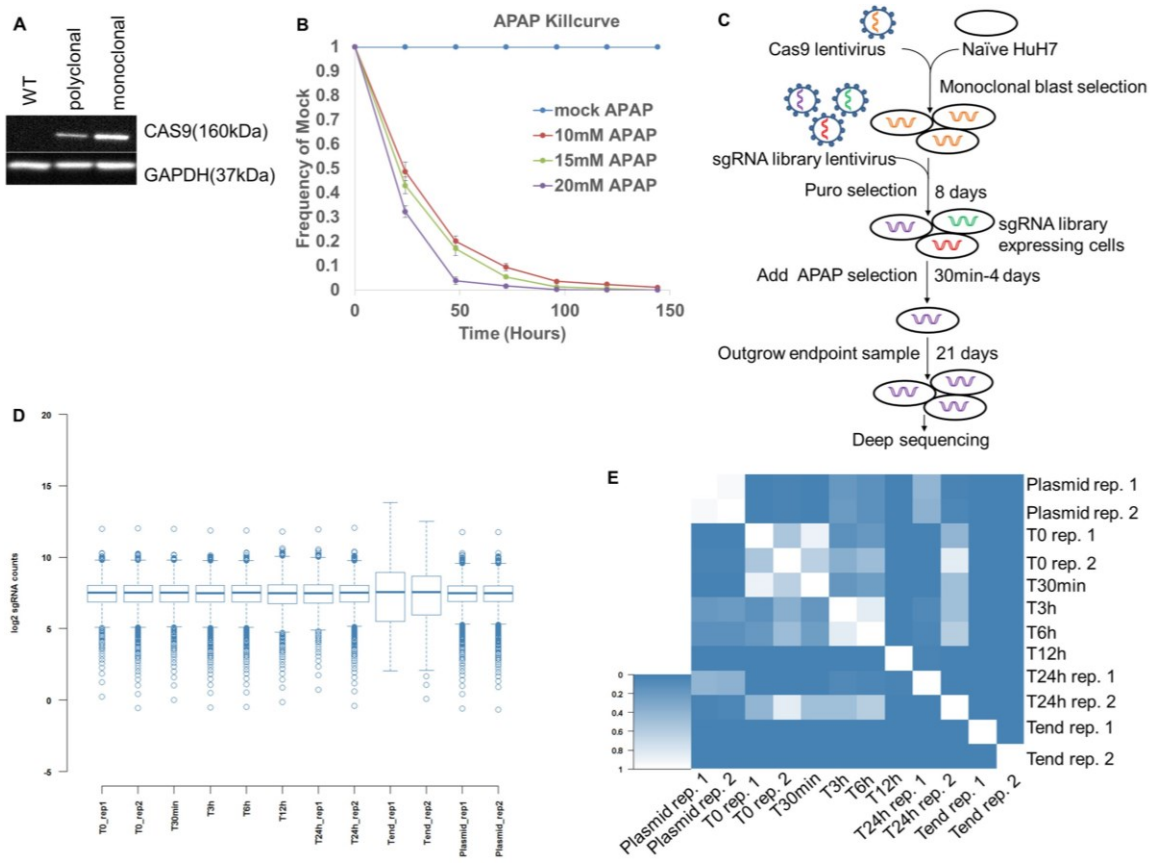

Figure 1 | Genome-scale positive and negative screening using CRISPR/Cas9. A Expression levels of Cas9 in polyclonal and Monoclonal HuH7-Cas9 cell line. **B** Relative growth of HuH7-Cas9/GuidePuro when treated with and without APAP. **C** Timeline of APAP resistance screen in HuH7 hepatocellular carcinoma cells. **D** Box-plot showing the distribution of $\log_2$ median-normalized sgRNA read count frequencies of the plasmid library (plasmid) and post-lentiviral transduction for baseline (T0), early APAP treatment time points (T30min-24h), and the endpoint (4 days APAP treatment and 21 days outgrowth) conditions. **E** Rank correlation p-values of median-normalized sgRNA read counts between treatment conditions.

sgRNA read counts were scored and ranked to determine the gene-level and protein-level negative and positive screen rankings of individual time points and combined time points using RRA (supplementary table 4-19). The 4 day APAP treated (end) samples were compared with the untreated sample, revealing a number of genes containing sgRNA that were significantly decreased with APAP treatment (negatively selected, potentially essential) and significantly increased with APAP treatment (positively selected, potentially

susceptible) (figure 2 A-B). These gene knock-outs were significantly differentially expressed in a sample where almost all of the Huh7 have been killed by APAP. The ranked gene lists underwent GSEA pathway analysis against the All Gene Ontology and KEGG pathway gene sets, that returned statistically significant, highly ranked essential pathways in the negative screen analysis as well as a number of novel pathways in both the negative and positive screen analysis (figure 2 C-E). Essential Kegg pathways are highly ranked in the negative screen after drug treatment, including ribosome and spliceosome pathways. Analysis of Gene Ontology pathways reveals other pathways important to cellular function are highly negatively selected and apoptotic processes are highly positively selected.

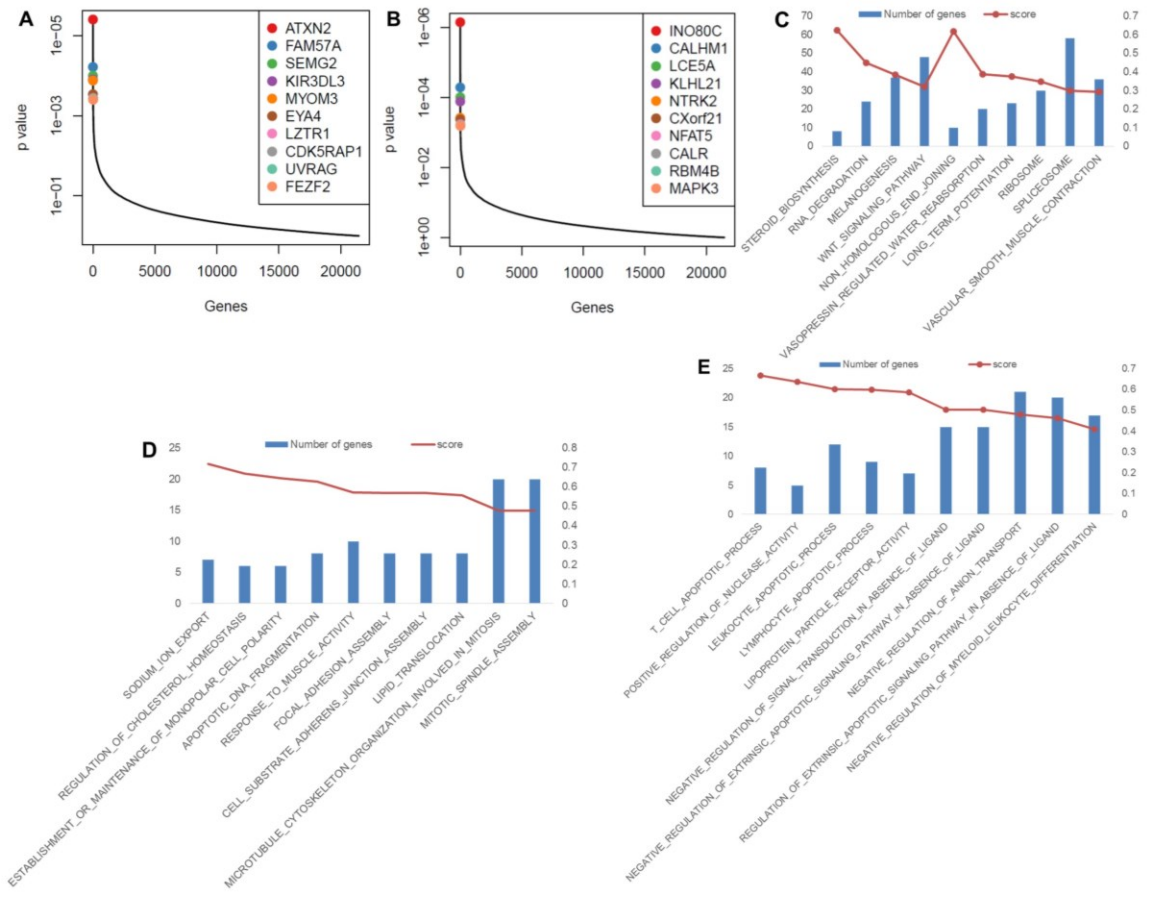

Figure 2 | Positive and negative screening reveal top gene and pathway candidates after 4 days of APAP treatment. A Identification of top candidate genes using the p-

values from positive RRA analysis of the 4d and T0 samples. Genes with the most positively selected sgRNAs are highlighted. **B** Identification of top candidate genes using the p-values from negative RRA analysis of the 4d and T0sample. Genes with the most negatively selected sgRNAs are highlighted. **C** Top 10 Kegg pathways negatively selected in the endpoint sample compared with the T0 sample. **D** Top 10 Gene Ontology pathways negatively selected in the endpoint sample compared with the T0 sample. **E** Top 10 Gene Ontology pathways positively selected in the endpoint sample compared with the T0 sample.

At 24h APAP treatment, we observed a significantly different distribution of genes representing highly significant positive and negative changes in sgRNA expression (figure 3 A-B). Pathway analysis by GSEA using the KEGG and Gene Ontology gene sets returned a number of novel pathways (figure 3 C-E). The top negatively selected Gene Ontology pathway after 24 hours of APAP treatment was *regulation of skeletal muscle contraction*. The top biological network identified from this pathway by Ingenuity Pathway Analysis (Qiagen) was *lipid metabolism, small molecule biochemistry and organ morphology*, focusing around calcium signaling (figure 3 F). This correlates with existing literature suggesting that calcium imbalance may affect APAP-induced hepatotoxicity[115-116]. Our data provide new and previously unrevealed targets for further experimentation.

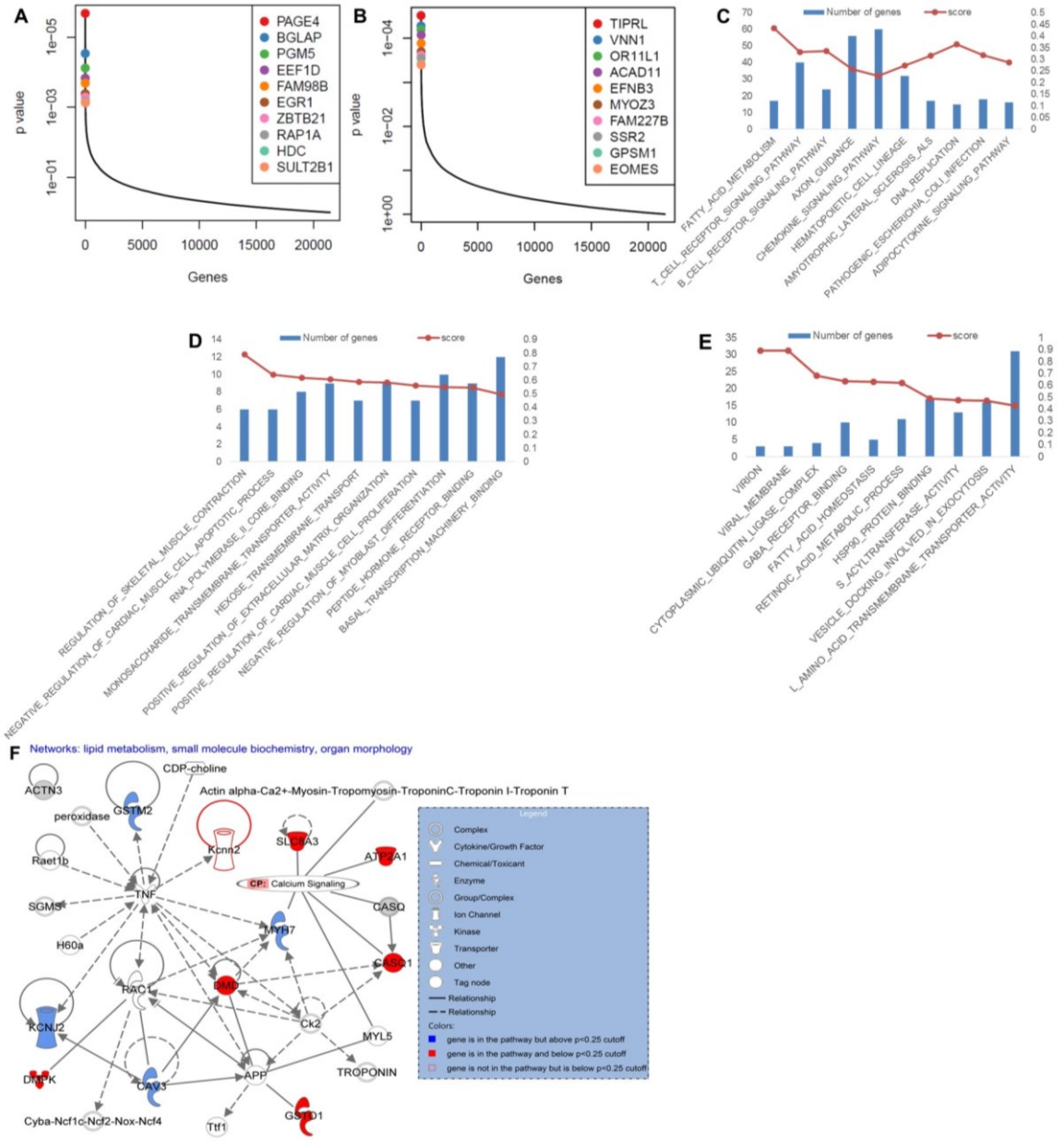

Figure 3 | Highly ranked genes and pathways after 24 hours of APAP treatment. A Identification of top candidate genes using the p-values from positive RRA analysis of the 24h and T0 samples. Genes with the most positively selected sgRNAs are highlighted. **B** Identification of top candidate genes using the p-values from negative RRA analysis of the 24h and T0 sample. Genes with the most negatively selected sgRNAs are highlighted. **C** Top 10 Kegg pathways negatively selected in the 24h sample compared with the T0 sample. **D** Top 10 Gene Ontology pathways negatively selected in the 24h sample compared with the T0 sample. **E** Top 10 Gene Ontology pathways positively selected in the 24h sample compared with the T0 sample. **F** Top biological network identified by IPA from the top essential Gene Ontology pathway, regulation of skeletal muscle contraction, at 24h of APAP treatment.

We next sought to rank genes by time groups rather than specific time points with two main goals: 1) identify genes that were ranked highly (positive or negative) in early time points (30min-24h APAP exposure) vs. no treatment and 2) identify genes that were ranked highly (positive or negative) in all pooled APAP treated samples vs. no treatment. A literature search of the top 100 ranked genes (positively and negatively ranked, respectively) for each of these combinations of time points identified 44 unique genes (of 716 total unique genes queried) that were already associated with APAP and a vast majority that do not have previous associations with acetaminophen in the literature (table 1).

Table 1: The top 100 genes for various APAP treatment times were queried in pubmatrix to determine novelty.

PubMatrix	APAP	acetaminophen	hepatotoxic	hepatotoxicity	acute liver injury	acute liver failure
24h pos. top 100 genes + APAP	7	7	6	14	11	8
24h neg. top 100 genes + APAP	5	5	5	5	5	5
4d pos. top 100 genes + APAP	7	6	6	8	6	8
4d neg. top 100 genes + APAP	7	7	2	8	8	4
all pos. top 100 genes + APAP	2	1	0	3	4	4
all neg. top 100 genes + APAP	6	6	4	7	6	4
30min-24h pos. top 100 genes + APAP	7	7	2	5	5	5
30min-24h neg. top 100 genes + APAP	6	6	4	7	5	5
genes in all 8 top 100 lists	800					
unique genes in all 8 top 100 lists	716					
unique genes with APAP hits	44(APAP), 42(acetaminophen)					

We then grouped genes that were highly ranked at independent time points to isolate early and late acting genes. While a few genes contained sgRNA that are significantly enriched (or depleted) across all early time points, many were unique to the individual time points. While the sensitivity of the screen at very early times is likely lower than at later time points, early and late acting gene groups that were shared between time points or were unique to specific time points but represent statistically significant pathways may be important to drug response (figure 4 A-B). To identify knocked-out genes that have a global significance we compared all APAP-treated samples to the T0 samples (figure 4 C-D). To identify knocked-out genes that were important for the early APAP response we compared the 30min-24h APAP treated samples to the T0 samples (figure 4 E-F). These comparisons resulted in a number of highly significant genes.

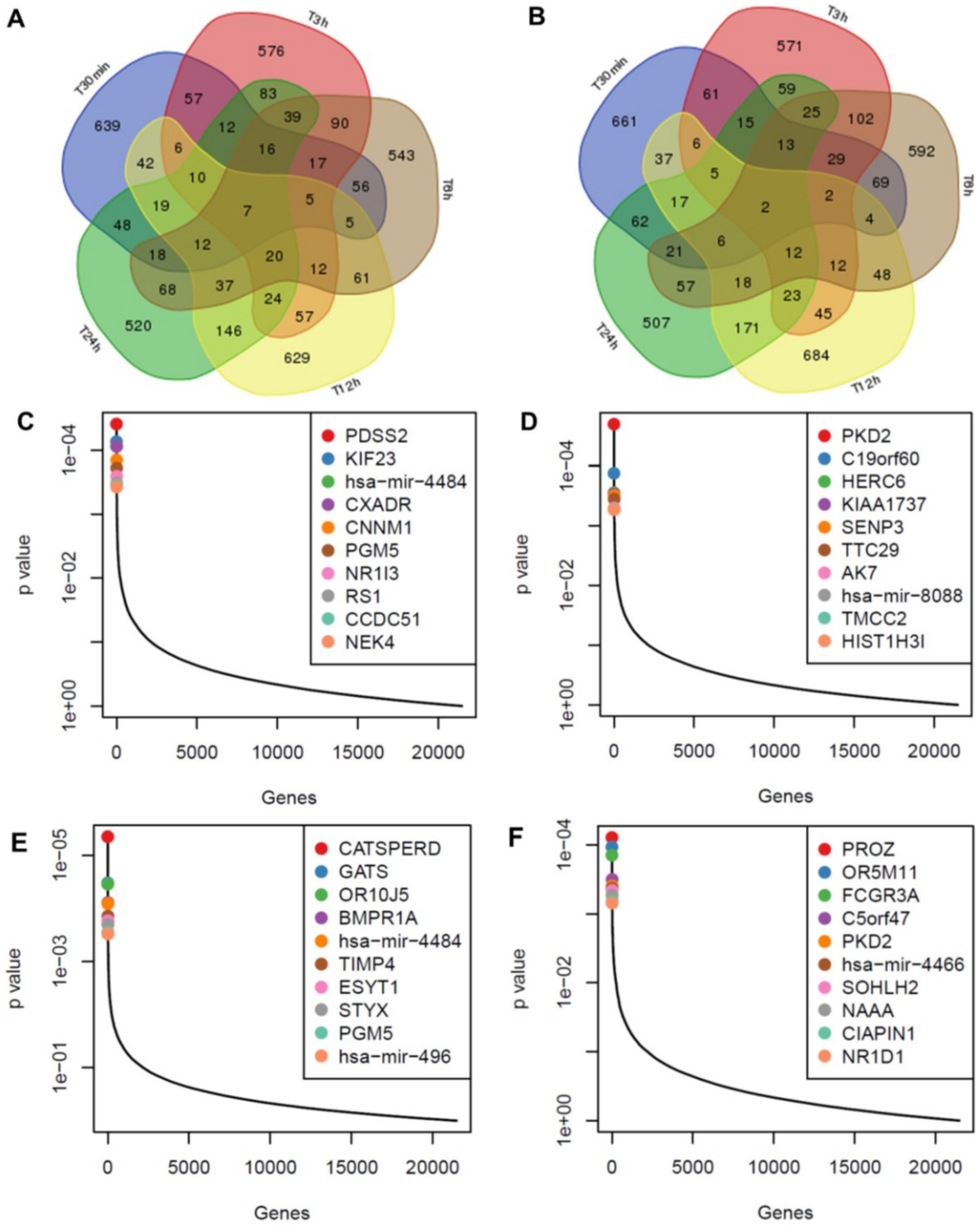

Figure 4 | Identification of gene hits across the APAP time course in the CRISPR/Cas9 screen. A, B Venn diagrams of differently expressed genes in HuH7 cells treated with 15 mM APAP for 5 early time points. The diagrams show the number of gene knockouts significantly enriched by the treatment (**A**) and depleted by the treatment (**B**) for 5 time points (P<0.05). The diagrams show the number of genes significantly modulated by the treatments. **C** Identification of top candidate genes using the p-values from positive RRA analysis based on all APAP time points vs. T0. Genes with the most positively selected

sgRNAs are highlighted. **D** Identification of top candidate genes using the p-values from negative RRA analysis based on all APAP time points vs. T0. Genes with the most negatively selected sgRNAs are highlighted. **E** Identification of top candidate genes using the p-values from positive RRA analysis based on intermediate (30min-24h) APAP time points vs. T0. Genes with the most positively selected sgRNAs are highlighted. **F** Identification of top candidate genes using the p-values from negative RRA analysis based on intermediate (30min-24h) APAP time points vs. T0. Genes with the most negatively selected sgRNAs are highlighted.

The RRA statistical method was chosen to rank gene knockouts because of its superior performance when compared with RSA and RIGER[100]. To validate our choice of statistical analysis method, we compared the RRA to the Maximum Likelihood Estimate algorithm (MLE), which has been shown to produce comparable gene ranking to RRA[117]. In a MLE analysis of all APAP time points compared with the T0 sample, 683 genes were statistically significant ($p<0.05$), of that 442 (65%) were also statistically significant ($p<0.05$) using the RRA method (v0.5.6) (supplementary table 20).

We suspect that NAD metabolism may play an important role in survival of acetaminophen injury and to this end we identified a number of genes involved in NAD metabolism that are also highly ranked in the CRISPR screen time points. A list of 48 genes identified based on Nikiforov *et al.*, 2015 was compared with statistically significant CRISPR hits ($p<0.05$)[118]. We identified 9 NAD metabolism genes in our screen data (supplementary table 21). Notably, NMNAT1 knockout is significantly depleted across all APAP-treated samples and individually at 24h and 4d treatments. Additionally, data from our lab suggest overexpression of NAMPT, a gene involved in NAD salvage, is protective against APAP-induced hepatotoxicity *in vivo*[105].

Discussion

This study has identified a number of novel and previously unrevealed regulators of APAP-induced hepatotoxicity by employing state of the art genome-wide CRISPR/Cas9 screen in a hepatocyte cell line. Selected targets have been validated in primary hepatocytes and cross-referenced in other available data sets of human and mouse involvement. Our study has illustrated the power of a genome-wide CRISPR/Cas9 screen to systematically identify novel genes involved in APAP induced hepatocyte toxicity and most importantly, it provide a rich resources for further experimentation to identify potential new diagnostic targets or to develop novel therapeutic modalities to APAP induced hepatocyte toxicity. Genes containing sgRNA that are significantly and consistently enriched or depleted across the gene are candidates for further study, both as biomarkers and as contributors to larger disease mechanisms. Gene knockouts that are extremely enriched or depleted are more likely to function in APAP mechanism without a redundant mechanism, as opposed to gene knockouts with little to no differential read count.

It is widely accepted that the cytochrome P450 isoform play an important role in APAP metabolism to NAPQI. While we expected to see the cytochrome P450 isoforms higher in the gene rankings of the negative screen, it is unsurprising that they are not highly ranked because HuH7 has low expression of some CYPs. It is suspected that multiple isoforms can regulate the metabolism of APAP, so it is possible that others are compensating for the knocked out isoform. The low expression of some CYPs in HuH7 arguably increases the potential for this system to reveal non-canonical mechanisms of survival and susceptibility.

Although there are always concerns when using a cell line to study a biological mechanism, HuH7 has been used successfully for studies of drug metabolism[95, 119]. To carry out the CRISPR/Cas9 screen it was necessary to use a cell line that could be transduced and didn't require differentiation. Whenever possible, we validated our findings in primary mouse hepatocytes.

Although few genes were completely removed from the pooled mutant cell population prior to APAP treatment, thousands were missing after 4 days of APAP treatment. Based on the kill curve 4 days of APAP treatment results in about 1% surviving cells, indicating a majority of the cells being killed. The survival of cells with low numbers of sgRNAs is only statistically important if the proportion within the surviving population is significantly different than the starting population consistently across multiple sgRNAs per gene. The early time points (30 minutes to 24 hours of APAP treatment) in this screen are based on traditional gene expression screening techniques. By considering the impact of drug selection at early time points we can better assess the early and late response genes involved in drug toxicity. We propose that a Wilcoxon Rank-Sum value of $p<10^{-10}$ may be too stringent for addressing finer scale effects of gene knockout.

Using GSEA pathway analysis our screen identified WNT signaling (Kegg gene set) as a very strongly depleted pathway and also identified positive regulation of Notch Signaling (GO, Gene Ontology gene set) as a significantly depleted pathway ($p<0.05$). Notch signaling has been previously identified as essential to survival of APAP[120]. To further validate our screening methodology, both spliceosome and ribosome Kegg pathways are among the most strongly depleted pathways after 4 days of APAP treatment. Our top negatively selected GO pathway after 24h APAP treatment, *regulation of skeletal*

muscle contraction, corroborates some existing work, suggesting that intracellular calcium may be important to response to APAP. However, the role of this pathway in APAP-induced hepatotoxicity is unclear.

The other top pathways included a variety of functions. At 24h APAP treatment the top GO pathway based on the positive (enriched) gene knockout ranking is *viron*. This could be resultant of the lentiviral process used to incorporate the sgRNA and Cas9 genomic sequence. At 4d APAP treatment the top pathway from the positive gene knockout ranking is *T-cell apoptotic process*. The top pathway from the negative gene knockout ranking at 4d APAP treatment is *sodium ion export*.

Based on Zhang *et al.* (Am J Pathol. In press, 2018) we identified NAD salvage, specifically the gene NAMPT, as a potentially important in protection against APAP-induced injury[105]. We extended this hypothesis to the genome-wide CRISPR screen of APAP-induced hepatotoxicity, assessing the presence of NAD metabolism genes among the top ranked genes ($p<0.05$). This analysis revealed that a number of NAD metabolism genes are represented in our highly enriched or depleted gene knockouts. NMNAT1 knockout was significantly depleted across the APAP screen, suggesting an important function in cell survival after APAP treatment. These genes that have known functions in NAD metabolism and whose knockout impacts survival of drug exposure in our CRISPR/Cas9 screen warrant additional mechanistic and population-based evaluation of their utility as biomarkers for liver injury.

CHAPTER 6

RESULTS PART 2

Overlapping analysis of our screen top hits with other gene expression acetaminophen datasets

In order to validate our results, we performed the overlapping analysis of our screen top hits with other gene expression acetaminophen datasets. We analyzed 2 human microarray datasets and 1 mouse RNA-sequence data set, all of that were collected after APAP exposure. In order to better understand the effect of APAP on the transcriptome and place this information within the context of our CRISPR/Cas9 knockout screen, we identified genes that were significantly enriched or depleted ($p<0.05$) in the CRISPR screen and in the transcriptome data.

Analysis of RNA-sequence from mice with acetaminophen-induced acute liver injury

In cuffdif, RNA-seq data from mice with and without APAP exposure (GSE110787) were compared to assess the effect of APAP exposure on gene transcription. 1,626 of 46,073 genes were statically, significantly and differentially expressed genes after APAP exposure with an unadjusted p-val <0.05. 1,025 genes have – $\log_2$ fold change with $p<0.05$ and 601 genes have + $\log_2$ fold change with $P<0.05$ (supplementary figure 3 A, supplementary table 22). Overlap between the genes that were highly ranked in the

CRISPR screen ($p<0.05$) and this analysis ($p<0.05$) represent genes that were validated *in vivo*. (figure 5 A-B, supplementary table 22).

Analysis of microarray of human liver biopsies from normal and acetaminophen-induced acute liver failure patients

Secondary data from human sources was used to cross-validate the CRISPR screen findings. In GEO2R, microarray data from 3 APAP-induced ALF liver samples were compared to 2 healthy liver samples (GSE74000). 1,679 of 54,675 probes have an FDR-adjusted p-value of <0.05. 1,251 probes have $-\log_2$ fold change with $p<0.05$ and 428 probes have $+\log_2$ fold change with $p<0.05$ (supplementary figure 3 B). We compared genes with $p<0.05$ to genes that were significantly enriched and depleted in our CRISPR screen ($p<0.05$) to identify overlap and ascertain the relationship between sgRNA depletion or enrichment and gene expression (figure 5 C-D).

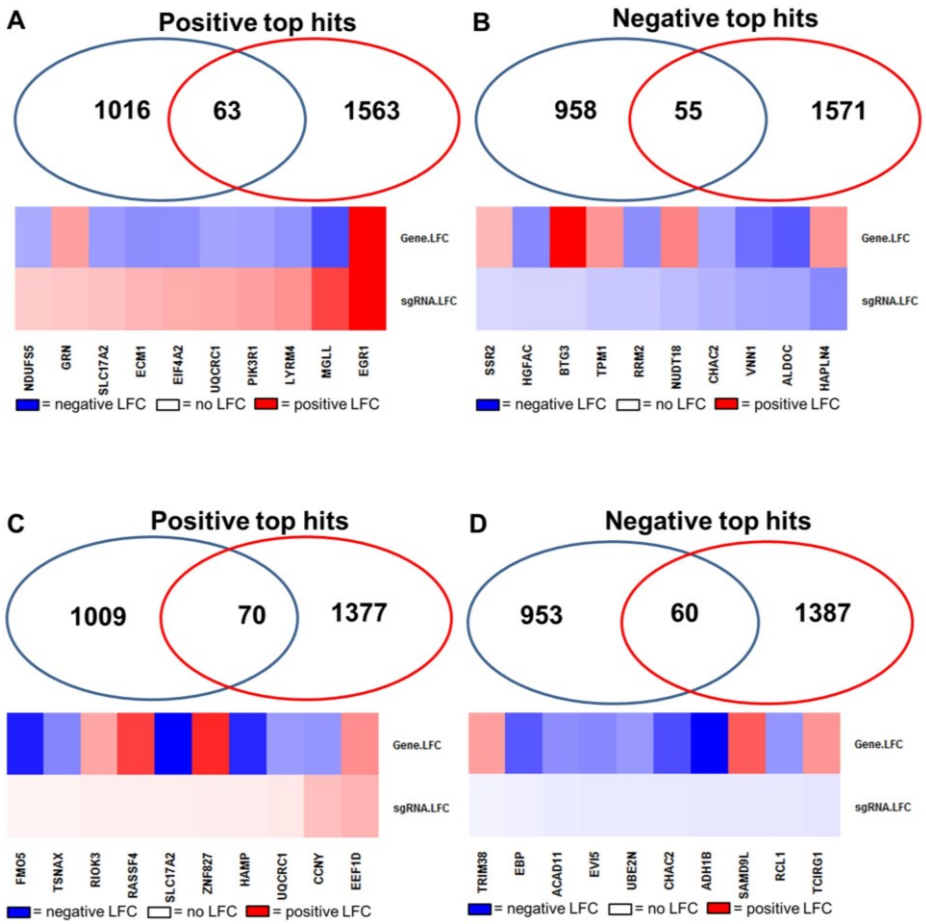

Figure 5 | Overlapping analysis of significant CRISPR/Cas9 screen with mouse ALI (GSE110787) and human ALF gene expression data (GSE74000). A Overlap of top positive CRISPR/Cas9 screen hits ($p<0.05$) at 24h with mouse RNA-Seq top hits at 24h APAP treatment ($p<0.05$), with heat map of the differential $\log_2$ fold change of the top 10 genes with the most positively selected sgRNAs (left to right). **B** Overlap of top negative CRISPR/Cas9 screen hits ($p<0.05$) at 24h with mouse RNA-Seq top hits at 24h APAP treatment ($p<0.05$), with heat map of the differential $\log_2$ fold change of the top 10 genes with the most negatively selected sgRNAs (left to right). **C** Overlap of top positive CRISPR/Cas9 screen hits ($p<0.05$) at 24h with ALF microarray dataset GSE74000 top hits at 24h ($p<0.05$), with hea tmap of the differential $\log_2$ fold change of the top 10 genes with the most positively selected sgRNAs (left to right) GSE74000; ALF healthy liver sample microarray data. **D** Overlap of top negative CRISPR/Cas9 screen hits ($p<0.05$) at 24h with ALF microarray dataset GSE74000 top hits at 24h ($p<0.05$), with heat map of the differential $\log_2$ fold change of the top 10 genes with the most negatively selected sgRNAs (left to right).

Analysis of microarray of human blood from normal and acetaminophen-dosed participants

A second dataset, GSE70748 was chosen to filter genes identified in the CRISPR screen that have also been identified in blood in humans who have been dosed with APAP (supplementary table 23). In GEO2R, microarray data from 12 APAP responder blood samples were compared to 32 non-responders using days 1 and 8 independently (GSE70784). This data represents a population of individuals who were dosed with APAP over a course of days, during that blood was collected daily. No probes had an FDR-adjusted p-value <0.05, so the unadjusted p-values were referenced. After 1 day of APAP dosing 362 of 20,173 probes have an unadjusted p-value <0.05, of that 148 probes have – $\log_2$ fold change with p<0.05 and 214 probes have + $\log_2$ fold change with P<0.05 (supplementary figure 4 A). After 8 days of APAP dosing 2445 of 20,173 probes had an unadjusted p-value <0.05, of that 314 probes have – $\log_2$ fold change with p<0.05 and 2,131 probes have + $\log_2$ fold change with P<0.05 (supplementary figure 4 B). We compared genes with p<0.05 to genes that were significantly enriched and depleted in our CRISPR screen (p<0.05) to identify overlap and ascertain the relationship between sgRNA depletion or enrichment and gene expression (figure 6 A-D).

Using the same GSE70784 dataset in GEO2R, microarray data from 12 APAP responder blood samples were compared to 10 placebo controls using days 1 and 8 independently. After 1 day of APAP dosing 697 of 20,173 probes had an unadjusted p-value <0.05. Of these, 244 probes have – $\log_2$ fold change with p<0.05 and 453 probes have + $\log_2$ fold change with P<0.05 (supplementary figure 4 C). After 8 days of APAP

dosing 1,801 of 20,173 probes had an unadjusted p-value <0.05, of that 1248 probes have – $\log_2$ fold change with $p<0.05$ and 553 probes have + $\log_2$ fold change with $P<0.05$ (supplementary figure 4 D). We compared genes with $p<0.05$ to genes that were significantly enriched and depleted in our CRISPR screen ($p<0.05$) to identify overlap and ascertain the relationship between sgRNA depletion or enrichment and gene expression (figure 6 E-H).

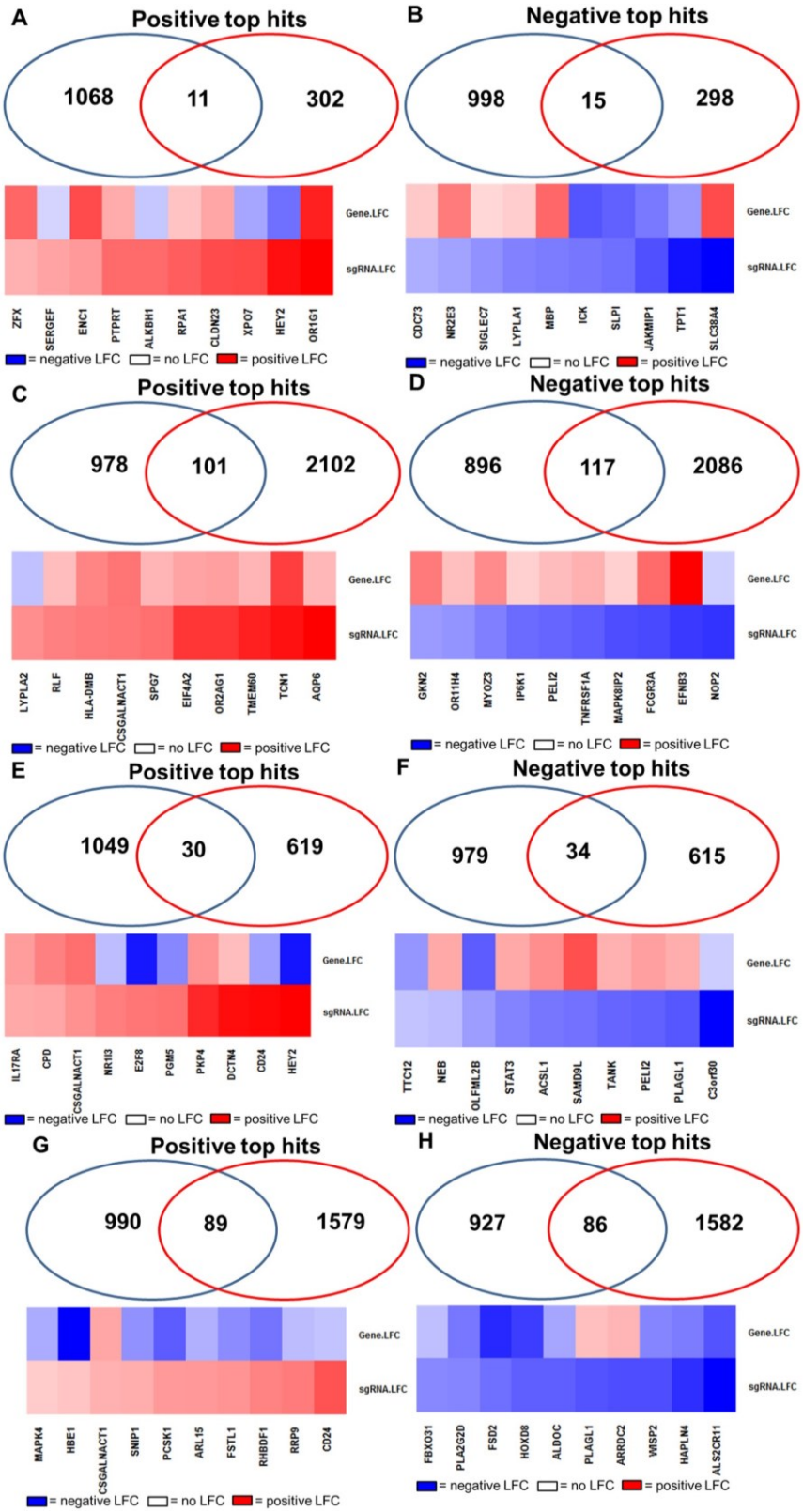

Figure 6 | Overlapping analysis of significant CRISPR/Cas9 screen hits with human ALI gene expression data (GSE70784). A Top positive CRISPR/Cas9 screen hits

($p<0.05$) at 24h overlapping APAP overdose microarray dataset GSE70784 responders vs. Non-responders (1 day) ($p<0.05$). Heat map of differential log_2 fold change of the top 10 genes with the most positively selected sgRNAs (left to right). **B** Top negative CRISPR/Cas9 screen hits ($p<0.05$) at 24h overlapping APAP overdose microarray dataset GSE70784 responders vs. Non-responders (1 day) ($p<0.05$). Heat map of differential log_2 fold change of the top 10 genes with the most negatively selected sgRNAs (left to right). **C** Top positive CRISPR/Cas9 screen hits ($p<0.05$) at 24h overlapping APAP overdose microarray dataset GSE70784 responders vs. Non-responders (8 days) ($p<0.05$). Heat map of differential log_2 fold change of the top 10 genes with the most positively selected sgRNAs (left to right). **D** Top negative CRISPR/Cas9 screen hits ($p<0.05$) at 24h overlapping APAP overdose microarray dataset GSE70784 responders vs. Non-responders (8 days) ($p<0.05$). Heat map of differential log_2 fold change of the top 10 genes with the most negatively selected sgRNAs (left to right). **E** Top positive CRISPR/Cas9 screen hits($p<0.05$) at 24h overlapping APAP overdose microarray dataset GSE70784 responders vs. Placebo (1 day) ($p<0.05$). Heatmap of differential log_2 fold change of the top 10 genes with the most positively selected sgRNAs (left to right). **F** Top negative CRISPR/Cas9 screen hits ($p<0.05$) at 24h overlapping APAP overdose microarray dataset GSE70784 responders vs. Placebo (1 day) ($p<0.05$). Heatmap of differential log_2 fold change of the top 10 genes with the most negatively selected sgRNAs (left to right). **G** Top positive CRISPR/Cas9 screen hits ($p<0.05$) at 24h overlapping APAP overdose microarray dataset GSE70784 responders vs. Placebo (8 days) ($p<0.05$). Heatmap of differential log_2 fold change of the top 10 genes with the most positively selected sgRNAs (left to right). **H** Top negative CRISPR/Cas9 screen hits ($p<0.05$) at 24h overlapping APAP overdose microarray dataset GSE70784 responders vs. Placebo (8 days) ($p<0.05$). Heatmap of differential log_2 fold change of the top 10 genes with the most negatively selected sgRNAs (left to right).

Identification of candidate genes from the overlapping gene sets

We then isolated only genes (or gene knockouts in the case of the CRISPR screen) that were significantly differentially expressed across the CRISPR, mouse, and human studies. 523 genes (369 unique) overlapped the mouse RNA-seq GSE110787 and CRISPR "top lists" (4d, 24h, Int, and All, $p<0.05$). 57 of the 67 unique genes overlapping CRISPR, Mouse, and GSE74000 $p<0.05$ lists were not previously reported to have a role in APAP metabolism, and 51/67 had consistent expression in mouse and GSE74000 and within CRISPR lists. When we compared the GSE70784 1 day responder vs. placebo to the

CRISPR and mouse RNA-seq datasets, 12 of the 16 overlapping unique genes were novel ($p<0.05$ overlap the main CRISPR analyses and the mouse RNA-seq) and 10 of the 16 had consistent expression between CRISPR analysis or between gene expression dataset. When we compared the GSE70784 8 day responder vs. placebo to CRISPR/Cas9 and mouse datasets 36 of the 38 overlapping unique genes were novel ($p<0.05$ overlap the main CRISPR analyses and the mouse RNA-seq) and 22 of the 38 have consistent expression between CRISPR analysis or between gene expression dataset The largest overlap with the CRISPR/Cas9 screen data was observed with the GSE70784 8d day responder vs. non-responder dataset (supplementary table 24). A number of the genes with significantly differential expression in the *in vivo* datasets had known relationships with APAP (top 100 genes per data set, analyzed using PubMatrix), although as previously seen with the CRISPR screen, many are novel findings (supplementary table 25).

Discussion

The analysis method used to rank genes from the genome-wide CRIPSR-Cas9 screen based significance and rank on a combination of highly differential sgRNA counts that are consistent across a gene. However it is still possible that the genes identified by this method may have poor clinical utility. To better identify genes that could have good utility as biomarkers, we cross-referenced 3 different studies of APAP-induced liver injury and failure.

The 3 gene expression datasets all used distinct sampling methodologies, that when combined, produced a comprehensive picture of changes in gene expression after APAP

overdose. GSE70784 consists of blood samples from participants that are dosed with the daily maximum of APAP daily for an extended time. These data reflect a more chronic drug exposure, and response to the drug is measured by ALT. GSE74000 consisted of liver biopsies from Livers being replaced after APAP-induced ALF and liver biopsies obtained from non-ALF donors. This dataset, although it contains few samples, represents differential gene expression in humans at the 4d-point of the disease. The mouse RNA-seq data GSE110787 provided an extremely controlled population with controlled APAP dosage, avoiding issues of inter-population variabilities that may affect studies in human populations.

This approach addresses APAP-induced liver injury in 2 distinct ways. First, we identified genes with a role in APAP metabolism by assessing the effect of gene knockouts on cell proliferation and survival. Next, we identified genes that were differentially expressed in response to APAP. The combination helps us to build hypotheses about the role of these genes in the disease process. This cross-validation with other APAP datasets is targeted at identifying genes that are important to APAP metabolism and may be novel diagnostic or therapeutic biomarkers. Genes that are highly ranked in the CRISPR screen ($p<0.05$) and whose RNA are expressed differentially at high enough levels that a blood sample (preferable) or liver biopsy (less preferable) could be used to detect changes in expression levels resultant from APAP overdose rapidly in clinic. Novel genes identified by this method that were highly ranked in the CRIPSR-Cas9 screen and in the gene expression data are the strongest candidates for further study. This method of candidate gene discovery was validated by the presence of genes that

already have known association with APAP metabolism among the top candidate genes. Selection of specific candidate genes is discussed in more detail in chapter 8.

CHAPTER 7

RESULTS PART 3

Acetaminophen-associated single nucleotide polymorphisms in the literature

We explored the candidate gene and genome-wide approaches that have identified 147 SNPs associated with either protection against or susceptibility to acetaminophen-induced hepatotoxicity (supplementary table 26). We then provided a reanalysis of the published SNP data using *in silico* tools to further uncover the biological relevance of the coding and non-coding variants (Heruth *et. al*. 2018, under review).

Court et al. evaluated the association with acetaminophen-induced hepatotoxicity in a panel of polymorphisms from genes encoding known acetaminophen metabolizing enzymes, including *UGT1A*, *UGT1A1*, *UGT1A6*, *UGT1A9*, *UGT2B15*, *SULTA1*, *CYP2E1*, and *CYP3A5* [50]. They also analyzed a polymorphism in *CD44* that associated with elevated serum alanine aminotransferase (ALT) levels in healthy volunteers who consumed the maximum recommended dose of acetaminophen for up to 2 weeks [37-38]. Three genes, *CYP3A5*, *UGT1A*, and *CD44*, contained SNPs with relatively weak associations with acetaminophen-induced liver injury in an Acute Liver Failure Study Group cohort of 260 Caucasian individuals that consists of 78 patients with intentional acetaminophen-overdose, 79 patients with unintentional acetaminophen-overdose, and 103 patients with ALF due to non-acetaminophen associated causes.

Moyer et al. utilized a human variation panel of 176 lymphoblastoid cell lines (HVP-LC) established from healthy donors [43]. The growth inhibitory effect of NAPQI

(IC_{50}) was determined for each cell line following 24 hours of treatment with 7 doses (0-100μM) of NAPQI. Initially, Moyer et al. examined the association of 716 SNPs, located in 31 GSH pathway genes, with NAPQI-IC_{50}. Moyer et al. extended their study to a genome-wide SNP analysis in that 1,008,202 SNPs were screened for association with NAPQI-IC_{50}.To identify SNPs associated with NAPQI-induced hepatotoxicity, GWAS was performed using Illumina Infinium HumanHap 550K and 510S bead chips and Affymetrix 6.0 GeneChips.

Two studies by Harrill et al. [38, 66] identified potential susceptibility targets using a panel of 36 inbred mouse strains to model genetic diversity. Fasting mice were treated with 300 mg/kg acetaminophen by intragastric dosing. Food was reintroduced after three hours of acetaminophen dosing. After 24 hours the mice were euthanized for analysis. The extent of liver injury was quantified by serum ALT levels. Haplotype-associated mapping and targeted sequencing were used to evaluate relationships of polymorphisms with ALT. Harrill *et al.* also performed mRNA microarray analyses on an Agilent Mouse Toxicology Array (#4121A) to identify gene expression biomarkers for acetaminophen hepatotoxicity in their panel of 36 inbred mouse strains [66].

To begin to understand the molecular mechanisms by that SNPs associate with a disease state, it is important to analyze the data at the gene level [121]. Here we analyzed coding and non-coding genes that contain or nearest neighbors to SNPs that have a significant association with acetaminophen sensitivity (supplementary tables 27-28). Genes positioned outside of protein-coding genes may be positioned in regulatory elements that have functional consequences on nearby genes. In total, Refseq, GENCODE, and Ensembl annotations predicted the 147 SNPs to be in or nearest neighbor to a combined 97

unique genes, including 60 protein-coding genes and 37 non-coding RNA genes. The newly compiled data are presented in supplementary tables 26-31.

Functional *in silico* analyses of SNPs associated with acetaminophen-induced hepatotoxicity

Analysis with HaploReg 4.1 (RefSeq) classified 84 intergenic and 63 intragenic SNPs, with 58 of the intragenic SNPs annotated functionally as 5'-UTR, intronic, or 3'-UTR (supplementary table 29). GENCODE annotation identified 79 and 68 intergenic and intragenic SNPs, respectively. 71 SNPs (48.3%) are associated with two or more transcripts, while 21 (14.3%) are within a single transcript (supplementary table 27). 55 SNPs (38.2%) are not located within a known transcript. 7 SNPs are located in the proximity of 5 miRNAs. In total, 58 SNPs are within or in the proximity of non-coding RNA genes.

Interestingly, several of the SNPs overlap regulatory regions including promoter and enhancer histone marks, DNases, and bound proteins. Several of the SNPs are predicted to alter TF binding sites (Supplementary Table 29). Genome Wide Annotation of VAriants (GWAVA) was used to score the functional relevance of the 147 SNPs (supplementary table 30) [111]. Five of the SNPs (rs2031920, rs8330, rs2524290, rs10929303 and rs1042640) have a high functional significance prediction using a model that accounts for nearby transcriptional start sites (TSS score >0.7) [122]. These predictions support the previous findings that rs2031920 and rs8330 effect the transcriptional regulation of CYP2E1 and UGT1A, respectively [48-49]. rs2524290 is located in the promoter region of

RAB3IL1, that encodes RAB3A Interacting Protein Like 1, a guanine nucleotide exchange factor. rs10929303 and rs1042640 are located in the 3' UTR of *UGT1A1* but are predicted to disrupt protein binding motifs. An additional 20 SNPs have a moderate functional significance with a TSS score >0.4. Further investigation of these SNPs is warranted to determine the roles of these potential regulatory regions and the corresponding genes in acetaminophen-induced hepatotoxicity.

The 72 protein-coding genes were assessed further for functional associations using Ingenuity Pathway Analysis (IPA)[123] in 2 steps. First, the 44 protein-coding genes corresponding to 84 intragenic SNPs were analyzed for biological significance. Next, following the lead of Zhang and Lupski [124], the list was expanded to include the 28 protein-coding genes that were nearest to the 63 intergenic SNPs. Inclusion of the additional genes enhanced the predicted associations with several canonical pathways that play a key role in hepatotoxicity and drug metabolism. The number of genes associated with *Glutathione redox reactions I*, *Xenobiotic metabolism signaling*, *LPS/IL-1 mediated inhibition of RXR function* and *Glutathione Biosynthesis* were enriched significantly when the intragenic SNPs were included in the analysis (table 2).

Table 2: Top canonical pathways predicted by Ingenuity Pathway Analysis.

Pathway*	Ratio of 44 genes containing SNPs#	P-value	Ratio of 72 genes containing or near SNPs&	P-value
Glutathione Redox Reactions I	8.33E-02	1.07E-03	2.50E-01	1.21E-10
Xenobiotic Metabolism Signaling	2.41E-02	1.68E-06	3.79E-02	2.32E-09
LPS/IL-1 Mediated Inhibition of RXR Function	2.25E-02	8.13E-05	3.15E-02	7.71E-06
Nicotine Degradation III	7.27E-02	4.50E-06	7.27E-02	3.06E-05
Glutathione Biosynthesis	NA	NA	6.67E-01	3.11E-05

*, Top 5 pathways for ratio of genes containing or near SNPs
#, number of genes with intragenic SNPs divided by total genes in the pathway
&, number of genes with intragenic and intergenic SNPs divided by total number of genes in pathway
NA, not applicable, no genes discovered in the pathway

For example, the *Glutathione redox reactions I* pathway included two genes (*GPX2* and *GSTP1*) with intragenic SNPs and an additional four genes (*GPX3*, *GSTA1*, *GPX4*, *GPX7*) near intergenic SNPs, while *Glutathione Biosynthesis* included no genes with intragenic SNPs and two genes (*GCLC*, *GSS*) near intragenic SNPs. As evidence that the enriched associations were not a random result of including an increased number of genes, the *Nicotine degradation III* pathway was not altered when the additional 28 genes were included in the analysis. The number of genes associated with Diseases and Disorders also increased significantly when both the intragenic and intergenic SNPs were considered (table 3).

Table 3: Top diseases and disorders predicted by Ingenuity Pathway Analysis.

Diseases and Disorders*	Genes#	Range of P-values#	Genes&	Range of P-values&
Metabolic Disease	6	6.02E-03 - 8.44E-06	13	9.70E-03 - 4.74E-07
Gastrointestinal Disease	39	1.00E-02 - 6.06E-06	63	9.70E-03 - 4.37E-06
Hepatic System Disease	25	1.00E-02 - 6.06E-06	39	9.70E-03 - 4.37E-06
Organismal Injury and Abnormalities	41	1.00E-02 - 6.06E-06	67	9.70E-03 - 4.37E-06
Inflammatory Disease	12	8.02E-03 - 2.67E-05	14	7.17E-03 - 1.29E-05

*, Top 5 diseases and disorders for combined genes with intragenic and intergenic SNPs
#, number of genes containing intragenic SNPs
&, number of genes containing intragenic and intergenic SNPs

Remarkably, 24 and 26 of the 28 protein-coding genes nearest to intragenic SNPs were associated with *Gastrointestinal Disease* and *Organismal Injury and Abnormalities*, respectively. These observations suggest strongly that the intragenic SNPs play a significant role in regulating cellular and molecular functions associated with acetaminophen-induced hepatotoxicity.

To determine what genetic associations have already been identified, a PubMatrix literature query [110] of the 72 protein-coding genes (supplementary table 29) against the terms “acetaminophen,” “disease,” “drug,” “hepatotoxicity,” “liver” and “metabolism” revealed that 56 and 55 of the genes have not been associated previously with “acetaminophen” or “hepatotoxicity,” respectively. Conversely, 67 and 51 genes have been linked previously to “disease” and “liver” (supplementary table 31).

We then cross-referenced the genes containing the147 APAP-associated SNPs with the findings of the genome-wide CRISPR/Cas9 knockout screen of APAP hepatotoxicity. 133 gene names were identified from the literature as nearest-neighbors or containing the 147 APAP injury-associated single nucleotide polymorphisms (SNPs). Of the genes

containing the 147 SNPs, 22 of the 133 gene names identified from RefSeq, GENCODE, and Ensembl (non-coding RNA genes) were significantly enriched or depleted in the CRISPR/Cas9 screen time points ($p<0.05$) (supplementary table 32, Shortt *et. al*. 2018, under review). Interestingly, ALCAM and RAP1GAP2 knockouts were both highly ranked at 4d and across all time points ($p<0.05$, enriched and depleted, respectively) of the CRISPR/Cas9 knockout screen. GSS and CPA6 knockouts were both highly ranked at 24h and across early time points (30min-24h) ($p<0.05$, enriched and depleted, respectively). STAB1 knockout was not significantly enriched at 24h or 4d, but emerged as significantly enriched across early time points (30min-24h, $p<0.05$) and all time points (30min-4d, $p<0.05$). These findings, in combination with known APAP-associated polymorphisms in these genes, suggest a direct role of these genes in APAP-induced liver injury.

Discussion

Non-coding SNPs (SNPs not located in a protein encoding gene) are commonly identified in GWAS, but have been under studied because of the difficulty in elucidating their biological function. Non-coding SNPs may be in linkage disequilibrium with the causal coding variant(s), however it is also possible they are positioned within regulatory regions, such as chromatin marks, enhancer elements, and DNase hypersensitivity regions, that have functional consequences on nearby genes [124]. They may also be located in non-protein encoding genes. Non-coding RNA genes produce functional RNAs (e.g., LINC, antisense, snRNA, miRNA) rather than mRNAs that encode proteins. Non-coding RNAs are associated with multiple biological functions, including the regulation of transcription,

mRNA processing, and translation [125]. Although several miRNAs have been associated with liver injury [126] and the interaction with 3'UTR SNPs [127], the mechanisms by which the non-coding RNA influence acetaminophen-induced hepatotoxicity remain to be elucidated further.

HaploReg 4.1, GWAVA, Ingenuity Pathway and PubMatrix analyses complement the genetic association studies and supports the need for further investigation into the biological processes and regulatory roles effected by the SNPs and the corresponding genes discussed here. The non-coding RNA genes described above have not been linked previously to APAP-induced hepatotoxicity. Interestingly, several of the SNPs overlap regulatory regions including promoter and enhancer histone marks, DNases, and bound proteins (supplementary table 29). Several of the SNPs are predicted to alter TF binding sites.

The pathways and networks obtained from the smaller, intragenic gene list, along with the expanded set that incorporates nearest neighbor intergenic SNP genes, support the idea that noncoding, intergenic SNPs may hold important predictive value when considering APAP-induced hepatotoxicity. In summary, similar pathways were predicted with the expanded gene list but with increased significance.

Although the application of genetic information has not yet been applied formally to acetaminophen dosing, the studies presented here provide the foundation for critical translational research in DILI. The identification of SNPs associated with a significant risk for acetaminophen-induced hepatotoxicity will provide potential targets for improved prognosis, prevention, and treatment. However, there remains very little human data investigating acetaminophen-induced hepatotoxicity. The majority of data has been

generated using either *in vitro* or animal models. The studies reviewed in this article provide a strong starting point for the validation of these findings and the further investigation of potentially promising acetaminophen susceptible biomarkers. The *in silico* analyses suggest that these 147 SNPs are present at biologically significant locations that may regulated and modify biological functions, including gene expression and alternative splicing. In addition, the identification of 41 novel non-coding RNA genes provides intriguing targets for further exploration.

Ultimately, these 147 SNPs will have to be examined experimentally to determine if they are intricately involved in acetaminophen metabolism or simply false-positives due to experimental limitations. The SNPs that were also identified in the CRISPR/Cas9 screen are extremely promising candidates for further evaluation. Further study of the polymorphisms in these genes could result in a diagnostic or prognostics SNP panel. Further study of the role of these genes could inform their use in targeted therapies.

The identification of SNPs associated with acetaminophen-induced hepatotoxicity will provide novel insights into the mechanisms of acetaminophen metabolism and the potential for therapeutic interventions. Additional GWAS studies, including whole genome sequencing and SNP-array assays, on larger cohorts of acetaminophen-induced ALI or ALF, and the inclusion of control populations that ingested the same dose of acetaminophen but did not develop ALI or ALF, are critical for the identification of additional biomarkers. Furthermore, the complex, and perhaps redundant, biochemical metabolism of acetaminophen in the liver suggests that it might be necessary to perform multi-loci, transcriptomic, or epigenetic analyses to identify regions associated with acetaminophen-induced hepatotoxicity rather than a single polymorphic allele.

CHAPTER 8

RESULTS PART 4

Validation of screening strategy

We considered genes for functional validation that were in the top 10 of a CRISPR list and were also significantly differentially expressed in the GEO or mouse RNA-seq datasets ($p<0.05$), with a preference for genes with a $p<0.05$ in multiple positive or negative ranked lists. Novelty was assessed by literature search and essentiality was determined from essentialgene.org. A number of genes that were highly ranked in the CRISPR screen (positive or negative) and overlapped with the other gene sets (human and mouse gene expression with and without APAP, $p<0.05$) are identified as essential genes (http://www.essentialgene.org/). These genes include PGM5, KIF23, C19orf60, BMPR1A, PDSS2, CXADR, SSR2, TMCC2, RDH13, and EGR1 (Supplementary Table 33). Additional genes that ranked highly in the CRISPR screen and overlapped with the other gene sets (human and mouse gene expression with and without APAP) have previously published relationships with APAP metabolism (pubmatrix.irp.nia.nih.gov). These genes include EGR1, VNN1, NR1I3. Genes that are highly ranked in our screen and previous publications support the selection method used to filter candidate genes. Novel, non-essential genes identified by this study for further study include LZTR1, NAAA, ATG2B, MYOZ3, EFNB3, OR5M11, FCGR3A, PROZ, EEF1D, ACAD11, and TMCC2 (supplementary table 33). These genes are pathogenic (positively ranked) or protective

(negatively ranked) and have potential for utility in development of diagnostic, risk-assessment, or therapeutic biomarkers.

Drug-gene interactions of candidate genes

Further analysis of top candidate genes described in this study (Supplementary Tables 21, 32, 33) identified a number of candidate drugs that may be suitable for re-purposing to treat APAP-induced hepatotoxicity. Of the 54 unique candidate genes that were analyzed, 153 drug-gene interactions were identified for 19 genes (supplementary table 34). Of these, 14 genes were annotated with drug-gene interactions of known effects (table 4).

Table 4: Top candidate genes with known drug effects annotated by the DRUG Gene Interaction Database (www.dgidb.org).

Gene	Gene Effect on ALF	Known Drug	Drug Effect	Drug Effect matches Gene Effect?
BMPR1A	susceptible (CRISPR screen)	CHEMBL3186227	inhibitor	yes
FCGR3A	protective (CRISPR screen)	GLOBULIN, IMMUNE	antagonist	no
NAAA	protective (CRISPR screen)	CARBENOXOLONE	inhibitor	no
NAAA	protective (CRISPR screen)	FLUFENAMIC ACID	inhibitor	no
NR1I3	susceptible (PMID: 12376703, and CRISPR screen)	PRASTERONE	activator	no
NR1I3	susceptible (PMID: 12376703, and CRISPR screen)	CHEMBL458603	agonist	no
NR1I3	susceptible (PMID: 12376703, and CRISPR screen)	CLOTRIMAZOLE	antagonist	yes
NR1I3	susceptible (PMID: 12376703, and CRISPR screen)	MECLIZINE	antagonist modulator	yes
PROZ	protective (CRIPSR screen)	MENADIONE	activator	yes
HSD11B1	susceptible (CRISPR screen)	CARBENOXOLONE	inhibitor	yes
HSD11B1	susceptible (CRISPR screen)	CHEMBL222670	inhibitor	yes
HSD11B1	susceptible (CRISPR screen)	CHEMBL2153191	inhibitor	yes
HSD11B1	susceptible (CRISPR screen)	CHEMBL2177609	inhibitor	yes
HSD11B1	susceptible (CRISPR screen)	PHENYLARSINE OXIDE	inhibitor	yes
HSD11B1	susceptible (CRISPR screen)	PREDNISONE	ligand	unknown
SIRT1	protective (PMID 29084443), susceptible (CRISPR screen)	CHEMBL257991	activator	unknown
SIRT1	protective (PMID 29084443), susceptible (CRISPR screen)	SODIUM LAURYL SULFATE	inhibitor	unknown
SIRT1	protective (PMID 29084443), susceptible (CRISPR screen)	CHEMBL420311	inhibitor	unknown
SIRT1	protective (PMID 29084443), susceptible (CRISPR screen)	SPLITOMICIN	inhibitor	unknown
SIRT3	susceptible (PMID 21720390, CRISPR screen)	SODIUM LAURYL SULFATE	inhibitor	yes
GPX2	protective (CRISPR screen)	GLUTATHIONE	cofactor	unknown
GPX4	protective (PMID 25962350), susceptible (CRISPR screen)	GLUTATHIONE	cofactor	unknown
GSS	protective (PMID 11287661), susceptible (CRISPR screen)	ACETYLCYSTEINE	stimulator	no
GSTP1	susceptible (PMID 11058152; CRIPSR screen)	EZATIOSTAT HYDROCHLORIDE	inhibitor	yes
KCNJ3	protective (CRISPR 4d), susceptible (CRISPR all APAP samples)	CHEMBL2409106	activator	unknown
KCNJ3	protective (CRISPR 4d), susceptible (CRISPR all APAP samples)	CHEMBL116590	channel blocker	unknown
KCNJ3	protective (CRISPR 4d), susceptible (CRISPR all APAP samples)	HALOTHANE	inhibitor	unknown
NAMPT	protective (Zhang *et al.* 2018, CRISPR screen)	TEGLARINAD CHLORIDE	inhibitor	no

Notably, 3 novel genes are targets of existing drugs that may be suitable re-purposed therapeutics against APAP-induced hepatotoxicity. BMPR1A, identified as a susceptible gene by the CRISPR/Cas9 screen, is inhibited by CHEMBL3186227. PROZ, identified as a protective gene by the CRISPR/Cas9 screen, is activated by Menadione. HSD11B1, a gene that was shown to be susceptible in the CRISPR/Cas9 screen, is inhibited by Carbenoloxone, CHEMBL222670, CHEMBL2153191, CHEMBL2177609, and Phenylarsine Oxide. An additional 3 genes, NR1I3, SIRT3, and GSTP1, have known roles in APAP hepatotoxicity that were correctly predicted by our CRIPSR-Cas9 screen and are targets of existing drugs that may be suitable for re-purposing[128-130]. These 6 genes are excellent candidate targets for re-purposing existing drugs to treat APAP-induced ALI and ALF. An additional 3 genes, SIRT1, GPX4, and GSS, were identified as targets of drugs with known gene interactions, however the CRISPR/Cas9 screen did not agree with the published gene role (protective or susceptible) in APAP-induced hepatotoxicity[131-133].

Functional validation of candidate genes

The screening strategy employed in the study resulted in the discovery of genes that were ranked among the 10 enriched or depleted knockouts at specific APAP treatment times or across the screen, and were also significantly enriched or depleted in APAP-treated gene expression data. From these genes, we selected LZTR1, PGM5, and NAAA for *in vitro* tests of gene knockdown. Lztr1, Nampt, Pgm5, and Naaa were knocked down

in vitro in primary mouse hepatocytes that were subsequently treated with and without APAP to assess relative changes in cellular survival.

Nampt knockdown by siRNA, measured by sqPCR, resulted in a significant decrease in cellular survival when compared with a scramble control after 3h APAP treatment (figure 7 A-B). Lztr1 knockdown by siRNA, measured by sqPCR, resulted in a significant increase in cellular survival when compared with a scramble control after 3h APAP treatment (figure 7 C-D). Pgm5 knockdown by siRNA resulted in a significant increase in cellular survival after 3h of APAP treatment when compared with the scrambled control (figure 7 E-F).

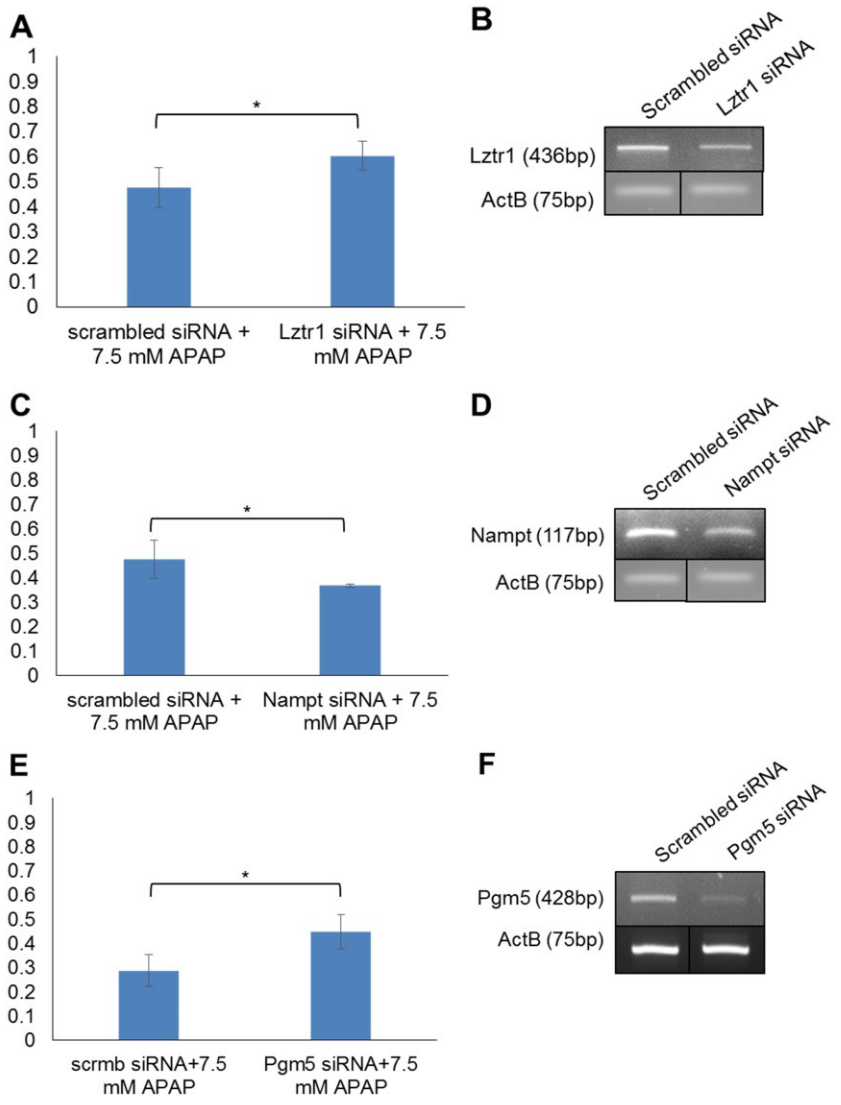

Figure 7 | Validation experiments in primary mouse hepatocytes. **A** Viability of primary mouse hepatocytes transfected with 25Mm scrambled or Lztr1 siRNA after treatment with 7.5mM APAP for 3h, normalized to Lztr1 siRNA transfected, untreated cells, measured by luminescent ATP assay. N=4 and error bars represent standard deviation. *, $p<0.05$. **B** sqPCR from cDNA prepared from RNA collected 25h post-transfection with 25Mm scrambled or Lztr1 siRNA. **C** Viability of primary mouse hepatocytes transfected with 25Mm scrambled or Nampt siRNA after treatment with 7.5mM APAP for 3h, normalized to Nampt siRNA transfected, untreated cells, measured by luminescent ATP assay. N=4 and error bars represent standard deviation. *, $p<0.05$. **D** sqPCR from cDNA prepared from RNA collected 25h post-transfection with 25Mm scrambled or Nampt siRNA. **E** Viability of primary mouse hepatocytes transfected with 50-100Mm scrambled or Pgm5 siRNA

after treatment with 7.5mM APAP for 3h, normalized to Pgm5 siRNA transfected, untreated cells, measured by luminescent ATP assay. N=4 and error bars represent standard deviation. *, $p<0.05$. **F** sqPCR from cDNA prepared from RNA collected 25h post-transfection with 50Mm scrambled or Pgm5 siRNA.

Although Naaa knockdown was confirmed, no effect on cellular survival of APAP was observed (data not shown). It is also possible that a complete NAAA knockout, rather than knockdown, is responsible for the protective effect and that low NAAA expression is enough for normal function. Overall, NAMPT, LZTR1, and PGM5 are strong candidate biomarkers of APAP-induced ALI and ALF. Additional studies are needed to confirm the roles of these genes in APAP-induced hepatotoxicity.

Discussion

Validation of the screen findings was sought at multiple steps in the analysis and by siRNA in primary hepatocytes. Inspection of the significant genes revealed overlap of the CRISPR/Cas9 knockout screen ($p<0.05$) with human microarray and mouse RNA-seq studies of APAP overdose ($p<0.05$). Several top genes identified from the screen for further study already had known associations with APAP in the literature. The presence of genes that are already known to be associated with acetaminophen hepatotoxicity in the overlap between the CRISPR/Cas9 gene knockouts and the expression datasets validates this method of candidate gene discovery.

Some of the genes identified from the screen for further study have been previously identified as essential. The presence of essential genes among the top candidates identified from both highly enriched and depleted gene knockouts suggests a number of essential

cellular functions may be affected by APAP overdose and toxicity. While these genes were not essential in our study, their relationship with APAP treatment would support their roles in critical cellular functions that, when disrupted, result in cell death.

We tested the effect of siRNA knockdown of *Lztr1*, *Nampt*, and *Pgm5* in primary mouse hepatocytes to validate our screen findings. We demonstrate that Leucine Zipper Like Transcription Regulator 1 (LZTR1) knockout and knockdown increase cellular survival of APAP-induced injury. LZTR1 has a positive LFC in the APAP-exposed human microarray data GSE70784, suggesting that the while the gene knockout increases survival of APAP, it is also elevated in APAP-treated subjects (supplementary table 29). LZTR1 mutations are associated with Noonan Syndrome 10, Schwannomatosis-2, gastric cancer, ventricular septal defects, and deletion of the gene may be associated with DiGeorge syndrome[134-138]. The GO annotations for LZTR1 include transcription factor activity and sequence-specific DNA binding. The protein localizes to the golgi, where it is thought to have a stabilizing effect.

Nicotinamide Phosphoribosyltransferase (NAMPT, PDB ID 4LVF.A) was selected for further study because although it is not significant in this screen, other lab data demonstrates a protective effect of overexpression against APAP-induced hepatotoxicity and Nampt has reduced expression in APAP-treated mice (LFC=-0.476, $p<0.05$)[105]. This in combination with the number of other NAD metabolism genes that are significantly ranked in this screen led us to validate the effect of NAMPT knockdown, which we found to increase susceptibility to APAP-induced injury. NAMPT protein is involved in the catalysis of the biosynthesis of the nicatinomide adenine dinucleotide. NAMPT's role in NAD salvage is thought to be important to a number of metabolism and aging-related

conditions[139-146]. It is involved in the NAD metabolism and Common Cytokine Receptor Gamma-Chain Family Signaling pathways. GO annotations include protein homodimerization activity and drug binding.

Phosphoglucomutase 5 (PGM5) knockdown increased cellular survival of APAP treatment, validating our CRISPR/Cas9 screen finding that knockout of the gene is protective. PGM5 has a negative LFC in the APAP-exposed human microarray data GSE70784, suggesting that the gene knockout increases survival of APAP exposure and gene expression is decreased after APAP exposure. PGM5 does not exhibit phosphoglucomutase activity and is a component of cell-cell and cell-matrix junctions. It is expressed at high levels in smooth muscle and is essential in the metabolism of galactose and glycogen and is involved in the Porphyrin and chlorophyll metabolism pathway. GO annotations include structural molecule activity, intramolecular transferase activity, and phosphotransferase activity. Abnormal expression and mutation of PGM5 are associated with a number of diseases, including Duchenne's Muscular Dystrophy and colorectal tumorigenesis, [147-148].

We attempted to validate the increased susceptibility of NAAA knockdown, however we were not able to reproduce this result in primary mouse hepatocytes. Although we were able to confirm knockdown of Naaa *in vitro*, we were not able to validate the increase in susceptibility observed in the CRISPR/CAS9 screen. It is possible that the effect is too small in the conditions used for the validation experiments. Further mechanistic studies are needed to evaluate the biological pathways in that these genes are acting to alter APAP metabolism. Further population studies of polymorphisms in these genes could yield susceptibility SNP panels. mRNA or protein expression of these genes, especially genes

that are also identified in GSE70784 in blood after APAP dosing, could have utility as biomarkers for diagnosis and prognosis.

To better control for potential differences in drug metabolism across systems and to identify the most promising candidate genes, the CRIPSR-Cas9 gene knockout rankings were cross-referenced with multiple human and mouse datasets to select the most promising candidate genes. We also identified genes with likely and known associations with APAP-induced hepatotoxicity (NAD metabolism and genes containing polymorphisms). These candidate genes were assessed for drugability by existing drugs as a means to more quickly bring forward new therapies. Indeed, 6 candidate genes (3 novel and 3 known) are targets for existing drugs that have an interaction predicted to be protective against APAP-induced hepatotoxicity.

CHAPTER 9

Conclusions

Collectively, this study has illustrated the power of a genome-wide CRISPR/Cas9 screen to systematically identify novel genes involved in APAP-induced hepatocyte toxicity and to provide potential new targets to develop novel therapeutic modalities. A negative selection screen for essential genes identified gene sets involved in fundamental processes, and a positive selection screen identified numerous genes potentially involved in pathogenic processes. These results inform the complex heterogenic nature of APAP toxicity and provide new targets for new mechanistic explorations and novel therapeutic modality developments. Combined with functional validations, this screening technique offers a robust and dynamic way to identify candidate genes for a variety of disease models. In this study we demonstrate that LZTR1 and PGM5 knockout and knockdown are protective against APAP–induced hepatotoxicity. Further experiments are warranted to evaluate the specific roles of these genes in the disease process.

The gene NAMPT is protective against APAP-induced ALI *in vivo*, although not identified directly by the sgRNA screen, we show knockdown increases susceptibility to APAP-induced hepatotoxicity. NAMPT has a known role in NAD salvage that warrants further study to identify if its protective effect is resultant of increased NAD supporting glutathione production and CYP function, or if it is protective by a novel mechanism.

These genes represent novel diagnostic and therapeutic targets for improving the care of acetaminophen overdose. Gene expression could be used to determine susceptibility

to APAP-hepatotoxicity as well diagnose and predict disease severity and outcome. Expression and function-associated variants in these genes could be used in risk-assessment genotyping panels. Furthermore, these genes represent novel biomarkers for personalized therapeutics. *In silico* analysis of candidate genes identified a number of the candidate genes that are targets for existing drugs. These existing drugs could be quickly re-purposed to treat and prevent APAP-induced ALF. Further studies are needed to better understand the functional role of the genes and pathways highlighted in this study.

Future Directions

This study identifies genetic components of acetaminophen-induced hepatocyte toxicity. Further studies are needed to better understand the functional role of the genes and pathways highlighted in this study. More validations in primary hepatocytes, animal models, patient populations and further investigation of the underlying molecular mechanisms are needed. Further research on the topic can include biological validation in cellular and mouse models, as well as in-depth study of the roles of the genes and pathways proposed in this study. Specifically, studies of the effects of overexpression of the functionally validated candidate genes in-vitro and of overexpression and knockdown/knockout in-vivo will further define the role of these genes. Larger-scale genome-wide studies as well as candidate gene approaches in human populations can contribute to our understanding of genetic variation that alters acetaminophen metabolism. Additional CRISPR/Cas9 knockout screening of non-coding RNAs associated with APAP-induced hepatotoxicity will advance our understanding of non-coding contributors to susceptibility to and pathogenesis of the disease process.

Possible implications of the study described here could include novel diagnostic and therapeutic targets or susceptibility and prognosis markers for acetaminophen-induced ALF. Drugable gene candidates also warrant further study as it is faster and cheaper to re-purpose existing drugs. This research has the potential to make a valuable contribution to the body of medical research by adding to our understanding of acute liver failure and acetaminophen metabolism. The findings in this study provide rich novel targets for further experimentation, which could lead to development of new and better diagnostic and therapeutic modalities to potentially enhance the frequency of good outcomes of acetaminophen-induced ALF.

APPENDIX A

SUPPLEMENTARY FIGURES

Supplementary Figure 1 | Amplicon sequencing strategy. The sequence of the sgRNA cassette labeled with the binding sites of the sequencing primers with different colors:pink, Illumina forward primer (P5 and seq); green, binding site of forward indexing primer; yellow, binding site of reverse indexing primer; red, Illumina reverse primer (seq); blue, Illumina P7 sequence.

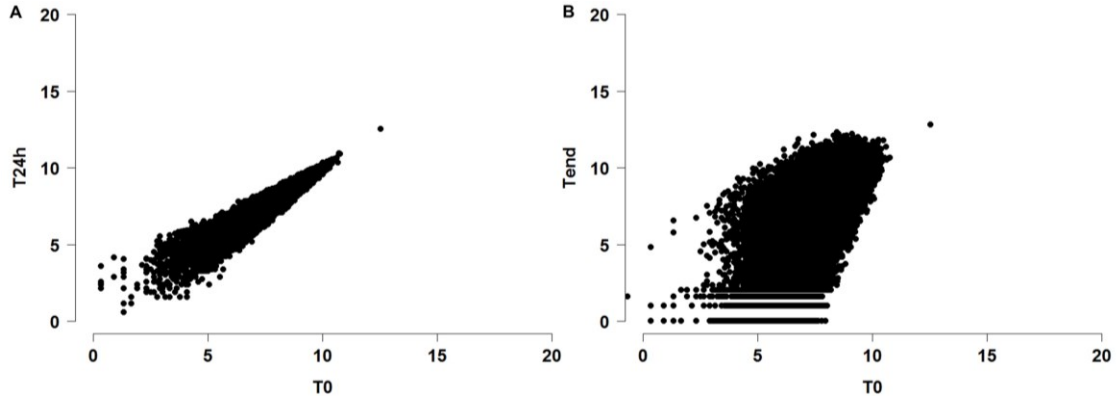

Supplementary Figure 2 | Scatterplots describing the distribution of read counts between samples. A Scatterplot showing enrichment and depletion of Log_2 sgRNA read counts after 24h APAP treatment. **B** Scatterplot showing enrichment and depletion of Log_2 sgRNA read counts after 4d APAP treatment and 21d outgrowth.

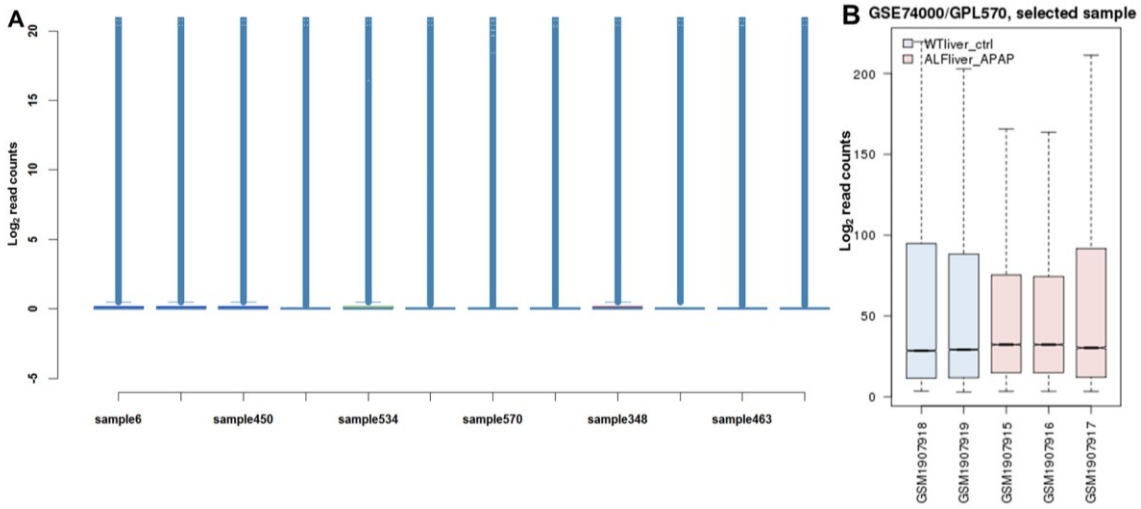

Supplementary Figure 3 | Box plots of mouse RNA-seq (GSE 110787) and human microarray samples (GSE74000) used to validate CRISPR/Cas9 screen hits. A Log_2 read counts of samples with and without APAP treatment from RNA-sequenced mice. **B** Log_2 read counts for GSE74000, healthy liver control and APAP overdose samples.

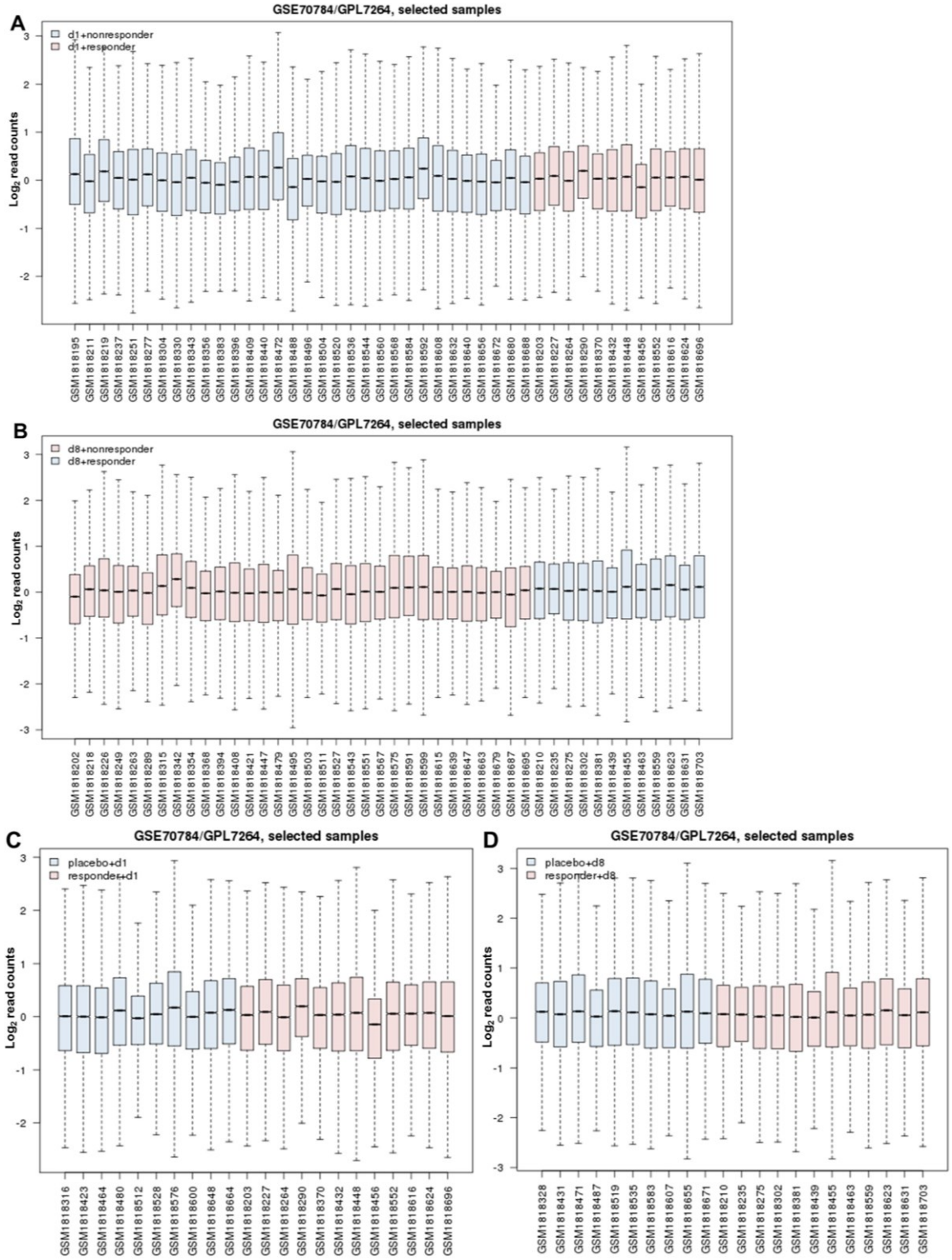

Supplementary Figure 4 | Box plots of human microarray samples (GSE70784) used to validate CRISPR/Cas9 screen hits. A Log_2 read counts from day 1 responder and nonresponder samples in GSE70784. **B** Log_2 read counts from day 8 responder and nonresponder samples in GSE70784. **C** Log_2 read counts from day 1 responder and placebo

samples in GSE70784. **D** Log_2 read counts from day 8 responder and placebo samples in GSE70784.

APPENDIX B

SUPPLEMENTARY TABLES

Supplementary Table 1: Primers used for sequencing, cloning, and sqPCR.

Name	Sequence	Details
PCR1 F1 primer	AATGGACTATCATATGCTTACCGTAACTTGAA AGTATTTCG	primer for readout PCR1
PCR1 R1 primer	CTTTAGTTTGTATGTCTGTTGCTATTATGTCTA CTATTCTTTCC	primer for readout PCR1
PCR2 F01	AATGATACGGCGACCACCGAGATCTACACTCT TTCCCTACACGACGCTCTTCCGATCTttcttgtggaaa ggacgaaacaccg	Illumina F (P5 & Illumina seq) with variable-length stagger for readout PCR2
PCR2 F02	AATGATACGGCGACCACCGAGATCTACACTCT TTCCCTACACGACGCTCTTCCGATCTattcttgtggaa aggacgaaacaccg	Illumina F (P5 & Illumina seq) with variable-length stagger for readout PCR2
PCR2 F03	AATGATACGGCGACCACCGAGATCTACACTCT TTCCCTACACGACGCTCTTCCGATCTgattcttgtgga aaggacgaaacaccg	Illumina F (P5 & Illumina seq) with variable-length stagger for readout PCR2
PCR2 F04	AATGATACGGCGACCACCGAGATCTACACTCT TTCCCTACACGACGCTCTTCCGATCTcgattcttgtgg aaaggacgaaacaccg	Illumina F (P5 & Illumina seq) with variable-length stagger for readout PCR2
PCR2 F05	AATGATACGGCGACCACCGAGATCTACACTCT TTCCCTACACGACGCTCTTCCGATCTtcgattcttgtg gaaaggacgaaacaccg	Illumina F (P5 & Illumina seq) with variable-length stagger for readout PCR2
PCR2 F06	AATGATACGGCGACCACCGAGATCTACACTCT TTCCCTACACGACGCTCTTCCGATCTatcgattcttgt ggaaaggacgaaacaccg	Illumina F (P5 & Illumina seq) with variable-length stagger for readout PCR2
PCR2 F07	AATGATACGGCGACCACCGAGATCTACACTCT TTCCCTACACGACGCTCTTCCGATCTgatcgattcttg tggaaaggacgaaacaccg	Illumina F (P5 & Illumina seq) with variable-length stagger for readout PCR2
PCR2 F08	AATGATACGGCGACCACCGAGATCTACACTCT TTCCCTACACGACGCTCTTCCGATCTcgatcgattctt gtggaaaggacgaaacaccg	Illumina F (P5 & Illumina seq) with variable-length stagger for readout PCR2
PCR2 F09	AATGATACGGCGACCACCGAGATCTACACTCT TTCCCTACACGACGCTCTTCCGATCTacgatcgattct tgtggaaaggacgaaacaccg	Illumina F (P5 & Illumina seq) with variable-length stagger for readout PCR2
PCR2 F10	AATGATACGGCGACCACCGAGATCTACACTCT TTCCCTACACGACGCTCTTCCGATCTttcttgtggaaa ggacgaaacaccg	Illumina F (P5 & Illumina seq) with variable-length stagger for readout PCR2
PCR2 F11	AATGATACGGCGACCACCGAGATCTACACTCT TTCCCTACACGACGCTCTTCCGATCTattcttgtggaa aggacgaaacaccg	Illumina F (P5 & Illumina seq) with variable-length stagger for readout PCR2
PCR2 F12	AATGATACGGCGACCACCGAGATCTACACTCT TTCCCTACACGACGCTCTTCCGATCTgattcttgtgga aaggacgaaacaccg	Illumina F (P5 & Illumina seq) with variable-length stagger for readout PCR2
PCR2 R01	CAAGCAGAAGACGGCATACGAGATAAGTAGA GGTGACTGGAGTTCAGACGTGTGCTCTTCCGA TCTctactattctttcccctgcactgt	Illumina R (P7 & Illumina seq) with barcode for readout PCR2

Supplementary Table 1. –Continued.

PCR2 R02	CAAGCAGAAGACGGCATACGAGATACACGAT CGTGACTGGAGTTCAGACGTGTGCTCTTCCGA TCTtctactattctttcccctgcactgt	Illumina R (P7 & Illumina seq) with barcode for readout PCR2
PCR2 R03	CAAGCAGAAGACGGCATACGAGATCGCGCGG TGTGACTGGAGTTCAGACGTGTGCTCTTCCGA TCTtctactattctttcccctgcactgt	Illumina R (P7 & Illumina seq) with barcode for readout PCR2
PCR2 R04	CAAGCAGAAGACGGCATACGAGATCATGATC GGTGACTGGAGTTCAGACGTGTGCTCTTCCGA TCTtctactattctttcccctgcactgt	Illumina R (P7 & Illumina seq) with barcode for readout PCR2
PCR2 R05	CAAGCAGAAGACGGCATACGAGATCGTTACC AGTGACTGGAGTTCAGACGTGTGCTCTTCCGA TCTtctactattctttcccctgcactgt	Illumina R (P7 & Illumina seq) with barcode for readout PCR2
PCR2 R06	CAAGCAGAAGACGGCATACGAGATTCCTTGGT GTGACTGGAGTTCAGACGTGTGCTCTTCCGAT CTtctactattctttcccctgcactgt	Illumina R (P7 & Illumina seq) with barcode for readout PCR2
PCR2 R07	CAAGCAGAAGACGGCATACGAGATAACGCAT TGTGACTGGAGTTCAGACGTGTGCTCTTCCGA TCTtctactattctttcccctgcactgt	Illumina R (P7 & Illumina seq) with barcode for readout PCR2
PCR2 R08	CAAGCAGAAGACGGCATACGAGATACAGGTA TGTGACTGGAGTTCAGACGTGTGCTCTTCCGA TCTtctactattctttcccctgcactgt	Illumina R (P7 & Illumina seq) with barcode for readout PCR2
PCR2 R09	CAAGCAGAAGACGGCATACGAGATAGGTAAG GGTGACTGGAGTTCAGACGTGTGCTCTTCCGA TCTtctactattctttcccctgcactgt	Illumina R (P7 & Illumina seq) with barcode for readout PCR2
PCR2 R10	CAAGCAGAAGACGGCATACGAGATAACAATG GGTGACTGGAGTTCAGACGTGTGCTCTTCCGA TCTtctactattctttcccctgcactgt	Illumina R (P7 & Illumina seq) with barcode for readout PCR2
PCR2 R11	CAAGCAGAAGACGGCATACGAGATACTGTATC GTGACTGGAGTTCAGACGTGTGCTCTTCCGAT CTtctactattctttcccctgcactgt	Illumina R (P7 & Illumina seq) with barcode for readout PCR2
PCR2 R12	CAAGCAGAAGACGGCATACGAGATAGGTCGC AGTGACTGGAGTTCAGACGTGTGCTCTTCCGA TCTtctactattctttcccctgcactgt	Illumina R (P7 & Illumina seq) with barcode for readout PCR2
Nampt-Mouse-F	TGGCGCTTTGCTACAGAAGT	mouse qPCR, amplicon position: exon 9-10 (CDS), length: 117
Nampt-Mouse-R	TTGGGATCAGCAACTGGGTC	mouse qPCR, amplicon position: exon 9-10 (CDS), length: 117
mLztr1-set8-F	GCCCGTTCTAGCTACTTTGAG	mouse qPCR, amplicon position: exon 17/18-21 (CDS), length: 436bp
mLztr1-set8-R	GCTTGTCAGAGATGTGGGAG	mouse qPCR, amplicon position: exon 17/18-21 (CDS), length: 436bp
mPgm5-set5-F	ACCGTTATATGATCCTTGGCC	mouse qPCR, amplicon position: exon 6-9 (CDS), length: 428bp
mPgm5-set5-R	CTCCAGTCCCTCGTAATCAAAC	mouse qPCR, amplicon position: exon 6-9 (CDS), length: 428bp
ActB-F	CTTTGCAGCTCCTTCGTTGC	mouse qPCR, amplicon position: 5'UTR-exon 1, length: 79bp
ActB-R	GTCGACGACCAGCGCA	mouse qPCR, amplicon position: 5'UTR-exon 1, length: 79bp

Supplementary Table 2: Alignment metrics for the CRISPR/Cas9 APAP screen.

Label	Total reads /sample	Total mapped reads /sample	Freq mapped genes /sample	Zerocounts /sample
Plasmid_rep1	46103448	35778757	0.78	1
Plasmid_rep2	47102021	37808035	0.80	0
T0_rep1	36989846	20480799	0.55	12
T0_rep2	45321323	36048480	0.80	2
T30min	36441473	24184285	0.66	15
T3h	42968606	34715794	0.81	2
T6h	41412350	33900076	0.82	5
T12h	35096028	27235534	0.78	4
24h_rep1	40517754	14730530	0.36	19
24h_rep2	40473783	32073043	0.79	2
4d_rep1	31545812	10868034	0.34	4957
4d_rep2	42953904	34098492	0.79	1257
Total_rep1	311075317	201893809	0.65	
Total_rep2	175851031	140028050	0.80	
Total	486926348	341921859	0.70	

Supplementary Table 3: Wilcoxon Rank-Sum Test p-values for the CCRISPR/Cas9 screen samples.

Label	Plasmid rep. 1	Plasmid rep. 2	T0 rep. 1	T0 rep. 2	T30min	T3h	T6h	T12h	24h rep. 1	24h rep. 2	4d rep. 1	4d rep. 2
Plasmid rep. 1	1.00E+00	9.59E-01	3.83E-03	2.47E-02	5.44E-03	1.96E-01	1.33E-01	1.07E-03	4.16E-01	3.92E-02	7.51E-211	2.63E-66
Plasmid rep. 2	9.59E-01	1.00E+00	4.07E-03	2.62E-02	6.13E-03	2.08E-01	1.39E-01	1.06E-03	3.92E-01	4.18E-02	1.77E-211	1.62E-66
T0 rep. 1	3.83E-03	4.07E-03	1.00E+00	5.44E-01	8.87E-01	1.34E-01	1.90E-01	5.91E-08	1.37E-03	4.05E-01	3.05E-198	1.86E-56
T0 rep. 2	2.47E-02	2.62E-02	5.44E-01	1.00E+00	6.37E-01	3.77E-01	4.69E-01	8.80E-07	8.69E-03	8.41E-01	1.58E-200	4.49E-58
T30min	5.44E-03	6.13E-03	8.87E-01	6.37E-01	1.00E+00	1.74E-01	2.31E-01	8.54E-08	2.25E-03	4.83E-01	4.59E-199	5.74E-57
T3h	1.96E-01	2.08E-01	1.34E-01	3.77E-01	1.74E-01	1.00E+00	8.52E-01	3.15E-05	6.26E-02	4.81E-01	7.40E-203	3.07E-60
T6h	1.33E-01	1.39E-01	1.90E-01	4.69E-01	2.31E-01	8.52E-01	1.00E+00	1.55E-05	4.27E-02	6.03E-01	3.79E-203	1.23E-59
T12h	1.07E-03	1.06E-03	5.91E-08	8.80E-07	8.54E-08	3.15E-05	1.55E-05	1.00E+00	2.23E-02	1.38E-06	2.95E-218	5.30E-70
24h rep. 1	4.16E-01	3.92E-01	1.37E-03	8.69E-03	2.25E-03	6.26E-02	4.27E-02	2.23E-02	1.00E+00	1.22E-02	3.81E-206	1.74E-62
24h rep. 2	3.92E-02	4.18E-02	4.05E-01	8.41E-01	4.83E-01	4.81E-01	6.03E-01	1.38E-06	1.22E-02	1.00E+00	8.10E-203	1.49E-58
4d rep. 1	7.51E-211	1.77E-211	3.05E-198	1.58E-200	4.59E-199	7.40E-203	3.79E-203	2.95E-218	3.81E-206	8.10E-203	1.00E+00	3.50E-73
4d rep. 2	2.63E-66	1.62E-66	1.86E-56	4.49E-58	5.74E-57	3.07E-60	1.23E-59	5.30E-70	1.74E-62	1.49E-58	3.50E-73	1.00E+00

Supplementary Table 4: Enriched gene knockouts ranked by RRA analysis of the CRISPR/Cas9 screen 30min-4d APAP treatment vs. T0.

ID	sgRNA	Pos score	Pos p-value	Pos rank	Pos good sgRNA	Pos lfc
PDSS2	6	7.75E-06	5.56E-05	1	3	0.9457
KIF23	6	1.48E-05	9.76E-05	2	4	0.59281
hsa-mir-4484	4	1.70E-05	6.71E-05	3	1	2.9828
CXADR	6	1.70E-05	0.0001077	4	5	0.60028
CNNM1	6	2.77E-05	0.00016466	5	4	0.55475
PGM5	6	3.84E-05	0.0002207	6	5	0.56592
NR1I3	6	5.27E-05	0.0002802	7	5	0.45067
RS1	6	7.11E-05	0.00035216	8	2	0.80817
CCDC51	6	7.66E-05	0.00036968	9	1	1.4295
NEK4	6	8.26E-05	0.00040059	10	4	0.6183
TM4SF5	6	9.81E-05	0.00047669	11	2	0.74329
NETO1	6	0.00011428	0.00055141	12	5	0.35556
WFIKKN2	6	0.00011712	0.00056617	13	2	0.94383
GLYATL3	6	0.00012513	0.00059385	14	3	0.64176
CTNND2	6	0.00012767	0.00060815	15	2	1.1465
RXFP1	6	0.00013562	0.00064689	16	4	0.47969
hsa-mir-3667	4	0.00015321	0.00061506	17	3	0.33794
PLP1	6	0.0001724	0.00081686	18	5	0.34928
CHST4	6	0.00017874	0.00084753	19	1	1.4723
TMEM229B	6	0.00018836	0.00089642	20	4	0.61343
KPNA7	6	0.00022854	0.0010532	21	4	0.48639
GUCY2F	6	0.00024923	0.0011469	22	3	0.71776
IQCE	6	0.00025408	0.0011686	23	4	0.47943
DET1	6	0.00026497	0.0012161	24	5	0.38933
TM2D2	6	0.00027997	0.0012876	25	2	0.75432
ZNF2	6	0.00028086	0.0012926	26	2	1.1893
TRIM37	6	0.00030257	0.0013793	27	3	0.55012
TMEM60	6	0.00030447	0.0013867	28	2	0.9665
XRN2	6	0.00032385	0.0014688	29	4	0.53972
PIGV	6	0.00033192	0.0015011	30	2	0.93384
HOXD12	6	0.00033951	0.0015343	31	2	0.87919
KHDRBS3	6	0.00034392	0.00155	32	5	0.39681
HTR3A	6	0.00035572	0.0016058	33	5	0.48482
SLITRK4	6	0.00036497	0.0016422	34	4	0.67464
RAB41	6	0.00037236	0.0016773	35	4	0.47937
TFIP11	6	0.00038298	0.001729	36	2	1.1676
CBFA2T3	6	0.00038485	0.0017359	37	4	0.45563
FAF2	6	0.00039675	0.0017862	39	4	0.38135
TRPV6	6	0.00039963	0.0017949	40	4	0.55701

Supplementary Table 5: Depleted gene knockouts ranked by RRA analysis of the CRISPR/Cas9 screen 30min-4d APAP treatment vs. T0.

ID	sgRNA	Neg score	Neg p-value	Neg rank	Neg good sgRNA	Neg lfc
PKD2	6	4.51E-06	3.25E-05	1	3	-1.5917
C19orf60	6	2.55E-05	0.00014829	2	1	-1.7353
HERC6	6	5.94E-05	0.00031526	3	4	-0.78428
KIAA1737	6	6.23E-05	0.00032633	4	5	-0.55801
SENP3	6	6.65E-05	0.00034524	5	3	-0.89267
TTC29	6	7.66E-05	0.00038168	6	2	-1.3568
AK7	6	0.00011033	0.00055187	7	5	-0.59964
hsa-mir-8088	4	0.00011567	0.00046239	8	4	-0.81305
TMCC2	6	0.00011568	0.00057079	9	5	-0.46257
HIST1H3I	6	0.00011761	0.00058047	10	4	-0.81016
C5orf34	6	0.00011854	0.00058508	11	3	-1.0994
CYB5B	6	0.00012767	0.00062014	12	3	-0.71493
H3F3B	6	0.00012922	0.0006289	13	3	-0.88598
TAT	6	0.00017355	0.00083369	14	3	-1.1348
GLB1L3	5	0.00017609	0.00083231	15	5	-0.38086
WDR25	6	0.00017874	0.0008586	16	2	-1.2777
OAZ1	6	0.0001804	0.0008669	17	5	-0.6531
CENPA	6	0.00018117	0.00087151	18	3	-0.79542
SSFA2	6	0.00018359	0.00088904	19	4	-0.71874
PEX11A	6	0.00018498	0.00089504	20	3	-0.7544
ANKRD13B	6	0.00019191	0.00092317	21	3	-1.0923
hsa-mir-6839	4	0.00019627	0.00076727	22	3	-0.88662
TIGD2	6	0.00019763	0.00094485	23	5	-0.58574
ADAMTS15	6	0.0002298	0.0010698	25	3	-1.479
SNRPD1	6	0.00024615	0.0011423	26	3	-1.1914
KLHL2	6	0.00025963	0.0012013	27	2	-0.92905
NUBPL	6	0.00027857	0.0012903	28	3	-1.0675
EIF4ENIF1	6	0.00028086	0.0013019	29	2	-1.1856
hsa-mir-498	4	0.00028087	0.0010814	30	2	-0.78968
MNX1	6	0.00028982	0.0013374	31	5	-0.43006
DICER1	6	0.00029364	0.0013554	32	3	-0.62626
KRT85	6	0.00033046	0.0015034	33	4	-0.77437
SMAP2	6	0.00033186	0.0015094	34	5	-0.34947
ADCY9	6	0.00033192	0.0015099	35	1	-1.2071
SSPO	6	0.00034304	0.0015525	36	5	-0.55715
hsa-mir-3929	4	0.00036053	0.0013849	37	3	-0.97941
ALPPL2	6	0.00036267	0.0016413	38	3	-0.81703
GPR107	6	0.00037868	0.0017128	39	5	-0.46629
RAB24	6	0.00038012	0.0017197	40	4	-0.87477

Supplementary Table 6: Enriched gene knockouts ranked by RRA analysis of the CRISPR/Cas9 screen 30min-24h APAP treatment vs. T0.

ID	sgRNA	Pos score	Pos p-value	Pos rank	Pos good sgRNA	Pos lfc
CATSPERD	6	1.20E-06	8.53E-06	1	4	0.87111
GATS	6	7.21E-06	5.14E-05	2	3	0.63212
OR10J5	6	7.55E-06	5.37E-05	3	5	0.4469
BMPR1A	6	1.64E-05	0.00010493	4	5	0.29969
hsa-mir-4484	4	1.70E-05	6.71E-05	5	1	2.6355
TIMP4	6	2.79E-05	0.0001672	6	3	0.67637
ESYT1	6	3.49E-05	0.00021148	7	4	0.51038
STYX	6	4.03E-05	0.00023408	8	6	0.32595
PGM5	6	5.68E-05	0.00031849	9	6	0.30323
hsa-mir-496	4	6.14E-05	0.00023869	10	4	0.26194
EMC8	6	7.55E-05	0.00040289	11	4	0.40301
LOC643669	6	7.66E-05	0.00040704	12	2	1.2731
RETNLB	6	9.00E-05	0.00048961	13	3	0.44105
RPL13A	6	9.15E-05	0.00049629	14	6	0.28236
AP5S1	6	9.57E-05	0.00052189	15	3	0.41817
RASSF4	6	9.60E-05	0.00052282	16	5	0.42009
AIM2	6	9.99E-05	0.00054496	17	5	0.46325
FRYL	6	0.0001017	0.0005551	18	5	0.37196
FAM194B	6	0.00010702	0.00058647	19	3	0.5383
MPV17L	6	0.00011014	0.00060538	20	2	0.93129
DCN	6	0.00012767	0.00069071	21	2	0.69049
NUCB1	6	0.00013616	0.00073775	22	6	0.20616
SLC43A1	6	0.0001527	0.00083139	24	4	0.38929
ATXN3L	6	0.00015596	0.00085214	25	6	0.21101
NDUFS5	6	0.00016076	0.00087705	26	6	0.30749
TM4SF5	6	0.00017361	0.00094762	27	3	0.49386
SESN2	6	0.00017874	0.00097898	28	4	0.19759
ITIH2	6	0.00018493	0.001021	29	6	0.20532
GSTP1	6	0.00019946	0.0010851	30	2	0.5513
TP53I13	6	0.00021365	0.0011575	31	6	0.24655
PFKFB1	6	0.0002298	0.001234	32	2	1.2147
FBXL20	6	0.00023294	0.0012525	33	5	0.28205
QRSL1	6	0.0002394	0.0012852	34	5	0.3129
NUDT2	6	0.00024602	0.0013171	35	5	0.24332
KHDRBS3	6	0.00024836	0.0013323	36	5	0.29467
CD55	6	0.00026429	0.0014185	37	3	0.42614
TES	6	0.00026491	0.0014218	38	3	0.51684
GLYATL3	6	0.00026678	0.0014296	39	3	0.44454
NR1I3	6	0.00028086	0.0014983	40	4	0.28284

Supplementary Table 7: Depleted gene knockouts ranked by RRA analysis of the CRISPR/Cas9 screen 30min-24h APAP treatment vs. T0.

ID	sgRNA	Neg score	Neg p-value	Neg rank	Neg good sgRNA	Neg lfc
PROZ	6	1.52E-05	9.85E-05	1	3	-0.55952
OR5M11	6	1.91E-05	0.00011739	2	4	-0.6621
FCGR3A	6	2.55E-05	0.00014829	3	3	-0.34113
C5orf47	6	6.10E-05	0.00033325	4	3	-0.52808
PKD2	6	7.66E-05	0.00040704	5	4	-0.58533
hsa-mir-4466	4	8.37E-05	0.00033279	6	4	-0.39367
SOHLH2	6	9.05E-05	0.00049191	7	3	-0.54426
NAAA	6	0.00010807	0.00059108	8	4	-0.50403
CIAPIN1	6	0.00012767	0.00069071	9	3	-0.2787
NR1D1	6	0.00013891	0.00075021	10	4	-0.5877
SH3D21	6	0.00014111	0.00076451	11	5	-0.55614
ZNF776	6	0.00015003	0.00082032	12	4	-0.67762
hsa-mir-3201	4	0.00016173	0.00064781	13	4	-0.36678
PPP1R26	6	0.00017838	0.0009776	14	6	-0.22734
PLXDC1	6	0.00017874	0.00097898	15	3	-0.4942
RASGEF1B	6	0.00020879	0.0011326	16	2	-0.72315
hsa-mir-4521	4	0.00022551	0.00088673	17	4	-0.37679
EFNB3	6	0.0002298	0.001234	18	2	-0.56097
hsa-mir-331	4	0.00024601	0.00095454	19	3	-0.45414
GAL3ST4	6	0.00024972	0.0013401	20	5	-0.36374
CCDC19	6	0.00028086	0.0015108	21	4	-0.37326
RAB3GAP2	6	0.00029997	0.0015989	22	5	-0.35747
CABIN1	6	0.00031478	0.0016755	23	3	-0.60778
PSRC1	6	0.00031826	0.0016902	24	4	-0.38892
SOX6	6	0.00033086	0.0017525	26	6	-0.22492
OLFM4	6	0.00033192	0.0017585	27	3	-0.49955
hsa-mir-4281	4	0.00035512	0.0013637	28	3	-0.86949
hsa-mir-8063	4	0.00035746	0.0013733	29	2	-0.68673
MUC4	6	0.00036599	0.0019231	30	4	-0.32442
HMMR	6	0.00036766	0.0019305	31	4	-0.36554
NLRP5	6	0.00037541	0.0019674	32	4	-0.3908
HSDL2	6	0.00037826	0.001979	33	5	-0.29211
CCDC169-SOHLH2	5	0.00037996	0.0017608	34	3	-0.40926
WRAP53	6	0.00038082	0.0019928	35	3	-0.40888
RCN3	6	0.00038277	0.0020016	36	3	-0.76598
AP4B1	6	0.00038298	0.002002	37	3	-0.32839
PPM1G	6	0.00038502	0.0020089	38	4	-0.37103
PXDN	6	0.00039281	0.0020417	39	5	-0.26842
SLC35D3	6	0.00039783	0.0020578	40	5	-0.307

Supplementary Table 8: Enriched gene knockouts ranked by RRA analysis of the CRISPR/Cas9 screen 30min APAP treatment vs. T0.

ID	sgRNA	Pos score	Pos p-value	Pos rank	Pos good sgRNA	Pos lfc
hsa-mir-629	4	1.31E-05	5.19E-05	1	2	1.1437
KAT7	6	1.93E-05	0.00011785	2	5	0.82194
SRSF1	6	2.55E-05	0.00014829	3	3	0.51229
CATSPERD	6	4.88E-05	0.00027744	4	4	0.95801
F8	6	5.54E-05	0.00031018	5	5	0.66691
CCNY	6	7.66E-05	0.00040704	6	3	0.24045
hsa-mir-6831	4	9.24E-05	0.00036323	7	4	0.4178
KIF2B	6	9.75E-05	0.00052789	8	3	0.68703
ANK1	6	0.00010535	0.0005754	9	4	0.60448
SFTPA1	6	0.00011544	0.00062936	10	5	0.6241
OR2AG1	6	0.00011942	0.00065104	11	5	0.73872
AXIN1	6	0.00012767	0.00069071	12	4	0.36959
SAT1	6	0.00013246	0.00071608	13	3	0.94749
OR2T33	6	0.00013785	0.0007456	14	6	0.34869
ATP7B	6	0.00014873	0.00081109	15	4	0.8474
TSC22D1	6	0.0001651	0.00089873	16	3	0.69373
CDK18	6	0.00016874	0.0009181	17	6	0.44218
LOC643669	6	0.00017874	0.00097898	18	2	1.6648
SETMAR	6	0.00020346	0.0011005	19	6	0.4566
MSRA	6	0.00020451	0.0011072	20	5	0.46454
hsa-mir-671	4	0.00020826	0.00081386	21	4	0.43091
CPQ	6	0.00021258	0.0011515	22	2	0.89045
hsa-mir-1283-1	4	0.00022408	0.00088305	23	3	0.53965
C5orf64	6	0.0002298	0.001234	24	3	0.33194
TMEM165	6	0.00024959	0.0013397	25	6	0.26639
SLC2A12	6	0.00025306	0.0013581	26	5	0.5113
CD163	6	0.00026405	0.0014167	27	4	0.58326
ZNF257	6	0.00027228	0.0014591	28	4	0.63291
PCED1B	6	0.00028086	0.0015108	29	3	0.36349
STXBP2	6	0.00029129	0.0015597	30	6	0.34082
SESN2	6	0.00031363	0.0016713	31	4	0.76548
AAED1	6	0.00032051	0.0017017	32	4	0.66596
hsa-mir-4484	4	0.00032342	0.0012437	33	3	0.52471
RAB7L1	6	0.00033192	0.0017585	34	4	0.59309
RAB3B	6	0.00034332	0.0018148	35	4	0.63844
FBXL20	6	0.00036933	0.001949	36	5	0.47368
C5orf51	6	0.00037181	0.0019665	37	4	0.58045
CREB3L3	6	0.00038298	0.0020278	38	3	0.21435
USP25	6	0.00039139	0.0020689	39	5	0.59887

Supplementary Table 9: Depleted gene knockouts ranked by RRA analysis of the CRISPR/Cas9 screen 30min APAP treatment vs. T0.

ID	sgRNA	Neg score	Neg p-value	Neg rank	Neg good sgRNA	Neg lfc
CRYBB1	6	2.13E-05	0.00012892	1	5	-0.77782
HAUS8	6	2.44E-05	0.00014644	2	6	-0.42961
TNFRSF10C	6	2.55E-05	0.00014829	3	3	-0.34479
NHEJ1	6	2.89E-05	0.00017273	4	6	-0.50827
hsa-mir-6775	4	3.62E-05	0.0001386	5	4	-0.52897
HIP1R	6	4.62E-05	0.00026637	6	5	-0.5242
SRP19	6	5.03E-05	0.0002862	7	5	-0.40136
COL9A3	6	7.32E-05	0.00038998	8	6	-0.38037
MAPK11	6	7.66E-05	0.00040704	9	2	-0.57421
C17orf105	6	0.00010542	0.00057632	10	5	-0.49927
hsa-mir-6846	4	0.00011213	0.0004504	11	4	-0.57785
OAZ1	6	0.00012767	0.00069071	12	3	-0.46701
hsa-mir-4788	4	0.00013378	0.00054034	13	2	-0.84262
GSDMC	6	0.00014477	0.00078941	14	3	-0.8266
TTC9	6	0.00017874	0.00097898	15	2	-0.5821
IRF2BPL	6	0.00018144	0.00099697	16	4	-0.38708
hsa-mir-7850	4	0.00018725	0.00072945	17	2	-0.6255
ASAH2	6	0.00019729	0.0010781	18	6	-0.33131
AZGP1	6	0.0002298	0.001234	19	1	-1.109
ANKRD66	6	0.00023819	0.0012793	20	4	-0.58655
RAP2A	6	0.00024452	0.0013078	21	5	-0.54024
SPANXF1	5	0.00024562	0.0011556	22	4	-0.52934
hsa-mir-4270	4	0.00024978	0.00096607	23	3	-0.61801
PRLR	6	0.0002747	0.001473	24	4	-0.62035
ARHGEF2	6	0.00029689	0.0015846	25	3	-0.58824
GUCY2C	6	0.00032762	0.0017373	26	5	-0.42311
GMDS	6	0.00033116	0.0017543	27	2	-1.0905
CYP26C1	6	0.00033192	0.0017585	28	1	-0.86341
ACTR3B	5	0.00034747	0.001627	29	3	-0.50374
TXNRD3NB	6	0.00034956	0.0018489	30	3	-0.72464
OR10G8	6	0.00035528	0.0018823	31	4	-0.65745
CSNK1A1	6	0.00036565	0.0019296	32	3	-0.76362
PSENEN	6	0.00037695	0.0019942	33	5	-0.43933
SOHLH2	6	0.00038023	0.0020112	34	4	-0.84114
ZFP30	6	0.00038298	0.0020278	35	2	-0.55655
RNMTL1	6	0.00040071	0.0021081	36	4	-0.47957
TCL1B	6	0.00041106	0.0021708	37	6	-0.239
CPXM2	6	0.00041237	0.0021801	38	3	-0.47961
CYP2S1	6	0.00041496	0.0021897	39	4	-0.49216

Supplementary Table 10: Enriched gene knockouts ranked by RRA analysis of the CRISPR/Cas9 screen 3h APAP treatment vs. T0.

ID	sgRNA	Pos score	Pos p-value	Pos rank	Pos good sgRNA	Pos lfc
CPE	6	1.11E-05	7.91E-05	1	6	0.35521
HES6	6	2.31E-05	0.00014137	3	6	0.35138
C5orf64	6	2.55E-05	0.00014829	4	3	0.26997
RTBDN	6	2.59E-05	0.00015013	5	3	0.7885
IQCE	6	5.69E-05	0.00031872	6	4	0.50013
POLR2C	6	6.05E-05	0.00033094	7	6	0.31181
SLITRK1	6	6.30E-05	0.00034339	8	2	0.93917
GP9	6	6.76E-05	0.00036507	9	6	0.42265
CDHR4	6	7.66E-05	0.00040704	10	5	0.371
KPNA3	6	8.47E-05	0.00045686	11	6	0.48675
GTF2E2	6	8.96E-05	0.0004873	12	4	1.0284
AKR7A2	6	9.58E-05	0.00052189	13	6	0.316
ANKRD7	6	0.00011641	0.00063674	14	4	0.88174
hsa-mir-4484	4	0.00011916	0.000479	15	2	1.7943
LCMT2	6	0.00012767	0.00069071	16	2	1.7217
CLCN6	6	0.00012836	0.0006944	17	5	0.39548
TEX33	6	0.00014663	0.00080002	18	3	0.61369
RDH13	6	0.00015194	0.00082908	19	3	1.2339
STAMBPL1	6	0.00015845	0.00086506	20	4	0.55147
BGLAP	5	0.00019151	0.00090242	21	2	1.9002
AP3M1	6	0.00021252	0.0011515	22	5	0.41577
AFF1	6	0.00021364	0.0011575	23	4	0.48661
FAM194B	6	0.00021413	0.0011621	24	4	0.61065
PIGO	6	0.00021504	0.0011662	25	6	0.26571
LEFTY1	6	0.00022883	0.0012271	26	4	0.55873
ZNF524	6	0.00023056	0.0012373	27	4	0.68207
ST8SIA5	6	0.00023402	0.0012592	28	3	0.56604
PDSS2	6	0.00024005	0.0012899	29	3	0.79873
PRPS1L1	6	0.00024601	0.0013171	30	4	0.51425
SPATA31A1	3	0.00025007	0.00073222	31	3	0.45463
CSN3	6	0.00026374	0.0014158	32	3	0.60568
TNNT3	6	0.00027631	0.0014813	33	6	0.44574
CPNE5	6	0.00028086	0.0015108	34	2	1.1177
C16orf71	6	0.00028212	0.0015149	35	5	0.45673
PTPRT	6	0.00028321	0.0015205	36	5	0.47812
GDPD3	6	0.0002963	0.0015823	37	4	0.52214
MAST4	6	0.00029994	0.0015989	38	3	0.78261
KCNA1	6	0.00031931	0.0016958	39	5	0.71872
hsa-mir-106b	4	0.00032543	0.0012502	40	2	0.55078

Supplementary Table 11: Depleted gene knockouts ranked by RRA analysis of the CRISPR/Cas9 screen 3h APAP treatment vs. T0.

ID	sgRNA	Neg score	Neg p-value	Neg rank	Neg good sgRNA	Neg lfc
GDF15	6	5.55E-06	4.13E-05	1	3	-0.92515
RAD51AP2	6	1.92E-05	0.00011739	2	5	-0.66697
BLID	6	2.55E-05	0.00014829	3	3	-0.26669
EIF2S3	6	2.58E-05	0.00015013	4	5	-0.44464
FAM63A	6	3.31E-05	0.00019949	5	5	-0.33166
DPM1	6	3.54E-05	0.00021332	6	4	-0.47327
ACMSD	6	3.56E-05	0.00021425	7	5	-0.5557
STK19	6	4.29E-05	0.00024976	8	4	-0.66472
UROD	6	4.31E-05	0.00025022	9	4	-0.55998
FOXG1	6	5.68E-05	0.00031849	10	6	-0.55571
STARD7	6	5.69E-05	0.00031849	11	5	-0.64105
TMSB15B	3	6.38E-05	0.00019303	12	3	-0.2882
PRPF31	6	7.66E-05	0.00040704	13	2	-0.81686
ITLN2	6	9.38E-05	0.00051175	14	4	-0.615
RAB3GAP2	6	0.00010196	0.00055695	15	5	-0.39493
RAPSN	6	0.00011232	0.00061553	16	5	-0.47682
NEB	6	0.00012258	0.00066442	17	6	-0.2515
ZNF611	4	0.00014182	0.00057401	18	4	-0.60071
FAM167B	6	0.00014242	0.00077442	19	4	-0.56612
AP4B1	6	0.00014953	0.00081663	20	4	-0.49354
ARL5B	6	0.00015106	0.00082493	21	6	-0.25585
CD84	6	0.00015219	0.00083092	22	6	-0.30523
SPANXF1	5	0.00015543	0.00073176	23	4	-0.3949
LAPTM5	6	0.00016981	0.0009241	24	4	-0.56437
IFNG	6	0.00017209	0.00093886	25	3	-0.56892
SIVA1	6	0.00017818	0.00097622	26	3	-0.66867
HDGFRP2	6	0.00017874	0.00097898	27	2	-1.0114
TBC1D21	6	0.00019212	0.0010542	28	6	-0.31215
C1orf43	6	0.00022074	0.0011921	29	5	-0.33197
GINS4	6	0.0002298	0.001234	30	4	-0.54694
DNM1	6	0.00023825	0.0012797	31	5	-0.45568
AUP1	6	0.00026264	0.0014102	32	3	-0.60157
hsa-mir-4681	4	0.00027224	0.0010519	33	4	-0.37647
CMTM1	4	0.00027303	0.0010551	34	4	-0.39637
EIF1AD	6	0.00027997	0.0015053	35	3	-0.742
SERPINF1	6	0.00028086	0.0015108	36	5	-0.3583
STK38L	6	0.00028865	0.0015435	37	6	-0.25919
LDOC1	6	0.00029041	0.0015537	38	3	-0.45134
hsa-mir-942	4	0.0002956	0.00114	39	3	-0.47037

Supplementary Table 12: Enriched gene knockouts ranked by RRA analysis of the CRISPR/Cas9 screen 6h APAP treatment vs. T0.

ID	sgRNA	Pos score	Pos p-value	Pos rank	Pos good sgRNA	Pos lfc
LOC643669	6	3.84E-06	2.74E-05	1	3	0.96959
RAB41	6	1.03E-05	7.45E-05	2	4	0.51956
SNRNP70	6	1.21E-05	8.42E-05	3	3	0.89968
SRSF1	6	2.55E-05	0.00014829	4	3	0.38277
STYX	6	3.16E-05	0.00019211	5	4	0.69453
AKR7A2	6	4.37E-05	0.00025253	6	5	0.36009
SPATS1	6	4.97E-05	0.00028251	7	6	0.29516
CCDC71	6	6.70E-05	0.00036184	8	6	0.34472
RETNLB	6	7.51E-05	0.00039966	9	3	0.56409
CCNY	6	7.66E-05	0.00040704	10	3	0.35893
NPFF	6	9.17E-05	0.00050114	11	6	0.46028
hsa-mir-4800	4	9.89E-05	0.00039459	12	3	0.57866
CTNND2	6	0.00010271	0.00055972	13	3	0.49469
NUDCD3	6	0.00010338	0.00056294	14	2	1.2832
WDR24	6	0.00010476	0.00057125	15	6	0.36501
SMARCA2	6	0.00011143	0.00061045	16	4	0.54585
PDP2	6	0.00011559	0.00062982	17	5	0.57918
SIRT1	6	0.0001253	0.00067503	18	5	0.56079
GPS2	6	0.00012767	0.00069071	19	2	1.9818
ASXL1	6	0.00013614	0.00073775	20	5	0.63292
TSPAN13	6	0.00014346	0.00078065	21	6	0.26872
SPAG6	6	0.00015658	0.00085675	22	6	0.29197
OR52I2	6	0.00017189	0.00093747	23	3	0.66348
R3HDM1	6	0.00017201	0.00093793	24	4	0.44622
SOGA3	6	0.00017361	0.00094762	25	3	1.1267
NPTX1	6	0.00017874	0.00097898	26	4	0.26695
hsa-mir-150	4	0.0001891	0.00073775	27	4	0.64051
LYG1	6	0.00021232	0.0011506	28	6	0.31616
SSTR2	6	0.00021725	0.0011773	29	3	0.5415
FASTKD3	6	0.00021736	0.0011778	30	4	0.44421
ARHGAP27	6	0.00021867	0.0011847	31	5	0.46813
FMNL2	6	0.00022289	0.0012008	32	5	0.55852
BAX	6	0.00022795	0.0012257	33	4	0.46007
HIST1H2AM	6	0.0002298	0.001234	34	1	3.3758
BGLAP	5	0.00023406	0.0010994	35	3	0.60159
PGGT1B	6	0.00024455	0.0013078	36	6	0.43196
ME1	6	0.00024701	0.0013226	37	6	0.3376
TIMP4	6	0.00026703	0.0014324	38	3	0.75619
CARM1	6	0.00026787	0.0014352	39	4	0.40124

Supplementary Table 13: depleted gene knockouts ranked by RRA analysis of the CRISPR/Cas9 screen 6h APAP treatment vs. T0.

ID	sgRNA	Neg score	Neg p-value	Neg rank	Neg good sgRNA	Neg lfc
ASB10	6	8.47E-06	6.07E-05	1	5	-0.54332
DRAP1	6	1.37E-05	9.29E-05	3	5	-1.1001
ACOT1	6	1.65E-05	0.00010585	4	2	-0.84258
PNMAL1	6	2.55E-05	0.00014829	5	3	-0.35088
LMTK3	6	3.15E-05	0.00019165	6	2	-0.68178
OR5AU1	6	4.72E-05	0.00027052	7	3	-0.43634
CSF2	6	6.68E-05	0.00036184	8	3	-0.49177
FIGN	6	6.82E-05	0.00036876	9	6	-0.31215
C1orf43	6	6.93E-05	0.00037614	10	5	-0.48234
hsa-mir-1248	4	7.08E-05	0.00027836	11	3	-0.65237
BZW2	6	7.33E-05	0.00038998	13	3	-0.48134
GPR37L1	6	8.71E-05	0.00047162	14	5	-0.57205
hsa-mir-196a-2	4	0.00011916	0.000479	15	3	-0.58026
TRIM33	6	0.00012698	0.00068702	16	5	-0.29048
HIST1H2BD	6	0.00012767	0.00069071	17	2	-0.79881
MGAT4A	6	0.00012798	0.00069163	18	4	-0.52264
YIPF7	6	0.00012872	0.00069809	19	2	-0.6191
LRRN1	6	0.00015582	0.00085122	20	6	-0.36718
IL1R2	6	0.00018182	0.0010011	21	3	-0.71554
hsa-mir-548ab	4	0.00018428	0.00072184	22	2	-0.68659
TMEM215	6	0.00020403	0.0011044	23	5	-0.3895
CD84	6	0.00020598	0.001116	24	5	-0.42474
ATP1A1	6	0.00020936	0.0011363	25	4	-0.44064
DYNC1LI2	6	0.0002298	0.001234	26	1	-1.0698
GALNT5	6	0.00023033	0.0012364	27	4	-0.51196
TSSK6	6	0.00024467	0.0013083	28	5	-0.39479
IFI27	6	0.00025937	0.0013899	29	5	-0.45498
hsa-mir-372	4	0.00026635	0.0010288	30	3	-0.68708
ZBTB38	6	0.00028086	0.0015108	31	3	-0.24388
STOX2	6	0.00033192	0.0017585	32	4	-0.50216
PROCA1	6	0.00033362	0.0017686	33	3	-0.68802
ZNF609	6	0.00035161	0.0018636	34	2	-0.75098
MTX2	6	0.00035346	0.0018747	35	6	-0.2695
hsa-mir-302d	4	0.00035833	0.0013761	36	3	-0.53077
MBD2	6	0.00036395	0.0019236	37	3	-0.52941
DAW1	6	0.00038298	0.0020278	38	1	-0.68703
TBP	6	0.0003896	0.002062	39	6	-0.35758
RPN1	6	0.00040224	0.0021155	40	5	-0.52792
KDELR2	6	0.00040864	0.0021565	41	4	-0.41677

Supplementary Table 14: Enriched gene knockouts ranked by RRA analysis of the CRISPR/Cas9 screen 12h APAP treatment vs. T0.

ID	sgRNA	Pos score	Pos p-value	Pos rank	Pos good sgRNA	Pos lfc
OTUD3	6	1.56E-05	0.00010032	1	3	0.83868
GATS	6	1.79E-05	0.00011231	2	4	0.77141
BMPR1A	6	1.93E-05	0.00011785	3	6	0.41848
CUL4B	6	1.96E-05	0.00012015	4	6	0.36531
SCUBE2	6	2.14E-05	0.00012892	5	5	0.68204
NR3C1	6	2.52E-05	0.00014783	6	4	0.80561
C14orf159	6	2.55E-05	0.00014829	7	3	0.237
PIK3R1	6	2.78E-05	0.00016674	8	4	0.66259
TES	6	5.91E-05	0.00032679	9	3	0.72636
ZW10	6	6.08E-05	0.00033279	10	6	0.48035
C5orf64	6	7.66E-05	0.00040704	11	4	0.20738
ZNF613	6	8.02E-05	0.00042826	12	6	0.60179
DEFB114	6	0.00010702	0.00058647	13	4	0.5274
LIX1	6	0.00011211	0.00061414	14	6	0.466
HIST1H2AM	6	0.00012767	0.00069071	15	1	3.7898
DUSP2	6	0.00014087	0.00076405	16	3	0.8838
CD1B	6	0.00014721	0.00080371	17	5	0.64858
KCNJ3	6	0.00015128	0.00082585	18	6	0.32044
KLHL15	6	0.00015275	0.00083139	19	5	0.59454
KIAA0895	6	0.00015518	0.00084707	20	5	0.48535
SSBP2	6	0.00015763	0.00085952	21	5	0.52499
EVI5L	6	0.00016031	0.00087428	22	3	0.85075
GRB7	6	0.00016553	0.00090242	23	5	0.75454
IRF1	6	0.0001694	0.00092225	24	6	0.37856
MTA1	6	0.00017874	0.00097898	25	1	3.2361
FSTL1	6	0.00018744	0.0010334	26	4	0.70639
WRB	6	0.00018815	0.0010348	27	5	0.62386
ATPAF2	6	0.00019034	0.001044	28	2	0.98707
PGM5	6	0.00019139	0.0010491	29	6	0.48176
RREB1	6	0.00019572	0.0010698	30	4	0.76125
VIT	6	0.00019583	0.0010708	31	6	0.36793
GAREM	6	0.0001967	0.0010758	32	3	0.74914
PRDM11	6	0.00020842	0.0011293	33	5	0.60209
MICAL3	6	0.00021313	0.0011538	34	5	0.61197
AIM2	6	0.00022164	0.0011939	35	5	0.67795
EZH1	6	0.00023319	0.0012539	36	6	0.38361
GOLGA2	6	0.00024713	0.0013231	37	4	0.67385
PSMB11	6	0.00026098	0.0013983	38	6	0.40166
ARID3A	6	0.00026827	0.0014361	39	4	0.5301

Supplementary Table 15: Depleted gene knockouts ranked by RRA analysis of the CRISPR/Cas9 screen 12h APAP treatment vs. T0.

ID	sgRNA	Neg score	Neg p-value	Neg rank	Neg good sgRNA	Neg lfc
QRFP	6	7.00E-06	5.10E-05	1	6	-0.71124
hsa-mir-6840	4	1.21E-05	4.82E-05	2	4	-0.58806
hsa-mir-6805	4	1.33E-05	5.28E-05	3	4	-0.69571
hsa-mir-4449	4	2.23E-05	9.06E-05	5	3	-0.99791
FAM110D	6	2.55E-05	0.00014829	6	2	-1.021
RPL3L	6	4.79E-05	0.00027329	8	4	-1.1242
hsa-mir-3201	4	6.35E-05	0.00024653	9	4	-1.0169
hsa-mir-6772	4	6.65E-05	0.00026037	10	4	-0.57996
RNF25	6	6.83E-05	0.00036922	11	5	-0.70265
EPB42	6	7.66E-05	0.00040704	12	2	-1.039
hsa-mir-1180	4	7.70E-05	0.00030511	13	3	-0.89839
ABI1	6	8.07E-05	0.00043057	14	6	-0.50071
hsa-mir-4674	4	8.83E-05	0.00034893	15	4	-0.52824
HOOK2	6	9.29E-05	0.00050852	16	6	-0.56762
MAGEH1	6	9.35E-05	0.00051129	17	6	-0.4293
ILKAP	6	0.00010968	0.00060215	18	5	-0.71864
CBX8	6	0.00012637	0.00068148	19	5	-0.75639
ZNF776	6	0.00013183	0.00071377	20	6	-0.43882
LPL	6	0.00013757	0.00074513	21	6	-0.47907
hsa-mir-3128	4	0.00016674	0.00066303	22	2	-1.1344
hsa-mir-6068	4	0.00016996	0.00067318	23	2	-1.0814
ATAD3B	6	0.00017874	0.00097898	24	3	-0.90913
TC2N	6	0.00019991	0.001086	26	5	-0.50035
hsa-mir-4532	4	0.00020684	0.00080971	27	3	-1.6694
C1orf56	6	0.0002187	0.0011852	28	6	-0.48476
TMC4	6	0.0002214	0.0011935	29	6	-0.73446
NOL3	6	0.0002298	0.001234	30	5	-0.44867
UBXN7	6	0.00024216	0.0012995	31	6	-0.56121
hsa-mir-4469	4	0.00025373	0.00098267	32	4	-0.66196
HDGFRP3	6	0.00025498	0.001365	33	5	-0.59283
hsa-mir-4324	4	0.00025629	0.00099282	34	3	-0.59911
TACSTD2	6	0.00026402	0.0014162	35	3	-1.0601
BRAP	6	0.00028086	0.0015108	36	3	-0.37861
MAPK13	6	0.00028769	0.0015399	37	5	-0.71997
H2AFJ	6	0.00029098	0.0015569	38	5	-0.83708
hsa-mir-4466	4	0.0003011	0.001157	41	3	-1.2671
ZNF768	6	0.0003037	0.001621	42	6	-0.33605
UGT2B15	4	0.00030925	0.0011875	43	2	-0.96415
RAC2	6	0.00032657	0.0017317	45	5	-0.56381

Supplementary Table 16: Enriched gene knockouts ranked by RRA analysis of the CRISPR/Cas9 screen 24h APAP treatment vs. T0.

ID	sgRNA	Pos score	Pos p-value	Pos rank	Pos good sgRNA	Pos lfc
PAGE4	6	3.80E-07	3.00E-06	1	6	0.50966
BGLAP	5	4.12E-06	1.91E-05	2	2	1.6481
PGM5	6	1.34E-05	9.13E-05	3	6	0.39874
EEF1D	6	2.55E-05	0.00014829	4	2	1.6816
FAM98B	6	3.61E-05	0.00021701	5	3	0.617
EGR1	6	7.66E-05	0.00040704	6	2	1.4603
ZBTB21	6	9.87E-05	0.00053481	7	5	0.79106
RAP1A	6	0.00012767	0.00069071	8	2	0.86814
HDC	6	0.00013846	0.0007479	9	5	0.37985
SULT2B1	6	0.00014774	0.00080556	10	6	0.26799
RFPL3	6	0.00015617	0.00085353	11	6	0.2974
OR10J5	6	0.00017189	0.00093747	12	4	0.63468
HIST1H2AM	6	0.00017874	0.00097898	13	2	1.5416
PDCD5	6	0.00018409	0.0010163	14	4	0.64129
SLC43A1	6	0.0001928	0.0010592	15	5	0.44453
REST	6	0.0001964	0.0010731	16	3	0.46524
HBE1	6	0.0002102	0.0011432	17	6	0.23558
RBM10	6	0.0002298	0.001234	18	2	1.6083
FAM120A	6	0.00023414	0.0012603	19	4	0.49317
CSGALNACT1	6	0.0002408	0.0012949	20	5	0.31133
ADCY9	6	0.00025774	0.0013784	21	3	0.61489
TSNAX	6	0.0002633	0.0014139	22	6	0.26452
UQCRC1	6	0.00027027	0.0014462	23	4	0.48922
PCED1B	6	0.00028086	0.0015108	24	1	2.811
TMEM60	6	0.00029838	0.0015901	25	4	0.51151
RASSF4	6	0.00031826	0.0016902	26	5	0.35433
ENAM	6	0.00033192	0.0017585	27	4	0.2781
USP10	6	0.00035221	0.0018659	28	5	0.2809
RRP9	6	0.00037015	0.0019582	29	4	0.52246
C4orf22	6	0.00037197	0.0019674	30	5	0.3168
HES5	6	0.00037573	0.0019886	31	5	0.37072
AKAP9	6	0.00038298	0.0020278	32	4	0.38815
PECR	6	0.00041903	0.0022091	33	4	0.41854
XPR1	6	0.00042456	0.0022363	34	4	0.48323
SDS	6	0.00043403	0.0022815	35	5	0.42734
hsa-mir-4804	4	0.00044577	0.0016925	36	4	0.2922
FMO5	6	0.0004667	0.0024383	37	6	0.23512
CIDEC	6	0.00047506	0.0024785	38	6	0.33006
NTN5	6	0.00047801	0.0024912	39	5	0.42811

Supplementary Table 17: Depleted gene knockouts ranked by RRA analysis of the CRISPR/Cas9 screen 24h APAP treatment vs. T0.

ID	sgRNA	Neg score	Neg p-value	Neg rank	Neg good sgRNA	Neg lfc
TIPRL	6	5.52E-06	4.08E-05	1	5	-0.42208
VNN1	6	1.06E-05	7.73E-05	2	4	-0.51134
OR11L1	6	1.35E-05	9.20E-05	3	5	-0.43335
ACAD11	6	1.71E-05	0.00010816	4	5	-0.40344
EFNB3	6	2.55E-05	0.00014829	6	2	-0.6828
MYOZ3	6	3.94E-05	0.00022993	7	4	-0.43961
FAM227B	6	4.77E-05	0.0002719	8	4	-0.57481
SSR2	6	5.64E-05	0.0003171	10	6	-0.23165
GPSM1	6	7.66E-05	0.00040704	11	2	-0.48187
EOMES	6	7.96E-05	0.00042457	12	5	-0.47969
RCL1	6	9.10E-05	0.00049376	13	4	-0.47733
POFUT1	6	0.00010169	0.0005551	14	5	-0.34436
SDC1	6	0.00013778	0.0007456	15	2	-0.76185
BABAM1	6	0.00017628	0.00096284	16	5	-0.45825
hsa-mir-3140	4	0.00017768	0.00070454	17	3	-0.45661
GKN2	6	0.00017874	0.00097898	18	3	-0.34985
SUZ12	6	0.00017977	0.00098544	19	6	-0.38846
hsa-mir-4449	4	0.00019735	0.00077189	20	3	-0.48835
GLI3	6	0.0002068	0.001122	21	5	-0.38439
IP6K1	6	0.00022379	0.0012036	22	5	-0.51206
PPM1M	6	0.00022415	0.0012055	23	3	-0.5059
NSUN5	6	0.00022709	0.0012225	24	2	-0.87854
OR2T34	6	0.0002298	0.001234	25	2	-0.54416
TNFRSF1A	6	0.00024106	0.0012959	26	3	-0.55964
TGFBR3L	6	0.00024836	0.0013323	27	5	-0.50034
BTG3	6	0.00024944	0.0013378	28	6	-0.25213
hsa-mir-4707	4	0.00025534	0.00098959	29	2	-0.73793
CAMK1	6	0.00025664	0.0013729	30	5	-0.41143
SHPRH	6	0.00028086	0.0015108	31	3	-0.28086
TACSTD2	6	0.00029994	0.0015989	33	3	-0.62317
TSPAN2	6	0.00030333	0.0016187	34	2	-0.89357
FOXF1	6	0.00033434	0.0017737	35	4	-0.38978
GSDMB	6	0.00033858	0.0017931	36	6	-0.36549
MAPK8IP2	6	0.00033942	0.0017981	37	3	-0.61229
KCTD11	6	0.00039433	0.0020472	39	5	-0.36608
TMEM41A	6	0.00040652	0.0020984	40	4	-0.36943
hsa-mir-1324	4	0.00040662	0.0015542	41	2	-0.49281
HIST1H2AL	6	0.00041091	0.0021192	42	4	-0.46954
PELI2	6	0.00041523	0.0021353	43	3	-0.5315

Supplementary Table 18: Enriched gene knockouts ranked by RRA analysis of the CRISPR/Cas9 screen 4d APAP treatment vs. T0.

ID	sgRNA	Pos score	Pos p-value	Pos rank	Pos good sgRNA	Pos lfc
ATXN2	6	7.01E-07	5.77E-06	1	4	2.8779
FAM57A	6	1.26E-05	8.74E-05	2	4	2.5453
SEMG2	6	1.97E-05	0.00012015	3	6	1.3511
KIR3DL3	6	2.55E-05	0.00014829	4	3	0.6228
MYOM3	6	2.69E-05	0.00016074	5	5	1.888
EYA4	6	5.74E-05	0.00031895	6	4	2.1426
LZTR1	6	7.32E-05	0.00038998	7	5	1.9547
CDK5RAP1	6	7.51E-05	0.00040013	8	5	1.7195
UVRAG	6	7.66E-05	0.00040704	9	3	1.6195
FEZF2	6	8.06E-05	0.00043057	10	5	1.6874
C1QTNF5	6	8.26E-05	0.0004421	11	4	1.8882
TNFRSF25	6	8.47E-05	0.00045686	12	3	2.1064
NLRC3	6	9.73E-05	0.00052789	13	6	1.5065
SMIM4	6	0.00011389	0.00062014	14	6	1.7844
hsa-mir-3683	4	0.00011916	0.000479	15	2	1.9545
TMPRSS6	6	0.00012767	0.00069071	16	5	0.48736
hsa-mir-4327	4	0.00015321	0.00061506	17	2	2.6477
SIK2	6	0.000156	0.0008526	18	5	0.83149
ENPP7	6	0.00016992	0.0009241	19	6	1.3272
C12orf77	6	0.0001762	0.00096284	20	3	2.6334
DEFB118	6	0.00017861	0.00097852	21	6	1.2257
FEM1C	6	0.00020342	0.0011001	22	4	1.9684
CRISP1	6	0.00020503	0.0011095	23	4	1.5127
C9orf91	6	0.00020746	0.0011252	24	5	1.651
ESRRA	6	0.00021269	0.0011519	25	5	2.1654
PSMC5	6	0.00022442	0.0012064	26	5	1.6159
HLA-DPB1	6	0.00023005	0.001235	27	3	2.1053
LPXN	6	0.00027024	0.0014458	28	4	1.7911
SOD2	6	0.00028086	0.0015108	29	3	0.58993
hsa-mir-4752	4	0.00028949	0.0011169	30	3	1.6833
B3GALT5	6	0.00029928	0.0015938	31	3	1.8816
SLCO2A1	6	0.00030233	0.0016123	32	6	1.6761
LGALS3	6	0.00030789	0.0016422	33	3	2.5551
IL1RL1	6	0.00031723	0.0016861	34	5	1.9972
NADK2	6	0.00033192	0.0017585	35	2	3.2826
TAS2R20	6	0.00035363	0.0018752	37	5	1.7274
ABCB10	6	0.00037015	0.0019582	38	4	1.8988
hsa-mir-504	4	0.00037244	0.0014361	39	3	2.4877
IQCB1	6	0.00037517	0.001984	40	4	1.5882

Supplementary Table 19: Depleted gene knockouts ranked by RRA analysis of the CRISPR/Cas9 screen 4d APAP treatment vs. T0

ID	sgRNA	Neg score	Neg p-value	Neg rank	Neg good sgRNA	Neg lfc
INO80C	6	2.99E-08	2.31E-07	1	5	-2.0821
CALHM1	6	1.07E-05	7.77E-05	2	6	-3.3159
LCE5A	6	2.01E-05	0.00012108	3	5	-2.2661
KLHL21	6	2.55E-05	0.00014829	4	2	-1.8677
NTRK2	6	7.66E-05	0.00040704	5	3	-3.8148
CXorf21	6	8.68E-05	0.00047116	6	4	-1.1478
NFAT5	6	0.00011624	0.00063444	7	4	-2.4115
CALR	6	0.00012358	0.00066811	8	4	-2.7166
RBM4B	6	0.00012466	0.00067226	9	6	-2.6964
MAPK3	6	0.00012767	0.00069071	10	5	-1.8917
hsa-mir-4717	4	0.00014428	0.00058232	11	4	-1.6209
LCMT1	6	0.00014459	0.00078895	12	4	-2.087
AK7	6	0.00015873	0.00086552	13	5	-3.1668
TSSK2	6	0.00017627	0.00096284	14	5	-3.5813
EARS2	6	0.00017874	0.00097898	15	5	-1.8177
LINGO1	6	0.00018208	0.0010034	16	6	-1.8333
hsa-mir-6892	4	0.0002222	0.00087659	17	4	-2.8944
ATG2B	6	0.0002298	0.001234	18	2	-3.6526
SH3GLB2	6	0.00024589	0.0013161	19	5	-2.6298
HYPK	6	0.00024814	0.0013304	20	4	-2.1598
GSG1L	6	0.00025317	0.0013581	21	5	-2.3702
ACBD3	6	0.00026187	0.0014052	22	6	-2.2593
MTMR12	6	0.00026917	0.0014388	23	4	-2.1953
SLC3A2	6	0.00027914	0.0015002	24	6	-2.2157
TMEM215	6	0.00028086	0.0015108	25	5	-1.1434
AK6	6	0.00028655	0.0015366	26	4	-2.1069
MAMDC2	6	0.00030754	0.0016413	27	5	-1.4796
CHMP1A	6	0.00032762	0.0017373	28	5	-1.7902
ERMN	6	0.00033192	0.0017585	30	6	-0.97693
MAPK9	6	0.00033748	0.0017885	31	4	-2.8254
MYOG	6	0.00035314	0.0018724	32	5	-1.6799
TRPC7	6	0.00035559	0.0018839	33	4	-2.3862
PHB2	6	0.00035575	0.0018844	34	4	-2.1601
TM6SF2	6	0.00038298	0.0020278	35	4	-1.4028
DICER1	6	0.00039301	0.0020754	36	5	-2.072
C1orf95	6	0.00041291	0.0021828	37	6	-2.4832
hsa-mir-4270	4	0.00041852	0.0015906	38	3	-2.5061
DMGDH	6	0.00042055	0.0022183	39	5	-2.2022
BCAS3	6	0.0004259	0.0022432	40	4	-2.3394

Supplementary Table 20: Genes ranked by Maximum Likelihood Estimate comparing all APAP samples to T0.

Gene	sgRNA	Beta	Z value	P-value
hsa-mir-519c	3	0.62184	7.8712	0.001873
hsa-mir-611	4	-0.38341	-5.5104	0.002795
ATXN7L1	6	0.5016	10.354	0.0041
hsa-mir-6729	4	0.49166	7.1337	0.004305
ZNF776	6	-0.31595	-6.2515	0.005069
PKD2	6	-0.30637	-5.9898	0.005618
PGM5	6	0.45058	9.2391	0.005618
hsa-mir-3667	4	0.44758	7.4561	0.005693
hsa-mir-548i-4	3	0.44338	6.0099	0.005888
hsa-mir-4745	4	-0.30223	-4.5899	0.005926
hsa-mir-8088	4	-0.30191	-4.3664	0.005935
LOC388813	5	0.44244	7.0175	0.005935
CYB5R3	6	0.43842	8.3189	0.006149
hsa-mir-940	4	-0.29317	-4.9592	0.006597
hsa-mir-3929	4	-0.28944	-4.5263	0.00682
hsa-mir-6839	4	-0.28804	-4.7414	0.006904
CTDP1	6	0.41036	7.9603	0.007519
hsa-mir-346	4	-0.27647	-4.2813	0.007882
PDSS2	6	0.40502	7.9945	0.007892
SHC3	6	0.40446	8.1923	0.00792
CXADR	6	0.40409	7.9601	0.007938
NR1I3	6	0.40377	8.0512	0.007975
hsa-mir-2392	4	0.40319	6.2329	0.008013
hsa-mir-6719	4	0.39518	6.0495	0.008553
PTPRT	6	0.39483	7.5349	0.008553
PDLIM7	6	0.39414	7.6306	0.008665
hsa-mir-3151	4	0.39175	6.1599	0.008823
GPRIN1	6	-0.26558	-4.9772	0.008842
hsa-mir-506	4	0.39113	6.5232	0.008851
hsa-mir-6845	4	-0.26173	-4.0798	0.009159
OSBPL9	4	0.38179	5.8574	0.009541
NUP62CL	6	0.38158	7.9489	0.009541
hsa-mir-548f-4	3	-0.25804	-3.3301	0.009569
PXDN	6	-0.25612	-5.1054	0.009783
MAPK10	6	0.37439	7.6531	0.010286
hsa-mir-4270	4	-0.2537	-4.2933	0.010295
hsa-mir-4466	4	-0.25314	-3.8864	0.010379
GHRH	6	0.36919	7.5375	0.010836
hsa-mir-504	4	0.36901	6.4193	0.010845
hsa-mir-4313	4	-0.24881	-3.8792	0.010892

Supplementary Table 21 Significant gene hits from the APAP time points (p<0.05) were compared with a list of 48 genes with known roles in NAD metabolism.

4d pos p<0.05	4d neg p<0.05	24h pos p<0.05	24h neg p<0.05	30min-24h pos p<0.05	30min-24h neg p<0.05	all pos p<0.05	all neg p<0.05
NADK2	NMNAT1	HSD11B1	NMNAT1	HSD11B1	NMNAT1	NADK2	NMNAT1
SIRT3		NADSYN1		SIRT1			
NADSYN1							
SLC36A4							
NUDT9							
SLC25A17							

Supplementary Table 22: Most significant genes differentially expressed with and without APAP treatment from RNA-sequenced mice (p<0.05).

Gene	log_2(fold_change)	Test statistic	p-value
Dnajc12	1.8521	3.78614	5.00E-05
Tff3	2.67264	3.70363	5.00E-05
Abcc4	1.81514	3.36102	5.00E-05
Gsta1	1.66224	3.07492	5.00E-05
Derl3	1.75233	2.95514	5.00E-05
Nipal1	1.86904	2.90845	5.00E-05
Tcf24	2.46792	2.81794	5.00E-05
Socs2	1.60733	2.78214	5.00E-05
Scara5	1.44466	2.75335	5.00E-05
Arntl	1.66518	2.6448	5.00E-05
Asns	1.71814	2.52692	5.00E-05
Gm6484	1.56456	2.47812	5.00E-05
Tnfrsf12a	1.3779	2.43612	5.00E-05
Csf2rb2	1.96996	2.41819	5.00E-05
Srxn1	1.15006	2.40386	5.00E-05
Creld2	1.26828	2.39791	5.00E-05
Slc1a4	1.4146	2.38864	5.00E-05
Dhrs9	1.38945	2.38317	5.00E-05
Hes1	1.54994	2.3744	5.00E-05
Igfbp1	0.98216	2.34434	5.00E-05
Socs3	1.484	2.31186	5.00E-05
Efna1	0.981277	2.27729	5.00E-05
Sept11	1.08833	2.2209	5.00E-05
Abhd2	0.979515	2.17504	5.00E-05
Slc41a2	1.25408	2.12833	5.00E-05
Chka	1.59289	2.04586	5.00E-05
Kcnq1ot1	0.868679	2.04195	5.00E-05
Litaf	0.859747	2.03045	5.00E-05
Gas6	0.808195	1.9904	5.00E-05
Fndc3b	1.11942	1.68965	5.00E-05
Tef	-1.05904	-1.61622	5.00E-05
Pklr	-1.63238	-1.66792	5.00E-05
Gys2	-1.30449	-1.70762	5.00E-05
Dpp4	-0.905014	-1.86888	5.00E-05
Galm	-0.775005	-1.89618	5.00E-05
Slc1a2	-2.4172	-1.90821	5.00E-05
Homer2	-0.814433	-1.90821	5.00E-05
Acy3	-0.778139	-1.91211	5.00E-05
Ddah1	-0.856776	-1.95112	5.00E-05

Supplementary Table 23: Description of participants used in the GSE70784 analysis.

Group	Number of participants	Gender (% male)*	Age (years)	Ethnicity**
Responder	12	6 (50%)	32.8	C:8, H:4, C/H:0, A:0, AA:1
non-responder	32	20 (62.5%)	33.8	C:8, H:13, C/H:1, A:1, AA:9
Placebo	10	7 (70%)	25.8	C:4, H:5, C/H:0, A:0, AA:1
Total	54	33 (61.1%)	32.1	C: 20, H: 22, C/H: 1, A:1, AA:1

*, number males

**, ethnicity: c= caucasian, h=hispanic, aa=african american, a=asian

Supplementary Table 24: Significant gene hits from the APAP time points (p<0.05) were compared with significantly associated genes from other datasets studying the effects of APAP (GSE74000, ALF healthy liver sample microarray data; GSE70784, d1 and d8 APAP responder and non-responder blood sample microarray data; GSE70784, d1 and d8 APAP responder and placebo blood sample microarray data; and mouse 24h +/- APAP RNA-seq data).

Dataset	4d positive p<0.05	4d negative p<0.05	24h positive p<0.05	24h negative p<0.05	T30min-24h positive p<0.05	T30min-24h negative p<0.05	All positive p<0.05	All negative p<0.05
GSE70784 d1 APAP responder vs. non-responder p<0.05	12	11	15	12	12	19	18	10
GSE70784 d8 APAP responder vs. non-responder p<0.05	98	101	117	94	111	96	100	108
GSE70784 d1 APAP responder vs. placebo p<0.05	22	30	34	20	40	21	31	25
GSE70784 d8 APAP responder vs. placebo p<0.05	91	89	86	68	82	72	72	81
GSE74000 ALFp<0.05	67	63	70	60	81	61	67	57
GSE110787 mouse 24h +/- APAP p<0.05	86	57	63	55	64	58	73	67

Supplementary Table 25: Top 100 significantly associated genes (p<0.05) from other datasets studying the effects of APAP (GSE74000, ALF healthy liver sample microarray data; GSE70784, d1 and d8 APAP responder and non-responder blood sample microarray data; GSE70784, d1 and d8 APAP responder and placebo blood sample microarray data; and mouse 24h +/- APAP RNA-seq data) were queried in pubmatrix to determine novelty.

Dataset	Analysis type	APAP	Acetaminophen	Hepatotoxic	Hepatotoxicity	Acute liver injury	Acute liver failure
GSE110787 mouse RNA-Seq top 100 genes	Gene expression LFC	15	15	12	24	26	17
GSE74000 top 100 genes	Gene expression LFC	12	12	9	15	15	10
GSE70784 d1 responder vs. nonresponder top 100 genes	Gene expression LFC	8	8	7	14	14	10
GSE70784 d8 responder vs. nonresponder top 100 genes	Gene expression LFC	7	7	4	9	9	7
GSE70784 d1 responder vs. placebo top 100 genes	Gene expression LFC	9	9	6	10	13	8
GSE70784 d8 responder vs. placebo top 100 genes	Gene expression LFC	10	10	14	17	17	13
genes in all top 100 lists	600						
unique genes in all top 100 lists	586						
unique genes with APAP hits	60						

Supplementary Table 26: Summary of 147 APAP-associated SNPs.

SNP	Position*	Alleles#	MAF^	Reference	Reference p-value
rs10110651	Chr8:36989597	T/C	0.278754	Moyer 2011	2.14E-05
rs10144421	Chr14:95445498	T/C	0.384385	Moyer 2011	8.77E-05
rs10186482	Chr2:151625463	A/G	0.45647	Moyer 2011	6.87E-05
rs1042640	Chr2:233772898	C/G	0.178914	Court 2013	
rs10485114	Chr6:115807742	C/T	0.222444	Moyer 2011	4.01E-05
rs10508010	Chr13:94974756	A/C	0.30012	Moyer 2011	2.50E-03
rs10511137	Chr3:88463052	A/G	0.330671	Moyer 2011	3.18E-07
rs10515465	Chr5:134931867	G/C	0.157348	Moyer 2011	5.69E-05
rs10849421	Chr12:6217842	G/A	0.394968	Moyer 2011	4.15E-05
rs10852886	Chr17:6789522	A/T	0.475439	Moyer 2011	7.50E-05
rs10929303	Chr2:233772770	C/T	0.247604	Court 2013	
rs11070109	Chr13:95111572	C/T	0.0565096	Moyer 2011	3.80E-02
rs11129122	Chr3:23671125	A/G	0.220847	Moyer 2011	4.97E-05
rs11153350	Chr6:112257182	G/A	0.153554	Moyer 2011	2.54E-05
rs11248859	Chr16:1191997	G/A	0.276358	Moyer 2011	6.18E-05
rs11611637	Chr12:97291586	T/C	0.285343	Moyer 2011	8.78E-05
rs11766607	Chr7:49480023	A/G	0.136581	Moyer 2011	2.06E-05
rs1189434	Chr13:95084938	G/A	0.0972444	Moyer 2011	6.00E-03
rs1189436	Chr13:95084146	G/A	0.0986422	Moyer 2011	9.00E-03
rs1189437	Chr13:95083350	T/G	0.125799	Moyer 2011	1.11E-02
rs1189439	Chr13:95082712	C/T	0.194089	Moyer 2011	3.09E-02
rs11909987	Chr21:42402293	C/A	0.413139	Moyer 2011	3.62E-05
rs12107308	Chr3:88433203	C/G	0.193291	Moyer 2011	4.09E-06
rs12120268	Chr1:52587287	C/A	0.0551118	Moyer 2011	3.98E-02
rs12267329	Chr10:1633353	A/G	0.400559	Moyer 2011	6.71E-05
rs12584534	Chr13:95103296	C/T	0.175319	Moyer 2011	4.37E-02
rs12700386	Chr7:22723390	C/G/A	0.133187	Moyer 2011	6.20E-05
rs13015146	Chr2:202197380	T/C	0.434305	Moyer 2011	9.49E-05
rs13101122	Chr3:88458699	T/C	0.463259	Moyer 2011	8.35E-06
rs13204006	Chr6:21946381	A/G	0.165735	Moyer 2011	7.85E-05
rs13326165	Chr3:52498102	G/A	0.197284	Moyer 2011	7.92E-05
rs1343151	Chr1:67253446	G/A	0.337859	Moyer 2011	1.91E-05
rs1354510	Chr1:165206278	A/G	0.280351	Moyer 2011	7.78E-05
rs1356553	Chr6:53424785	T/G	0.451677	Moyer 2011	2.12E-02
rs1372940	Chr18:30437953	C/T	0.0700879	Moyer 2011	5.74E-05
rs1377392	Chr6:53433687	C/T	0.345048	Moyer 2011	8.80E-03
rs1380292	Chr8:21246897	A/G	0.236821	Moyer 2011	7.64E-05
rs1467558	Chr11:35208126	C/T	0.0609026	Court 2014, Harrill 2009	4.50E-02
rs1532815	Chr1:165210852	A/T	0.33147	Moyer 2011	6.04E-07
rs1536343	Chr13:39101284	C/T	0.0541134	Moyer 2011	7.28E-05

Supplementary Table 26. –Continued.

rs1599096	Chr8:21260713	C/T	0.263578	Moyer 2011	6.86E-05
rs16851554	Chr2:214159668	T/G	0.149561	Moyer 2011	2.46E-05
rs16900696	Chr5:31113307	C/G	0.0760783	Moyer 2011	7.12E-05
rs16950155	Chr13:94799401	C/G	0.0636981	Moyer 2011	4.16E-02
rs16950190	Chr13:94809909	C/T	0.0539137	Moyer 2011	1.27E-02
rs17310467	Chr20:34957813	A/G/T	0.0810703	Moyer 2011	4.20E-03
rs17413355	Chr7:78356266	C/T	0.142173	Moyer 2011	8.50E-05
rs17469886	Chr8:27725811	C/A	0.0419329	Moyer 2011	3.52E-05
rs1751043	Chr13:95076266	G/A	0.0972444	Moyer 2011	6.00E-03
rs17559005	Chr3:88463389	T/C	0.330471	Moyer 2011	3.18E-07
rs17640676	Chr2:154791307	G/T	0.227835	Moyer 2011	2.09E-05
rs1764425	Chr13:95352239	G/A	0.189696	Moyer 2011	3.20E-02
rs1766908	Chr13:95352874	C/T	0.186901	Moyer 2011	1.88E-02
rs1876381	Chr8:82046088	T/C	0.159944	Moyer 2011	9.60E-06
rs1902023	Chr4:68670366	C/A	0.453474	Court 2017	
rs1925851	Chr13:94968444	C/T	0.491613	Moyer 2011	2.28E-02
rs1925856	Chr13:94964357	A/G	0.491214	Moyer 2011	4.00E-03
rs1925860	Chr13:94993427	C/T	0.327276	Moyer 2011	2.00E-03
rs1982562	Chr3:88459217	G/A	0.463259	Moyer 2011	1.28E-05
rs1989983	Chr17:50633170	G/A	0.199481	Moyer 2011	3.84E-02
rs2031920	Chr10:133526341	C/T	0.0670926	Ueshima 1996	NA
rs2064504	Chr20:45775071	G/A	0.389976	Moyer 2011	8.52E-05
rs2074451	Chr19:1107036	G/T	0.391973	Moyer 2011	7.90E-03
rs2082603	Chr4:178754241	C/T	0.329673	Moyer 2011	3.43E-05
rs2089515	Chr8:57014167	C/T	0.230431	Moyer 2011	9.91E-05
rs2209631	Chr13:39100885	A/G	0.0541134	Moyer 2011	7.28E-05
rs2218988	Chr7:134879612	T/C	0.24361	Moyer 2011	9.50E-05
rs2344953	Chr3:88483065	G/A	0.272564	Moyer 2011	5.59E-06
rs2397105	Chr6:52788526	A/G	0.276757	Moyer 2011	4.80E-02
rs2397132	Chr6:52877418	A/G	0.138778	Moyer 2011	2.80E-02
rs2524290	Chr11:61920202	G/A	0.308906	Moyer 2011	6.19E-05
rs2567513	Chr17:72696601	T/C	0.161142	Moyer 2011	6.66E-05
rs2720666	Chr8:128071213	A/G	0.24401	Moyer 2011	6.93E-05
rs2720667	Chr8:128071338	A/G	0.244209	Moyer 2011	5.73E-05
rs2737844	Chr14:64941791	A/G	0.428315	Moyer 2011	2.97E-02
rs2748991	Chr6:52731718	C/T/A	0.485224	Moyer 2011	2.08E-02
rs279874	Chr9:953057	G/C	0.394968	Moyer 2011	9.13E-05
rs2880961	Chr3:88475025	C/T	0.333666	Moyer 2011	1.88E-07
rs319590	Chr5:134919098	T/G	0.162939	Moyer 2011	2.76E-05
rs319594	Chr5:134914456	T/C	0.16274	Moyer 2011	6.51E-05
rs3208829	Chr6:112252087	C/G	0.160144	Moyer 2011	2.54E-05
rs33966381	Chr3:88463472	C/T	0.330871	Moyer 2011	3.18E-07

Supplementary Table 26. –Continued.

rs3744198	Chr17:74960029	G/A	0.244209	Moyer 2011	3.40E-05
rs3746165	Chr19:1102212	G/A	0.433706	Moyer 2011	2.78E-02
rs3746923	Chr21:42406235	C/T	0.429313	Moyer 2011	2.56E-05
rs3749166	Chr2:240598004	A/G	0.488219	Harrill 2009	
rs3795578	Chr1:204143856	G/A	0.403754	Moyer 2011	7.18E-06
rs3799732	Chr6:125253363	T/C	0.48103	Moyer 2011	6.49E-05
rs3825924	Chr15:100905695	G/A	0.213458	Moyer 2011	1.73E-05
rs3828599	Chr5:151022235	G/A	0.416933	Moyer 2011	1.80E-03
rs3857596	Chr6:50937354	C/T	0.176318	Moyer 2011	7.75E-05
rs3957358	Chr6:53446762	G/T	0.284345	Moyer 2011	4.18E-02
rs4148411	Chr17:50656384	G/C	0.149161	Moyer 2011	3.41E-02
rs4289753	Chr7:49516998	G/A	0.146565	Moyer 2011	7.19E-05
rs4495049	Chr4:126017998	C/A	0.0926518	Moyer 2011	9.43E-05
rs4563418	Chr3:88430636	G/A	0.211861	Moyer 2011	3.87E-05
rs4585742	Chr8:67822534	A/G	0.282348	Moyer 2011	6.05E-05
rs4710625	Chr6:66787937	C/G	0.464257	Moyer 2011	8.39E-05
rs4715210	Chr6:50929538	C/T	0.176118	Moyer 2011	7.75E-05
rs4715359	Chr6:52876817	A/G	0.272564	Moyer 2011	6.80E-03
rs4764486	Chr12:6218823	C/T	0.392971	Moyer 2011	5.27E-05
rs4773861	Chr13:95254618	C/T	0.0726837	Moyer 2011	3.34E-02
rs4869233	Chr5:95089838	T/C	0.322284	Moyer 2011	2.28E-05
rs5936441	ChrX:148242736	C/T	0.445828	Moyer 2011	5.38E-06
rs6032545	Chr20:45794066	G/T/A	0.495008	Moyer 2011	6.48E-05
rs6083315	Chr20:23883158	A/G	0.416933	Moyer 2011	7.52E-05
rs6124741	Chr20:45776008	T/C	0.493211	Moyer 2011	8.31E-05
rs6502555	Chr17:2826358	T/C	0.452875	Moyer 2011	3.11E-05
rs6553786	Chr4:174379453	C/T	0.197085	Moyer 2011	8.16E-05
rs6737742	Chr2:239294326	G/A	0.164537	Moyer 2011	5.53E-05
rs6789170	Chr3:107870704	G/T	0.072484	Moyer 2011	3.63E-05
rs6795028	Chr3:88431940	A/G	0.480831	Moyer 2011	6.05E-06
rs6809413	Chr3:88463299	G/A	0.463858	Moyer 2011	5.47E-06
rs6810790	Chr4:20514047	A/G	0.208466	Moyer 2011	8.17E-05
rs6852435	Chr4:174379628	T/C	0.226837	Moyer 2011	5.71E-06
rs6878801	Chr5:116872209	C/T	0.479832	Moyer 2011	6.77E-05
rs6922172	Chr6:53441156	C/T	0.0964457	Moyer 2011	2.60E-02
rs6949916	Chr7:49494648	A/G	0.11881	Moyer 2011	8.53E-05
rs707148	Chr5:151010686	T/G	0.319888	Moyer 2011	1.73E-02
rs718068	Chr8:21245385	T/C	0.247604	Moyer 2011	5.25E-05
rs7329514	Chr13:95264546	G/A	0.0792732	Moyer 2011	2.39E-02
rs7526132	Chr1:205584957	G/C	0.425919	Moyer 2011	3.87E-06
rs7665426	Chr4:174404535	G/T	0.214856	Moyer 2011	2.17E-05
rs766606	Chr13:95001913	A/C	0.335463	Moyer 2011	1.21E-02

Supplementary Table 26. –Continued.

rs7726138	Chr5:86826950	A/G	0.332069	Moyer 2011	5.44E-05
rs7738812	Chr6:88206884	A/T	0.0940495	Moyer 2011	8.52E-05
rs776746	Chr7:99672916	C/T	0.378594	Court 2014	3.40E-02
rs777952	Chr3:104727844	C/T	0.255192	Moyer 2011	5.73E-05
rs7987903	Chr13:94818417	T/C	0.0780751	Moyer 2011	4.80E-03
rs8001657	Chr13:95091793	C/T	0.184305	Moyer 2011	3.34E-02
rs8081984	Chr17:6783247	T/G	0.1252	Moyer 2011	7.46E-05
rs8177426	Chr5:151023379	G/A	0.249401	Moyer 2011	1.94E-02
rs8191438	Chr11:67583625	C/G	0.0469249	Moyer 2011	2.70E-02
rs8191439	Chr11:67583826	G/A	0.0469249	Moyer 2011	3.40E-02
rs8330	Chr2:233772999	C/G	0.254992	Court 2013	2.70E-02
rs908262	Chr2:239295827	C/A	0.186502	Moyer 2011	3.71E-05
rs9367532	Chr6:53446041	G/A	0.278554	Moyer 2011	1.57E-02
rs943005	Chr6:50898107	C/T	0.174321	Moyer 2011	7.78E-05
rs9473924	Chr6:50866444	G/T	0.356629	Moyer 2011	8.49E-05
rs9473932	Chr6:50890282	G/A	0.354633	Moyer 2011	3.26E-05
rs948999	Chr11:130828644	T/C	0.405351	Moyer 2011	6.95E-05
rs9508207	Chr13:28984557	C/T	0.216853	Moyer 2011	6.79E-05
rs9590150	Chr13:94978603	A/T	0.490615	Moyer 2011	2.78E-02
rs9590154	Chr13:94999100	T/G	0.311901	Moyer 2011	2.80E-02
rs9784215	Chr21:42403627	C/A	0.4373	Moyer 2011	2.73E-05
rs9984523	Chr21:41512104	C/T	0.0555112	Moyer 2011	8.76E-05
rs9997440	Chr4:31206989	A/T	0.116414	Moyer 2011	3.83E-05

*, GRCh38.p5; #, Major Allele/ Minor Allele; ^, 1000 Genome Phase 3

Supplementary Table 27: Summary of Ensembl GrCh38.p5 transcripts of 147 APAP-associated SNPs.

SNP	Transcripts*
rs10110651	ENST00000495560
rs10144421	ENST00000557275, ENST00000334258, ENST00000554873, ENST00000555759, ENST00000553340
rs10186482	ENST00000409198, ENST00000604864, ENST00000603639, ENST00000427231, ENST00000618972, ENST00000397345, ENST00000172853, LRG_202t1
rs1042640	ENST00000430892, ENST00000428446, ENST00000454283, ENST00000610772, ENST00000482026, ENST00000344644, ENST00000373445, ENST00000373450, ENST00000354728, ENST00000373414, ENST00000373424, ENST00000446481, ENST00000305139, ENST00000406651, ENST00000305208, ENST00000360418, ENST00000373426, ENST00000373409, ENST00000450233, LRG_733t1
rs10485114	
rs10508010	
rs10511137	
rs10515465	ENST00000254908, ENST00000512783, ENST00000504352, ENST00000510013, ENST00000454092, ENST00000509243, ENST00000498999, ENST00000580862
rs10849421	ENST00000382518, ENST00000543916, ENST00000536586, ENST00000382519, ENST00000546073, ENST00000538834, ENST00000538418, ENST00000009180, ENST00000382515, ENST00000610354, ENST00000617871
rs10852886	ENST00000321535, ENST00000572251, ENST00000575022, ENST00000571744
rs10929303	ENST00000430892, ENST00000428446, ENST00000454283, ENST00000610772, ENST00000482026, ENST00000344644, ENST00000373445, ENST00000373450, ENST00000354728, ENST00000373414, ENST00000373424, ENST00000446481, ENST00000305139, ENST00000406651, ENST00000305208, ENST00000360418, ENST00000373426, ENST00000373409, ENST00000450233, LRG_733t1
rs11070109	ENST00000376887, ENST00000536256, ENST00000629385
rs11129122	
rs11153350	ENST00000230538, ENST00000522006, ENST00000389463, ENST00000424408, ENST00000521398, ENST00000519932, ENST00000431543, ENST00000243219, ENST00000521690, ENST00000368638, ENST00000453937, ENST00000455073, ENST00000433684, ENST00000588837, ENST00000590293, ENST00000585450, ENST00000629766, ENST00000590804, ENST00000590584, ENST00000627025, ENST00000585504, ENST00000590673, ENST00000585611, ENST00000587816, LRG_433t1, LRG_433t2
rs11248859	ENST00000348261, ENST00000565831, ENST00000564954, ENST00000358590
rs11611637	
rs11766607	
rs1189434	ENST00000376887
rs1189436	ENST00000376887
rs1189437	ENST00000376887
rs1189439	ENST00000376887
rs11909987	ENST00000635189, ENST00000291535, ENST00000635108, ENST00000635325, ENST00000634453, ENST00000634718, ENST00000319294, ENST00000398367, ENST00000473381
rs12107308	ENST00000384586
rs12120268	
rs12267329	ENST00000381312
rs12584534	ENST00000376887, ENST00000536256, ENST00000629385

Supplementary Table 27. –Continued.

rs12700386	ENST00000325042, ENST00000404625, ENST00000426291, ENST00000401651, ENST00000485300, ENST00000407492, ENST00000401630, ENST00000406575, ENST00000258743
rs13015146	ENST00000498697, ENST00000469462, ENST00000541917, ENST00000475212
rs13101122	
rs13204006	ENST00000606851, ENST00000607048, ENST00000444265
rs13326165	ENST00000321725, ENST00000481607, ENST00000479355
rs1343151	ENST00000347310, ENST00000425614, ENST00000473881, ENST00000395227
rs1354510	ENST00000457106, ENST00000342310, ENST00000294816, ENST00000489443, ENST00000367893
rs1356553	
rs1372940	
rs1377392	
rs1380292	
rs1467558	ENST00000510619, ENST00000528869, ENST00000263398, ENST00000415148, ENST00000528086, ENST00000428726, ENST00000526669, ENST00000425428, ENST00000433892, ENST00000278386, ENST00000434472, ENST00000352818, ENST00000442151, ENST00000525211, ENST00000526000, ENST00000279452, ENST00000527889, ENST00000531873, ENST00000531110, ENST00000525685, ENST00000534296, ENST00000525688, ENST00000278385, ENST00000533222, ENST00000525241, ENST00000526553, ENST00000534082, ENST00000525293, ENST00000528672, ENST00000532339
rs1532815	ENST00000457106, ENST00000342310, ENST00000294816, ENST00000489443, ENST00000367893
rs1536343	ENST00000614005
rs1599096	
rs16851554	ENST00000331683, ENST00000406979, ENST00000452556, ENST00000451561, ENST00000480494
rs16900696	ENST00000523584
rs16950155	
rs16950190	
rs17310467	ENST00000216951
rs17413355	ENST00000354212, ENST00000419488, ENST00000629359, ENST00000626691, ENST00000522391, ENST00000519748, ENST00000520379, ENST00000630991, ENST00000628781, ENST00000634996, ENST00000535697, ENST00000628980, ENST00000450028, ENST00000421208
rs17469886	
rs1751043	ENST00000376887, ENST00000474158, ENST00000467685
rs17559005	
rs17640676	ENST00000295101, ENST00000493505, ENST00000544049
rs1764425	
rs1766908	
rs1876381	
rs1902023	ENST00000338206
rs1925851	
rs1925856	ENST00000563184
rs1925860	

Supplementary Table 27. –Continued.

rs1982562	
rs1989983	ENST00000502435, ENST00000505699, ENST00000502426, ENST00000285238, ENST00000515707, ENST00000513511, ENST00000427699
rs2031920	ENST00000622716, ENST00000488261, ENST00000463117, ENST00000541261, ENST00000477500, ENST00000541080, ENST00000421586, ENST00000418356, ENST00000480558, ENST00000252945
rs2064504	ENST00000481847, ENST00000337205, ENST00000243938, ENST00000474942, ENST00000372632, ENST00000372630, ENST00000471401, ENST00000493693, ENST00000487343, ENST00000462017, ENST00000467679, ENST00000490877, ENST00000408119
rs2074451	ENST00000631948, ENST00000622719, ENST00000634172, ENST00000631689, ENST00000632999, ENST00000612198, ENST00000361757, ENST00000438103, ENST00000587024, ENST00000587673, ENST00000586109, ENST00000354171, ENST00000589115, ENST00000611653, ENST00000593032, ENST00000588919, ENST00000585362, ENST00000614791, ENST00000587648, ENST00000592940, ENST00000587932, ENST00000585480, ENST00000622390, ENST00000616066
rs2082603	
rs2089515	
rs2209631	ENST00000614005
rs2218988	ENST00000417172, ENST00000436461, ENST00000422748, ENST00000454108, ENST00000430085, ENST00000482470, ENST00000361675, ENST00000361901, ENST00000489019, ENST00000445569, ENST00000435928
rs2344953	
rs2397105	ENST00000493331, ENST00000334575
rs2397132	ENST00000616666, ENST00000412182
rs2524290	ENST00000394836, ENST00000301773, ENST00000531922
rs2567513	ENST00000255559, ENST00000542342, ENST00000579988, ENST00000582769
rs2720666	ENST00000513868, ENST00000512617, ENST00000521600, ENST00000522875, ENST00000523190, ENST00000616386
rs2720667	ENST00000513868, ENST00000512617, ENST00000521600, ENST00000522875, ENST00000523190, ENST00000616386
rs2737844	ENST00000267512, ENST00000533601, ENST00000552941, ENST00000549987, ENST00000553743, ENST00000551823, ENST00000553522, ENST00000389614, ENST00000557049, ENST00000557323, ENST00000612794, ENST00000551947, ENST00000551093
rs2748991	
rs279874	ENST00000382276, ENST00000569227
rs2880961	
rs319590	ENST00000254908, ENST00000512783, ENST00000504352, ENST00000510013, ENST00000501056
rs319594	ENST00000254908, ENST00000512783, ENST00000504352, ENST00000510013
rs3208829	ENST00000230538, ENST00000522006, ENST00000389463, ENST00000424408, ENST00000521398, ENST00000519932, ENST00000431543, ENST00000243219, ENST00000521690, ENST00000368638, ENST00000453937, ENST00000455073, ENST00000433684, ENST00000588837, ENST00000590293, ENST00000585450, ENST00000629766, ENST00000590804, ENST00000590584, ENST00000628122, ENST00000627025, ENST00000585504, ENST00000590673, ENST00000585611, ENST00000587816, LRG_433t1, LRG_433t2
rs33966381	

Supplementary Table 27. –Continued.

rs3744198	ENST00000425042, ENST00000534480, ENST00000578002, ENST00000532894, ENST00000318565, ENST00000583244, ENST00000530857, ENST00000528902, ENST00000532900, ENST00000581676, ENST00000530904, ENST00000525128, ENST00000579818
rs3746165	ENST00000354171, ENST00000589115, ENST00000611653, ENST00000593032, ENST00000588919, ENST00000585362, ENST00000614791, ENST00000587648, ENST00000592940, ENST00000587932, ENST00000585480, ENST00000622390, ENST00000616066
rs3746923	ENST00000635189, ENST00000291535, ENST00000635108, ENST00000635325, ENST00000634453, ENST00000634718, ENST00000319294, ENST00000398367, ENST00000473381
rs3749166	ENST00000391984, ENST00000404753, ENST00000270364, ENST00000352879, ENST00000357048, ENST00000416591, ENST00000354082, ENST00000270361, ENST00000391983, ENST00000494738, ENST00000465943, ENST00000483602, ENST00000493058, ENST00000426297
rs3795578	ENST00000433869, ENST00000367201, ENST00000367202, ENST00000367197, ENST00000422072, ENST00000472340, ENST00000492392, ENST00000422699, ENST00000452983, ENST00000444817, ENST00000477125
rs3799732	ENST00000304877, ENST00000534000, ENST00000368402, ENST00000368388, ENST00000527711, ENST00000392483, ENST00000528193, ENST00000532978, ENST00000532429, ENST00000534199, ENST00000392482, ENST00000524679, ENST00000532423, ENST00000530868, ENST00000608456, ENST00000609477
rs3825924	ENST00000329841, ENST00000346623, ENST00000558869, ENST00000560351
rs3828599	ENST00000388825, ENST00000521722, ENST00000521650, ENST00000519214, ENST00000517973, ENST00000625178, ENST00000521632, ENST00000520597, ENST00000520059, ENST00000614343, ENST00000622181, ENST00000624359
rs3857596	
rs3957358	
rs4148411	ENST00000515585, ENST00000505699, ENST00000502426, ENST00000285238, ENST00000513511, ENST00000427699
rs4289753	
rs4495049	
rs4563418	ENST00000384586
rs4585742	
rs4710625	
rs4715210	
rs4715359	ENST00000616666, ENST00000412182
rs4764486	ENST00000382518, ENST00000543916, ENST00000536586, ENST00000382519, ENST00000546073, ENST00000538834, ENST00000538418, ENST00000009180, ENST00000382515, ENST00000610354, ENST00000617871
rs4773861	ENST00000376887, ENST00000536256, ENST00000629385
rs4869233	ENST00000515393, ENST00000503301, ENST00000513695
rs5936441	
rs6032545	ENST00000372622, ENST00000449078, ENST00000456939, ENST00000415790, ENST00000435014, ENST00000481847, ENST00000337205, ENST00000243938, ENST00000372632, ENST00000372630, ENST00000471401, ENST00000493693, ENST00000487343, ENST00000462017, ENST00000467679, ENST00000490877, ENST00000465935
rs6083315	ENST00000304710

Supplementary Table 27. –Continued.

rs6124741	ENST00000481847, ENST00000337205, ENST00000243938, ENST00000474942, ENST00000372632, ENST00000372630, ENST00000471401, ENST00000493693, ENST00000487343, ENST00000462017, ENST00000467679, ENST00000490877, ENST00000408119
rs6502555	ENST00000540393, ENST00000254695, ENST00000366401, ENST00000542807
rs6553786	ENST00000508815
rs6737742	ENST00000345617, ENST00000463007, ENST00000493582, ENST00000535493, ENST00000446876, ENST00000544989, ENST00000543185
rs6789170	ENST00000464359, ENST00000488852, ENST00000464823, ENST00000466155, ENST00000612802, ENST00000608110, ENST00000601930, ENST00000596110, ENST00000608306, ENST00000601385, ENST00000600749, ENST00000608647, ENST00000608137, ENST00000475362, ENST00000600240, ENST00000473528, ENST00000608307, ENST00000609429, ENST00000607880
rs6795028	ENST00000384586
rs6809413	
rs6810790	ENST00000503823, ENST00000504154, ENST00000273739, ENST00000503837, ENST00000622093
rs6852435	ENST00000508815
rs6878801	
rs6922172	
rs6949916	
rs707148	
rs718068	
rs7329514	ENST00000376887, ENST00000536256, ENST00000629385
rs7526132	ENST00000475956, ENST00000367147, ENST00000539267, ENST00000489709, ENST00000616173, ENST00000536357, ENST00000621216, ENST00000614644
rs7665426	
rs766606	
rs7726138	
rs7738812	
rs776746	ENST00000222982, ENST00000469887, ENST00000461920, ENST00000463364, ENST00000481825, ENST00000466061, ENST00000480723, ENST00000463907, ENST00000439761, ENST00000469622, ENST00000456417, ENST00000489231, ENST00000339843
rs777952	
rs7987903	
rs8001657	ENST00000376887, ENST00000536256, ENST00000629385
rs8081984	ENST00000321535, ENST00000572251, ENST00000575022
rs8177426	ENST00000388825, ENST00000521722, ENST00000521650, ENST00000519214, ENST00000517973, ENST00000625178, ENST00000521632, ENST00000520597, ENST00000520059, ENST00000614343, ENST00000622181
rs8191438	ENST00000398606, ENST00000398603, ENST00000494593, ENST00000489040, ENST00000498765, ENST00000467591, ENST00000495996, LRG_723t1
rs8191439	ENST00000398606, ENST00000398603, ENST00000494593, ENST00000489040, ENST00000498765, ENST00000467591, ENST00000495996, LRG_723t1

Supplementary Table 27. –Continued.

rs8330	ENST00000373424, ENST00000446481, ENST00000305139, ENST00000406651, ENST00000354728, ENST00000373414, ENST00000482026, ENST00000373409, ENST00000450233, ENST00000430892, ENST00000428446, ENST00000454283, ENST00000610772, ENST00000373426, ENST00000305208, ENST00000360418, ENST00000344644, ENST00000373445, ENST00000373450, LRG_733t1
rs908262	ENST00000345617, ENST00000463007, ENST00000493582, ENST00000535493, ENST00000446876, ENST00000544989, ENST00000543185
rs9367532	
rs943005	ENST00000402760
rs9473924	
rs9473932	
rs948999	
rs9508207	ENST00000612955
rs9590150	
rs9590154	
rs9784215	ENST00000635189, ENST00000291535, ENST00000635108, ENST00000635325, ENST00000634453, ENST00000634718, ENST00000319294, ENST00000398367, ENST00000473381
rs9984523	ENST00000332149, ENST00000458356, ENST00000454499, ENST00000424093, ENST00000497881, ENST00000463138, ENST00000398585
rs9997440	ENST00000515292

*GRCh38.p5

Supplementary Table 28: Summary of Ensembl GrCh38.p5 regulatory annotation of 147 APAP-associated SNPs.

SNP	Regulatory Features*	GrCh38 Compiled ENSEMBL Variant Consequence	Non-coding RNA biotype*	Non-coding RNA gene*	SIFT prediction	PolyPhen prediction	Amino acid
rs10110651		upstream gene variant	processed pseudogene	AC090453.1-001			
rs10144421		intron variant, non coding transcript variant	-				
rs10186482		intron variant	-				
rs1042640		upstream gene variant, 3 prime UTR variant, downstream gene variant, NMD transcript variant					
rs10485114			-				
rs10508010			-				
rs10511137			misc RNA	Y RNA.529-201			
rs10515465		intron variant, NMD transcript variant, non coding transcript variant, upstream gene variant, downstream gene variant	-				
rs10849421		intron variant, non coding transcript variant	-				
rs10852886		downstream gene variant, NMD transcript variant, intron variant	-				
rs10929303		upstream gene variant, 3 prime UTR variant, downstream gene variant, NMD transcript variant					
rs11070109		intron variant	-				
rs11129122			snRNA, miRNA	RNU6-788P-201, MIR548AC			
rs11153350		upstream gene variant, non coding transcript variant, intron variant, non coding transcript exon variant	antisense	RP11-506B6.6			
rs11248859		intron variant, upstream gene variant	-				
rs11611637			linc RNA, ncRNA	RP11-541G9.2-001, RMST			
rs11766607			linc RNA	AC010971.1-001			
rs1189434		intron variant	-				

Supplementary Table 28. –Continued.

rs1189436	ENSR0000 1619905, ENSR0000 1036605	intron variant, regulatory region variant	-	
rs1189437	ENSR0000 1036605	intron variant, regulatory region variant	-	
rs1189439		intron variant	-	
rs11909987		upstream gene variant	-	
rs12107308		downstream gene variant	misc RNA	Y RNA.529-201
rs12120268			-	
rs12267329		intron variant	-	
rs12584534		intron variant	-	
rs12700386		downstream gene variant, upstream gene variant	antisense	AC073072.5-001
rs13015146		downstream gene variant, non coding transcript variant, non coding transcript exon variant	processed pseudogene	DAZAP2P1-001
rs13101122			-	
rs13204006	ENSR0000 1213359	non coding transcript variant, regulatory region variant, intron variant	linc RNA	RP11-377N20.1, CASC15
rs13326165	ENSR0000 1479196	intron variant, regulatory region variant, non coding transcript variant	-	
rs1343151		intron variant, NMD transcript variant	-	
rs1354510		upstream gene variant, intron variant, non coding transcript variant	-	
rs1356553			-	
rs1372940			linc RNA, miRNA	RP11-675P14.1-001, MIR302F
rs1377392	ENSR0000 1496109	regulatory region variant	misc RNA	RN7SKP256-201
rs1380292	ENSR0000 1387319	regulatory region variant	linc RNA, ncRNA	RP11-24P4.1-001, RP11-24P4.1-002, LOC286114

Supplementary Table 28. –Continued.

rs1467558		upstream gene variant, downstream gene variant, intron variant, missense variant, non coding transcript variant, NMD transcript variant, non coding transcript exon variant,	-		tolerated	benign	I/T
rs1532815		non coding transcript variant, non coding transcript exon variant, intron variant	antisense	RP11-38C18.2			
rs1536343	ENSR0000 1508952	non coding transcript variant, regulatory region variant, intron variant	linc RNA	RP11-50D16.4			
rs1599096			linc RNA, ncRNA	RP11-24P4.1-001, RP11-24P4.1-001, LOC286114			
rs16851554		intron variant, NMD transcript variant, non coding transcript variant	-				
rs16900696	ENSR0000 1408138	non coding transcript variant, regulatory region variant, intron variant	antisense	RP11-152K4.2-001			
rs16950155			antisense	SOX21-AS1			
rs16950190			antisense	SOX21-AS1			
rs17310467		upstream gene variant	-				
rs17413355		intron variant, non coding transcript variant, upstream gene variant	pseudogene	RPL13AP17			
rs17469886	ENSR0000 1720964	regulatory region variant	-				
rs1751043		intron variant, upstream gene variant	-				
rs17559005			-				
rs17640676		intron variant, non coding transcript variant	-				
rs1764425			misc RNA	RNY4P27-201			
rs1766908			misc RNA	RNY4P27-201			
rs1876381			linc RNA	RP11-99H20.1-001, RP11-99H20.1-002			
rs1902023		missense variant			tolerated	benign	Y/D

Supplementary Table 28. –Continued.

rs1925851	ENSR00000518959	regulatory region variant	linc RNA	LINC00557
rs1925856		downstream gene variant	linc RNA	LINC00557
rs1925860			snRNA	RNU6-62P-201
rs1982562			misc RNA	Y RNA.529-201
rs1989983		upstream gene variant	antisense	CTB-22K21.2
rs2031920		non coding transcript variant, non coding transcript exon variant, downstream gene variant, intron variant, upstream gene variant	-	
rs2064504		non coding transcript variant, intron variant, downstream gene variant, upstream gene variant	-	
rs2074451	ENSR00000640654	downstream gene variant, regulatory region variant	-	
rs2082603			snoRNA, ncRNA	SNORD65.1-201, LINC01098
rs2089515	ENSR00001722376	regulatory region variant	-	
rs2209631		non coding transcript variant, intron variant	linc RNA	RP11-50D16.4
rs2218988	ENSR00001564179	intron variant, regulatory region variant, NMD transcript variant, non coding transcript variant	-	
rs2344953			misc RNA	Y RNA.529-201
rs2397105	ENSR00001704513	downstream gene variant, regulatory region variant	-	
rs2397132	ENSR00001704518, ENSR00001496077	intron variant, regulatory region variant, non coding transcript variant	-	
rs2524290	ENSR00000319346	upstream gene variant, regulatory region variant, 5 prime UTR variant	-	
rs2567513		intron variant, non coding transcript variant	-	
rs2720666	ENSR00001401713	non coding transcript variant, regulatory region variant, intron variant, downstream gene variant	-	
rs2720667		non coding transcript variant, intron variant, downstream gene variant	-	

Supplementary Table 28. –Continued.

rs2737844	ENSR0000 0419397	downstream gene variant, regulatory region variant, NMD transcript variant, intron variant	-		
rs2748991	ENSR0000 1218546	regulatory region variant	pseudogene	GSTA7P	
rs279874		intron variant	-		
rs2880961			misc RNA	Y RNA.529-201	
rs319590		intron variant, NMD transcript variant, non coding transcript variant, downstream gene variant	-		
rs319594		intron variant, NMD transcript variant, non coding transcript variant	-		
rs3208829	ENSR0000 1224733	intron variant, regulatory region variant, downstream gene variant, non coding transcript variant	-		
rs33966381			misc RNA	Y RNA.529-201	
rs3744198		synonymous variant, 3 prime UTR variant, NMD transcript variant, upstream gene variant, downstream gene variant	-		A
rs3746165		upstream gene variant	-		
rs3746923	ENSR0000 0185890	intron variant, regulatory region variant, NMD transcript variant, non coding transcript variant	-		
rs3749166		synonymous variant, intron variant, 3 prime UTR variant, NMD transcript variant, non coding transcript variant, non coding transcript exon variant, downstream gene variant, upstream gene variant	-		A
rs3795578		downstream gene variant, intron variant, upstream gene variant, non coding transcript variant	-		
rs3799732	ENSR0000 1499510	intron variant, regulatory region variant, downstream gene variant, non coding transcript variant, non coding transcript exon variant, NMD transcript variant	-		
rs3825924		splice region variant, intron variant, non coding transcript variant	-		

Supplementary Table 28. –Continued.

rs3828599	ENSR00001294023	intron variant, regulatory region variant, non coding transcript variant, NMD transcript variant, downstream gene variant, upstream gene variant	-	
rs3857596			-	
rs3957358			ncRNA	AL591034.1
rs4148411		upstream gene variant, NMD transcript variant, intron variant	-	
rs4289753			-	
rs4495049			lincRNA, miRNA	RP11-318I4.1-001, MIR2054
rs4563418		upstream gene variant	misc RNA	Y RNA.529-201
rs4585742			-	
rs4710625			snRNA, pseudogene	RNU7-66P-201, MCART3P
rs4715210			-	
rs4715359	ENSR00001496077	intron variant, regulatory region variant, non coding transcript variant	unprocessed pseudogene	GSTA10P
rs4764486	ENSR00000425731	intron variant, regulatory region variant, non coding transcript variant	-	
rs4773861	ENSR00001511482	intron variant, regulatory region variant	-	
rs4869233		intron variant, non coding transcript variant	-	
rs5936441			-	
rs6032545		intron variant, upstream gene variant	-	
rs6083315		upstream gene variant	-	
rs6124741		non coding transcript variant, intron variant, upstream gene variant	-	
rs6502555	ENSR00001339172	intron variant, regulatory region variant	-	
rs6553786		upstream gene variant	linc RNA, miRNA	RP11-51M24.1-001, MIR4276
rs6737742		intron variant, non coding transcript variant	-	

Supplementary Table 28. –Continued.

rs6789170		non coding transcript variant, intron variant	linc RNA	RP11-631B21.1, LINC00635			
rs6795028		downstream gene variant	misc RNA	Y RNA.529-201			
rs6809413			misc RNA	Y RNA.529-201			
rs6810790		intron variant	-				
rs6852435		upstream gene variant	linc RNA, miRNA	RP11-51M24.1-001, MIR4276			
rs6878801			linc RNA	CTC-472C24.1-001			
rs6922172	ENSR00001218714	regulatory region variant	ncRNA	AL591034.1			
rs6949916			linc RNA	AC010971.1-001			
rs707148			-				
rs718068			lincRNA, ncRNA	RP11-24P4.1-001, RP11-24P4.1-002, LOC286114			
rs7329514		intron variant	-				
rs7526132	ENSR00000671996	3 prime UTR variant, regulatory region variant, NMD transcript variant, missense variant, downstream gene variant	-		tolerated	benign	G/A
rs7665426			miRNA	MIR4276			
rs766606			snRNA	RNU6-62P-201			
rs7726138			linc RNA	CTC-493L21.2-001			
rs7738812			-				
rs776746		intron variant, splice acceptor variant, non coding transcript variant, non coding transcript exon variant, NMD transcript variant, downstream gene variant	-				
rs777952			miRNA	MIR548A3			
rs7987903			-				

Supplementary Table 28. –Continued.

rs8001657		intron variant, downstream gene variant	-	
rs8081984		intron variant, upstream gene variant	-	
rs8177426	ENSR0000 1294023, ENSR0000 1698982	intron variant, regulatory region variant, non coding transcript variant, NMD transcript variant, downstream gene variant, upstream gene variant	-	
rs8191438	ENSR0000 0564238	5 prime UTR variant, regulatory region variant, upstream gene variant	-	
rs8191439	ENSR0000 0564238	5 prime UTR variant, regulatory region variant, non coding transcript variant, non coding transcript exon variant, upstream gene variant	-	
rs8330		downstream gene variant, 3 prime UTR variant, NMD transcript variant, upstream gene variant	-	
rs908262	ENSR0000 0610600	intron variant, regulatory region variant, non coding transcript variant	-	
rs9367532			ncRNA	AL591034.1
rs943005		non coding transcript variant, non coding transcript exon variant	processed pseudogene	RP4-753D5.3-001
rs9473924			-	
rs9473932			-	
rs948999	ENSR0000 1608376	regulatory region variant	linc RNA	RP11-890B15.2-001, RP11-890B15.2-001
rs9508207		intron variant	-	
rs9590150			linc RNA	LINC00557-001
rs9590154			snRNA	RNU6-62P-201
rs9784215		intron variant, upstream gene variant	-	
rs9984523		upstream gene variant, intron variant	-	
rs9997440		non coding transcript variant, intron variant	linc RNA	RP11-617I14.1-001

*, GRCh38.p5

Supplementary Table 29: Summary of HaploReg v4.1 annotations of 147 APAP-associated SNPs.

SNP	GERP cons°	SiPhy cons°	Promoter histone marks	Enhancer histone marks	DNAse	Proteins bound	Motifs changed	NHGRI /EBI GWAS hits	GRASP QTL hits	eQTL hits	GEN CODE genes	RefSeq genes	dbSNP func. Annot.+
rs10110651										3 hits	53kb 3' of KCNU 1	53kb 3' of KCNU1	
rs10144421					SKIN,A DRL,MU S	GATA2	Nrf-2,TCF11: :MafG		1 hit	9 hits	SYNE 3	C14orf4 9	intronic
rs10186482							6 altered motifs			14 hits	NEB	NEB	intronic
rs1042640						CTCF,R AD21	BCL,TH AP1,YY 1				UGT1 A1	UGT1A 1	3'-UTR
rs10485114							Eomes			1 hit	134kb 3' of FRK	134kb 3' of FRK	
rs10508010							NRSF				13kb 3' of RP11-74A12. 2	45kb 3' of ABCC4	
rs10511137							4 altered motifs				32kb 3' of Y_RN A	305kb 3' of C3orf38	intronic
rs10515465							CTCF,Ra d21,SMC 3			9 hits	PCBD 2	PCBD2	intronic
rs10849421					BRST,S KIN		Gfi1,Hdx ,STAT			1 hit	CD9	CD9	intronic

Supplementary Table 29. –Continued.

rs10852886		BRST,SKIN,BRST		4 altered motifs	1 hit	11 hits	TEKT1	1.9kb 3' of FBXO39	
rs10929303			CTCF,RAD21	6 altered motifs			UGT1A1	UGT1A1	3'-UTR
rs11070109	LNG	PANC		TCF11::MafG,VDR	1 hit		ABCC4	ABCC4	intronic
rs11129122	LNG			5 altered motifs			30kb 5' of U6	64kb 3' of MIR548AC	
rs11153350	ESDR, ADRL, HRT	ESDR,ESDR,ADRL		Spz1		1 hit	RP11-506B6.6	2.6kb 5' of LAMA4	intronic
rs11248859	4 tissues			BHLHE40,STAT			CACNA1H	CACNA1H	intronic
rs11611637				4 altered motifs			15kb 5' of RP11-541G9.2	173kb 5' of RMST	
rs11766607	6 tissues	SKIN		RBP-Jkappa			225kb 3' of AC010971.1	294kb 5' of VWC2	
rs1189434	BLD, VAS, SKIN			Myc,XBP-1			ABCC4	ABCC4	intronic
rs1189436	4 tissues	9 tissues		Hand1	1 hit		ABCC4	ABCC4	intronic

Supplementary Table 29. –Continued.

rs1189437		BLD, VAS	BLD	AP-1,Pax-8	1 hit		ABCC4	ABCC4	intronic
rs1189439	BLD	BLD		4 altered motifs			ABCC4	ABCC4	intronic
rs11909987	BLD	4 tissues	BLD			5 hits	1.6kb 5' of UBASH3A	1.6kb 5' of UBASH3A	
rs12107308		BLD		5 altered motifs			1.9kb 3' of Y_RNA	275kb 3' of C3orf38	intronic
rs12120268		ESDR		HNF4	1 hit	5 hits	15kb 5' of GPX7	15kb 5' of GPX7	
rs12267329				Cdx,HNF4,TCF4			ADARB2	ADARB2	intronic
rs12584534		ESDR		8 altered motifs			ABCC4	ABCC4	intronic
rs12700386	6 tissues	18 tissues	29 tissues	Smad			2kb 3' of AC073072.5	3.8kb 5' of IL6	
rs13015146		BLD, ADRL, SPLN		Hdx	2 hits		AC079354.1	8.8kb 3' of SUMO1	
rs13101122				4 altered motifs	1 hit		27kb 3' of Y_RNA	301kb 3' of C3orf38	intronic
rs13204006		13 tissues	6 tissues	5 altered motifs			34kb 3' of RP11-377N20.1	FLJ22536	intronic

Supplementary Table 29. –Continued.

rs13326165			4 tissues	12 tissues	BLD,BLD			1 hit	3 hits	12 hits	STAB1	STAB1	intronic
rs1343151								2 hits	1 hit	1 hit	IL23R	IL23R	intronic
rs1354510				ESDR			Myf,RP58				LMX1A	LMX1A	intronic
rs1356553				BLD			Ik-1,Ik-2,PLZF				9.2kb 5' of 7SK	73kb 3' of GCLC	
rs1372940											275kb 5' of RP11-675P14.1	139kb 3' of MIR302F	
rs1377392			FAT, LIV, BLD	15 tissues		4 bound proteins					18kb 5' of 7SK	64kb 3' of GCLC	
rs1380292					31 tissues	CTCF,RAD21,SMC3	Arid5b,Evi-1				51kb 5' of RP11-24P4.1	252kb 3' of LOC286114	
rs1467558	yes	yes		4 tissues	BLD,SKIN,BLD	POL2				9 hits	CD44	CD44	missense
rs1532815								1 hit	1 hit		RP11-38C18.2	LMX1A	intronic
rs1536343				4 tissues	6 tissues		14 altered motifs				50kb 3' of NHLRC3	51kb 3' of NHLRC3	
rs1599096				BRST			6 altered motifs				37kb 5' of RP11-24P4.1	266kb 3' of LOC286114	
rs16851554	yes	yes									SPAG16	SPAG16	intronic

Supplementary Table 29. –Continued.

rs16900696	STRM	7 tissues	10 tissues	ERALPHA_A,GR	AP-1,Arid5a,Hoxa5			5 hits	RP11-152K4.2	80kb 5' of CDH6	
rs16950155		4 tissues	SKIN,LNG		8 altered motifs				85kb 3' of SOX21-AS1	87kb 5' of SOX21	
rs16950190			ADRL		Maf				95kb 3' of SOX21-AS1	98kb 5' of SOX21	
rs17310467		IPSC, MUS, LIV		ZNF274	8 altered motifs	1 hit		12 hits	2kb 5' of GSS	MYH7B	intronic
rs17413355		ESDR, BRN							MAGI2	RPL13AP17	intronic
rs17469886		5 tissues	SKIN		Rad21		2 hits	8 hits	7.5kb 3' of CCDC25	7.5kb 3' of CCDC25	
rs1751043		ESDR	MUS		5 altered motifs				ABCC4	ABCC4	intronic
rs17559005					7 altered motifs				32kb 3' of Y_RNA	305kb 3' of C3orf38	intronic
rs17640676		PANC			NRSF		1 hit		KCNJ3	KCNJ3	intronic
rs1764425	ESDR	CRVX		STAT1,STAT3	LXR,STAT			1 hit	16kb 5' of RNY4P27	51kb 5' of ABCC4	
rs1766908		LNG, CRVX	BRST,CRVX	JUND	GR,Nkx2,Nkx3			1 hit	17kb 5' of RNY4P27	51kb 5' of ABCC4	

Supplementary Table 29. –Continued.

rs1876381			ESC, IPSC	ESC, ESDR, IPSC		8 altered motifs			52kb 3' of RP11-99H20.1	204kb 5' of SNX16	
rs1902023			LIV, BRN, GI	LNG		Dbx1,Hoxd8,Zfp105			UGT2B15	UGT2B15	missense
rs1925851			15 tissues	8 tissues	13 tissues	BCL,NF-kappaB			7.1kb 3' of RP11-74A12.2	51kb 3' of ABCC4	
rs1925856	yes	yes		ESDR	ESDR,ESDR	Pitx2			3kb 3' of RP11-74A12.2	55kb 3' of ABCC4	
rs1925860				7 tissues		Irx,RP58			26kb 5' of RNU6-62	26kb 3' of ABCC4	
rs1982562									28kb 3' of Y_RNA	301kb 3' of C3orf38	intronic
rs1989983	yes	yes		5 tissues	LNG,BLD		1 hit	2 hits	1.2kb 5' of CTB-22K21.2	1.7kb 5' of ABCC3	
rs2031920			LIV			7 altered motifs			CYP2E1	1kb 5' of CYP2E1	

Supplementary Table 29. –Continued.

rs2064504			GI, PLCNT	BRST,BRN,GI		6 altered motifs	19 hits	90 hits	WFDC3	WFDC3	intronic
rs2074451			17 tissues	28 tissues	6 bound proteins		1 hit	3 hits	248bp 3' of GPX4	247bp 3' of GPX4	
rs2082603			5 tissues			4 altered motifs			68kb 5' of SNORD65	763kb 3' of LOC285501	
rs2089515			8 tissues	5 tissues		BAF155	1 hit		20kb 5' of IMPAD1	20kb 5' of IMPAD1	
rs2209631			BRN	IPSC,BRN,BRN					50kb 3' of NHLRC3	51kb 3' of NHLRC3	
rs2218988	yes		7 tissues			GCNF,Pax-6			CALD1	CALD1	intronic
rs2344953						8 altered motifs			52kb 3' of Y_RNA	325kb 3' of C3orf38	
rs2397105		LIV	6 tissues		FOXA1, FOXA2	Cdc5	1 hit	11 hits	3.1kb 3' of GSTA1	2.9kb 3' of GSTA1	
rs2397132			11 tissues	20 tissues	HDAC2	Pou3f2		1 hit	19kb 3' of GSTA3	19kb 3' of GSTA3	
rs2524290		GI, LNG, BLD	14 tissues	6 tissues	12 bound proteins	LRH1,Pax-5,Smad	1 hit	1 hit	RAB3IL1	2.7kb 5' of RAB3IL1	

Supplementary Table 29. –Continued.

rs2567513				ESDR, SKIN, GI	GI		AhR,BDP1,Egr-1				SLC39A11	SLC39A11	intronic
rs2720666				8 tissues	BLD,BLD,BLD	6 bound proteins	HNF4,RXRA,TCF4				PVT1	PVT1	intronic
rs2720667				8 tissues	6 tissues	4 bound proteins	6 altered motifs				PVT1	PVT1	intronic
rs2737844			LIV, GI	GI, PANC, SKIN	GI		Esr2		10 hits	66 hits	GPX2	GPX2	intronic
rs2748991			BRN	8 tissues	IPSC						18kb 3' of GSTA2	7.7kb 3' of GSTA7P	
rs279874							DMRT1, Zfp187		1 hit		DMRT1	DMRT1	intronic
rs2880961							4 altered motifs	1 hit	1 hit		44kb 3' of Y_RNA	317kb 3' of C3orf38	
rs319590	yes	yes		4 tissues			Pou3f2,Pou3f3			9 hits	PCBD2	PCBD2	intronic
rs319594					BLD		7 altered motifs		1 hit	9 hits	PCBD2	PCBD2	intronic
rs3208829			12 tissues	4 tissues	MUS	P300	7 altered motifs			1 hit	LAMA4	LAMA4	intronic
rs33966381							Foxf2,Foxk1,Hoxc10				32kb 3' of Y_RNA	306kb 3' of C3orf38	intronic
rs3744198				4 tissues	ESDR,MUS		4 altered motifs			5 hits	C17orf28	C17orf28	synonymous
rs3746165			8 tissues	20 tissues	33 tissues	CTCF	ERalpha-a		1 hit	4 hits	1.7kb 5' of GPX4	1.7kb 5' of GPX4	

Supplementary Table 29. –Continued.

rs3746923		BLD, GI, THYM	IPSC, BLD	THYM		5 altered motifs			5 hits	UBASH3A	UBASH3A	intronic
rs3749166	yes		GI, ADRL, LIV			4 altered motifs			8 hits	CAPN10	CAPN10	synonymous
rs3795578		LIV	6 tissues				1 hit			ETNK2	ETNK2	intronic
rs3799732		STRM	9 tissues	BRST,SKIN,MUS		Foxo		5 hits	13 hits	TPD52L1	TPD52L1	intronic
rs3825924			BLD	IPSC		Rad21				ALDH1A3	ALDH1A3	intronic
rs3828599		11 tissues	8 tissues	SKIN		7 altered motifs		3 hits	5 hits	GPX3	GPX3	intronic
rs3857596						DMRT5,Sox,THAP1		2 hits	1 hit	90kb 3' of TFAP2B	90kb 3' of TFAP2B	
rs3957358		BLD	BLD, SKIN		ZNF263	CEBPB, Nkx3				9.7kb 3' of AL591034.1	51kb 3' of GCLC	
rs4148411			LIV, GI, LNG			Nkx6-1,Pou4f3,Pou6f1		2 hits	3 hits	ABCC3	ABCC3	intronic
rs4289753						Zfp105				257kb 5' of VWC2	257kb 5' of VWC2	
rs4495049						GR		1 hit		53kb 5' of RP11-318I4.1	511kb 3' of MIR2054	

Supplementary Table 29. –Continued.

rs4563418					HP1-site-factor,Hoxa13,Hoxb13		1 hit		554bp 5' of Y_RNA	273kb 3' of C3orf38	intronic
rs4585742		ESDR, LIV			Irf,SIX5, p300				76kb 5' of CPA6	76kb 5' of CPA6	
rs4710625									59kb 5' of RNU7-66P	998kb 3' of MCART3P	
rs4715210		ESC, ESDR, BLD			11 altered motifs			1 hit	82kb 3' of TFAP2B	82kb 3' of TFAP2B	
rs4715359		13 tissues			5 altered motifs		1 hit	1 hit	20kb 3' of GSTA3	20kb 3' of GSTA3	
rs4764486		17 tissues	9 tissues		Sox,ZBRK1		1 hit	1 hit	CD9	CD9	intronic
rs4773861	LNG	13 tissues	4 tissues	GATA2	14 altered motifs			1 hit	ABCC4	ABCC4	intronic
rs4869233					6 altered motifs				MCTP1	MCTP1	intronic
rs5936441						1 hit			216kb 3' of FMR1NB	216kb 3' of FMR1NB	
rs6032545		BLD, MUS, BRST	BLD,MUS				4 hits	84 hits	DNTTIP1	DNTTIP1	intronic
rs6083315		PANC			FXR,Nkx2				3.4kb 5' of CST5	3.4kb 5' of CST5	

Supplementary Table 29. –Continued.

rs6124741		GI			Nanog,Osr		15 hits	84 hits	WFDC3	WFDC3	intronic
rs6502555		BLD	19 tissues	CTCF,RAD21	PU.1,VDR			1 hit	RAP1GAP2	RAP1GAP2	intronic
rs6553786		ESC, IPSC					1 hit	1 hit	3kb 5' of RP11-51M24.1	44kb 5' of MIR4276	
rs6737742	BLD, GI	17 tissues	6 tissues	5 bound proteins	CCNT2,GATA,TAL1			1 hit	HDAC4	HDAC4	intronic
rs6789170					CIZ,Foxo,Irf				RP11-631B21.1	LOC151658	intronic
rs6795028					GATA,HDAC2		1 hit		630bp 3' of Y_RNA	274kb 3' of C3orf38	intronic
rs6809413					RXRA,Zec				32kb 3' of Y_RNA	305kb 3' of C3orf38	intronic
rs6810790			BLD						SLIT2	SLIT2	intronic
rs6852435		ESC, IPSC	BLD			1 hit	1 hit	1 hit	3.2kb 5' of RP11-51M24.1	44kb 5' of MIR4276	
rs6878801					Evi-1,Pou2f2				42kb 5' of CTC-472C24.1	297kb 5' of SEMA6A	

Supplementary Table 29. –Continued.

rs6922172				10 tissues	8 tissues	PU1	NRSF,Rhox11		15kb 3' of AL591034.1	56kb 3' of GCLC	
rs6949916									240kb 3' of AC010971.1	279kb 5' of VWC2	
rs707148				LIV			Duxl,Hdx		9.9kb 5' of GPX3	9.7kb 5' of GPX3	
rs718068				MUS			Zfp691		53kb 5' of RP11-24P4.1	250kb 3' of LOC286114	
rs7329514				LNG, BLD			6 altered motifs	1 hit	ABCC4	ABCC4	intronic
rs7526132	yes	yes		BLD, GI, PANC	IPSC,BLD,BLD	CTCF,RAD21		4 hits	MFSD4	MFSD4	missense
rs7665426	yes		ESDR	ESC, IPSC	LNG		6 altered motifs	1 hit	19kb 5' of MIR4276	19kb 5' of MIR4276	
rs766606				IPSC	ESDR,THYM		4 altered motifs		17kb 5' of RNU6-62	18kb 3' of ABCC4	
rs7726138						CEBPB	TCF12		27kb 3' of CTC-493L2 1.2	206kb 3' of COX7C	
rs7738812								3 hits	41kb 5' of CNR1	41kb 5' of CNR1	

Supplementary Table 29. –Continued.

rs776746			BLD, GI	GI		4 altered motifs	6 hits	11 hits	CYP3A5	CYP3A5	splice donor
rs777952						GATA,Gfi1	6 hits		639kb 5' of ALCAM	501kb 5' of MIR548A3	
rs7987903						RBP-Jkappa			104kb 3' of SOX21-AS1	106kb 5' of SOX21	
rs8001657			IPSC, ESC			Foxj2			ABCC4	ABCC4	intronic
rs8081984								2 hits	FBXO39	FBXO39	intronic
rs8177426		10 tissues	16 tissues	17 tissues	5 bound proteins	Myb,YY1		4 hits	GPX3	GPX3	intronic
rs8191438		22 tissues		51 tissues	26 bound proteins	18 altered motifs			GSTP1	GSTP1	5'-UTR
rs8191439		23 tissues		52 tissues	26 bound proteins	ETF,SP1			GSTP1	GSTP1	5'-UTR
rs8330						PPAR,SP2			UGT1A1	UGT1A1	3'-UTR
rs908262		10 tissues	16 tissues	6 tissues		8 altered motifs		1 hit	HDAC4	HDAC4	intronic
rs9367532		BLD	ESDR, BLD	BLD		9 altered motifs	1 hit		10kb 3' of AL591034.1	51kb 3' of GCLC	
rs943005	yes					Foxc1,Pou3f2		1 hit	50kb 3' of TFAP2B	50kb 3' of TFAP2B	

Supplementary Table 29. –Continued.

rs9473924							PTF1-beta,VDR	1 hit			19kb 3' of TFAP2B	19kb 3' of TFAP2B
rs9473932	yes	yes		4 tissues							43kb 3' of TFAP2B	43kb 3' of TFAP2B
rs948999			MUS	8 tissues	SKIN,MUS,MUS		AP-1,ATF3		1 hit		16kb 3' of RP11-890B15.2	47kb 3' of SNX19
rs9508207			ESDR	6 tissues	HRT		5 altered motifs				40kb 5' of MTUS2	40kb 5' of MTUS2
rs9590150				FAT			HP1-site-factor				17kb 3' of RP11-74A12.2	41kb 3' of ABCC4
rs9590154					IPSC		Evi-1,Nkx6-1,Pou2f2				20kb 5' of RNU6-62	21kb 3' of ABCC4
rs9784215			BLD, THYM, GI	5 tissues	5 tissues		PU.1,SP1,STAT		5 hits		271bp 5' of UBASH3A	281bp 5' of UBASH3A
rs9984523				GI, KID, PANC	GI,KID, GI	ERALPHA_A,GR	6 altered motifs				TMPRSS2	3.9kb 5' of TMPRSS2

Supplementary Table 29. –Continued.

rs9997440	6 altered motifs	RP11-617I14.1	60kb 3' of PCDH7

°, sequence constraint predicted by GREP or SiPhy; +, Canonical Splicing

Supplementary Table 30: Summary of GWAVA analysis of 147 APAP-associated SNPs.

SNP	Region score	TSS score	Unmatched score
rs10110651	0.33	0.14	0.18
rs10144421	0.21	0.18	0.22
rs10186482	0.21	0.22	0.14
rs1042640	0.41	0.77	0.79
rs10485114	0.44	0.26	0.05
rs10508010	0.39	0.35	0.14
rs10511137	0.25	0.12	0.03
rs10515465	0.45	0.06	0.09
rs10849421	0.39	0.22	0.16
rs10852886	0.27	0.33	0.35
rs10929303	0.37	0.75	0.81
rs11070109	0.41	0.37	0.22
rs11129122	0.35	0.23	0.02
rs11153350	0.19	0.12	0.15
rs11248859	0.27	0.16	0.2
rs11611637	0.33	0.17	0.07
rs11766607	0.3	0.16	0.02
rs1189434	0.34	0.28	0.14
rs1189436	0.29	0.27	0.16
rs1189437	0.41	0.23	0.22
rs1189439	0.3	0.25	0.17
rs11909987	0.22	0.35	0.56
rs12107308	0.28	0.13	0.13
rs12120268	0.37	0.17	0.16
rs12267329	0.41	0.1	0.02
rs12584534	0.3	0.23	0.06
rs12700386	0.55	0.64	0.69
rs13015146	0.38	0.28	0.51
rs13101122	0.27	0.03	0.01
rs13204006	0.43	0.28	0.19
rs13326165	0.21	0.35	0.37
rs1343151	0.47	0.4	0.19
rs1354510	0.23	0.2	0.09
rs1356553	0.35	0.31	0.14
rs1372940	0.49	0.24	0.08
rs1377392	0.41	0.41	0.23
rs1380292	0.46	0.44	0.26
rs1467558	0.45	0.43	0.51
rs1532815	0.32	0.23	0.68
rs1536343	0.36	0.42	0.17

Supplementary Table 30. –Continued.

rs1599096	0.37	0.26	0.05
rs16851554	0.36	0.26	0.04
rs16900696	0.51	0.43	0.22
rs16950155	0.43	0.4	0.13
rs16950190	0.5	0.28	0.07
rs17310467	0.24	0.43	0.44
rs17413355	0.29	0.18	0.22
rs17469886	0.48	0.46	0.12
rs1751043	0.39	0.1	0.29
rs17559005	0.24	0.21	0.03
rs17640676	0.29	0.11	0.04
rs1764425	0.16	0.2	0.06
rs1766908	0.2	0.33	0.09
rs1876381	0.3	0.26	0.16
rs1902023	0.28	0.16	0.48
rs1925851	0.25	0.45	0.54
rs1925856	0.43	0.6	0.36
rs1925860	0.25	0.25	0.13
rs1982562	0.23	0.14	0
rs1989983	0.45	0.65	0.86
rs2031920	0.71	0.78	0.8
rs2064504	0.44	0.35	0.44
rs2074451	0.14	0.51	0.53
rs2082603	0.52	0.16	0.03
rs2089515	0.45	0.32	0.14
rs2209631	0.29	0.23	0.12
rs2218988	0.31	0.21	0.21
rs2344953	0.17	0.1	0
rs2397105	0.4	0.44	0.35
rs2397132	0.36	0.37	0.36
rs2524290	0.62	0.75	0.99
rs2567513	0.18	0.1	0.03
rs2720666	0.37	0.25	0.25
rs2720667	0.28	0.19	0.27
rs2737844	0.29	0.22	0.54
rs2748991	0.27	0.15	0.09
rs279874	0.26	0.26	0.05
rs2880961	0.32	0.09	0.01
rs319590	0.58	0.52	0.45
rs319594	0.4	0.1	0.08
rs3208829	0.38	0.38	0.47
rs33966381	0.29	0.14	0.03

Supplementary Table 30. –Continued.

rs3744198	0.37	0.54	0.88
rs3746165	0.19	0.3	0.71
rs3746923	0.19	0.21	0.34
rs3749166	0.49	0.43	0.83
rs3795578	0.36	0.28	0.46
rs3799732	0.29	0.31	0.5
rs3825924	0.27	0.22	0.23
rs3828599	0.18	0.25	0.61
rs3857596	0.18	0.2	0.01
rs3957358	0.25	0.27	0.07
rs4148411	0.34	0.28	0.22
rs4289753	0.38	0.16	0.03
rs4495049	0.39	0.13	0.01
rs4563418	0.35	0.08	0.22
rs4585742	0.45	0.37	0.13
rs4710625	0.26	0.23	0.03
rs4715210	0.31	0.21	0.09
rs4715359	0.32	0.12	0.16
rs4764486	0.18	0.29	0.16
rs4773861	0.29	0.27	0.2
rs4869233	0.47	0.31	0.15
rs5936441	0.28	0.17	0.01
rs6032545	0.1	0.03	0.21
rs6083315	0.53	0.32	0.33
rs6124741	0.17	0.39	0.46
rs6502555	0.31	0.25	0.19
rs6553786	0.22	0.21	0.1
rs6737742	0.21	0.18	0.33
rs6789170	0.3	0.12	0.05
rs6795028	0.3	0.08	0.14
rs6809413	0.19	0.16	0.02
rs6810790	0.1	0.16	0.01
rs6852435	0.25	0.25	0.17
rs6878801	0.33	0.21	0.02
rs6922172	0.35	0.34	0.25
rs6949916	0.25	0.15	0
rs707148	0.39	0.32	0.05
rs718068	0.33	0.27	0.03
rs7329514	0.19	0.14	0.02
rs7526132	0.47	0.38	0.55
rs7665426	0.36	0.34	0.08
rs766606	0.33	0.38	0.09

Supplementary Table 30. –Continued.

rs7726138	0.3	0.06	0
rs7738812	0.28	0.13	0.01
rs776746	0.33	0.19	0.49
rs777952	0.22	0.09	0.02
rs7987903	0.24	0.23	0.05
rs8001657	0.25	0.07	0.05
rs8081984	0.35	0.06	0.1
rs8177426	0.3	0.31	0.51
rs8191438	0.51	0.45	0.95
rs8191439	0.35	0.46	0.97
rs8330	0.46	0.76	0.75
rs908262	0.22	0.24	0.33
rs9367532	0.17	0.26	0.08
rs943005	0.43	0.02	0.49
rs9473924	0.38	0.27	0.16
rs9473932	0.4	0.46	0.28
rs948999	0.29	0.38	0.28
rs9508207	0.48	0.25	0.16
rs9590150	0.39	0.36	0.14
rs9590154	0.34	0.21	0.03
rs9784215	0.38	0.56	0.84
rs9984523	0.4	0.26	0.15
rs9997440	0.35	0.09	0.01

Supplementary Table 31: Pubmatrix analysis of protein-coding genes containing 147 APAP-associated SNPs.

Gene	acetaminophen	disease	drug	hepatotoxicity	liver	metabolism	toxicity
ABCC3	4	53	206	6	100	219	36
ABCC4	10	103	395	11	105	477	75
ADARB2	0	8	1	0	1	15	2
ALCAM	0	114	118	0	35	449	4
ALDH1A3	0	32	58	0	10	139	9
C14orf49	0	1	1	0	0	0	0
C17orf28	0	0	0	0	0	0	0
C3orf38	0	0	0	0	0	1	0
CACNA1H	1	59	149	0	1	247	11
CALD1	0	5	5	0	1	29	0
CAPN10	0	90	13	0	7	73	0
CCDC25	0	1	1	0	2	4	0
CD44	4	3142	4293	7	931	10946	397
CD9	0	251	288	0	47	1081	19
CDH6	0	10	6	0	4	34	1
CNR1	0	172	295	0	34	388	19
COX7C	0	6	6	0	2	24	1
CPA6	0	7	5	0	2	14	0
CST5	0	2	7	0	1	18	1
CYP2E1	316	1162	3425	506	3675	4943	1524
CYP3A5	96	817	7719	189	4582	8957	1170
DMRT1	0	30	77	0	22	351	25
DNTTIP1	0	0	0	0	0	9	0
ETNK2	0	2	2	0	2	4	0
FBXO39	0	1	1	0	0	4	0
FMR1NB	0	1	1	0	0	1	0
FRK	0	31	50	0	13	147	10
GCLC	25	161	409	40	157	604	178
GPX2	0	53	112	2	65	249	53
GPX3	3	108	131	3	64	370	26
GPX4	1	94	148	1	83	356	45
GPX7	0	10	17	1	6	48	6
GSS	2	539	267	1	40	524	28
GSTA1	8	115	243	17	148	431	105
GSTA3	0	16	36	3	30	65	18
GSTP1	24	1513	1966	31	791	3948	684
HDAC4	0	148	269	0	37	647	25
IL23R	0	524	71	0	19	245	1
IL6	14	3775	3639	16	782	8378	444
IMPAD1	0	2	1	0	0	2	0
KCNJ3	0	15	19	0	1	50	0
LAMA4	0	22	25	0	8	101	2

Supplementary Table 31. –Continued.

LMX1A	0	92	29	0	1	148	3
MAGI2	0	32	19	0	4	96	0
MCTP1	0	1	3	0	1	6	1
MFSD4	0	3	0	0	1	4	0
MTUS2	0	2	2	0	0	4	0
MYH7B	0	7	6	0	1	25	1
NEB	0	215	255	2	44	509	12
NHLRC3	0	1	0	0	0	0	0
PCBD2	0	1	0	0	0	1	0
PVT1	0	70	23	0	12	77	2
RAB3IL1	0	0	0	0	0	2	0
RAP1GAP2	0	1	1	0	0	8	0
SEMA6A	0	9	12	0	0	65	1
SLC39A11	0	1	1	0	0	4	0
SLIT2	0	82	68	0	16	342	7
SNX16	0	3	3	0	0	8	0
SNX19	0	7	1	0	1	9	0
SOX21	0	4	6	0	0	44	1
SPAG16	0	10	1	0	0	16	0
STAB1	0	24	14	0	19	74	1
SUMO1	0	194	245	0	47	1808	27
TEKT1	0	1	2	0	0	7	0
TFAP2B	0	44	11	0	3	77	1
TMPRSS2	1	303	156	0	6	587	12
TPD52L1	0	3	4	0	0	15	0
UBASH3A	0	18	0	0	1	8	0
UGT1A1	47	577	1436	41	905	1769	496
UGT2B15	6	23	148	2	114	219	14
VWC2	0	0	0	0	0	4	0
WFDC3	0	1	1	0	0	1	0

Pubmatrix returns the number of articles containing both search and modifier terms

Supplementary Table 32: Significant gene hits from the APAP time points (p<0.05) were compared to a list of 133 gene names with 147 known APAP injury-related SNPs.

4d pos. p<0.05	4d neg. p<0.05	24h pos. p<0.05	24h neg. p<0.05	30min-24h pos. p<0.05	30min-24h neg. p<0.05	all pos. p<0.05	all neg. p<0.05
ALCAM	SUMO1	GSS	NEB	GSTP1	CPA6	TMPRSS2	RAP1GAP2
GPX4	KCNJ3	IL23R	UGT2B15	GSS	GPX2	STAB1	SUMO1
UGT2B15	SNX16	SNX19	DNTTIP1	STAB1	UGT2B15	ALCAM	
	RAP1GAP2	MAGI2	CPA6	SLIT2		KCNJ3	
			FBXO39			MCTP1	
						TPD52L1	

Supplementary Table 33: Summary information about the top genes considered for further studies. Genes had to be ranked in the top 10 of a CRISPR screen gene list and also be significantly differentially expressed in another dataset (all p<0.05).

Gene	Full name	Protein Database ID	CRISPR gene ranking (p<0.05)	sgRNA lfc**	Other dataset (p<0.05)	Gene expression lfc**	Essential Gene (essentialgene.org)	APAP publications
LZTR1	Leucine Zipper Like Transcription Regulator 1		4d+*,	1.95	70784 D1(responder v non-responder), D8(responder v non-responder)	0.36 D1, 0.34 D8	no	no
NAAA	N-Acylethanolamine Acid Amidase		int-*, all-, 30min-, 3h-, 6h-	-0.5	70784 D8(responder v non-responder), 70784 D1(responder v placebo), 74000 ALF	0.2 in D8(resp. v nonresp.), 0.265 in D1(resp. v placebo), -2.99 in ALF	no	no
PGM5	Phosphoglucomutase 5		24h+*, int+*, all+*, 4d+, 3h+, 6h+, 12h+,	0.40, 0.30, 0.57	70784 D1(responder v placebo)	-0.33759	yes	no
ATG2B	Autophagy Related 2B		NA(4d- #18)	-3.65	70784 D1(responder v placebo), 70784 D8(responder v placebo)	0.202 D1, 0.218 D8	no	no
MYOZ3	Myozenin 3		24h-*, all-, int-, 4d-, 3h-, 6h-, 12h-	-0.44	70784 D8(responder v non-responder)	0.4	no	no
EFNB3	Ephrin B3	4BKF.C	24h-*, int-, 30min-, 3h+, 3h-, 6h+, 6h-	-0.68	70784 D8(responder v non-responder)	0.89	no	no
OR5M11	Olfactory Receptor Family 5 Subfamily M Member 11		int-*, all-, 24h-, 30min-, 3h-, 6h-	0.66	70784 D8(responder v non-responder)	0.21	no	no
FCGR3A	Fc Fragment Of IgG Receptor IIIa	3SGJ.C	int-*, 24h-, all-, 30min-, 6h-, 12h-	-0.34	70784 D8(responder v non-responder)	0.51	no	no

Supplementary Table 33. –Continued.

PROZ	Protein Z, Vitamin K Dependent Plasma Glycoprotein	3F1S.B	int-*, 24h-, 30min-, 6h-, 12h-	-0.56	70784 D8(responder v placebo)	-0.34908	no	no
EEF1D	Eukaryotic Translation Elongation Factor 1 Delta		24h+*, 3h+	1.68	74000 ALF	2.525	no	no
ACAD11	Acyl-CoA Dehydrogenase Family Member 11		24h-*, 3h-	-0.4	74000 ALF	-2.369	no	no
KIF23	Kinesin Family Member 23	3VHX.B	all+*, 24h+, int+, 6h+, 12h+	0.59	70784 D8(responder v placebo)	-0.37566	yes	no
C19orf60	Chromosome 19 Open Reading Frame 60		all-*, int-	-1.74	70784 D8(responder v non-responder), 70784 D8(responder v placebo)	0.16, 0.156	yes	no
BMPR1A	Bone Morphogenetic Protein Receptor Type 1A	1ES7.B	int+*, all+, 24h+, 6h+, 12h+	0.3	74000 ALF	-3.146	yes	no
PDSS2	Prenyl (Decaprenyl) Diphosphate Synthase, Subunit 2		all+*, int+, 4d+, 3h+, 12h+, 24h+	0.95	74000 ALF	-2.349	yes	no
CXADR	Coxsackie Virus And Adenovirus Receptor	1EAJ.A	all+*, int+, 3h+, 6h+, 12h+	0.6	74000 ALF	-2.497	yes	no

Supplementary Table 33. –Continued.

SSR2	Signal Sequence Receptor Subunit 2		24h-*, 30min-	-0.23	mouse RNA-Seq	0.41	yes	no
TMCC2	Transmembrane And Coiled-Coil Domain Family 2		all-*	-0.46	mouse RNA-Seq	-1.047	no	no
UVRAG	UV Radiation Resistance Associated		4d+ *, all-	1.62	mouse RNA-Seq	-0.48	yes	no
EGR1	Early Growth Response 1	4X9J.A	24h+*, int+, all+, 6h+	1.46	mouse RNA-Seq	1.468	yes	yes
VNN1	Vanin 1	4CYF.A	24h-*, 6h-	-0.51	mouse RNA-Seq	-0.851	no	yes
NR1I3	Nuclear Receptor Subfamily 1 Group I Member 3		all+*, int+, 24h+	0.45	70784 D1(responder v placebo), mouse RNA-Seq	-0.183, -0.857	no	yes

*, in top 10 genes; **, lfc=log fold change

Supplementary Table 34: All Drug-Gene interactions resultant from analysis of candidate genes by the Drug Gene Interaction Database (www.dgidb.org)

Gene	Drug	Interaction types	Sources	PubMed IDs
ALCAM	FLUOROURACIL		CIViC	24708484
BMPR1A	CHEMBL3186227	inhibitor	GuideToPharmacologyInteract	
FCGR3A	GLOBULIN, IMMUNE	antagonist	DrugBank	20441428|17351760|17911465
FCGR3A	FENTANYL		NCI	11772808
FCGR3A	EFALIZUMAB		DrugBank	17139284|17016423
FCGR3A	CETUXIMAB		PharmGKB|NCI|DrugBank	17139284|17704420|17016423
FCGR3A	INFLIXIMAB		PharmGKB	
FCGR3A	VINCRISTINE		PharmGKB	
FCGR3A	PENICILLIN G POTASSIUM		NCI	17257217
FCGR3A	NATALIZUMAB		DrugBank	17139284|17016423
FCGR3A	TRASTUZUMAB		PharmGKB|NCI|DrugBank	18089830|17363544
FCGR3A	ALEMTUZUMAB		DrugBank	15217834
FCGR3A	TOSITUMOMAB		DrugBank	17139284|17016423
FCGR3A	ABCIXIMAB		DrugBank	17139284|17016423
FCGR3A	PREDNISOLONE		NCI	17329922
FCGR3A	CHEMBL411250		NCI	1827816
FCGR3A	BEVACIZUMAB		DrugBank	17139284|17016423
FCGR3A	EPOETIN ALFA		NCI	1300984
FCGR3A	CHONDROITIN SULFATE		NCI	18006074
FCGR3A	GEMTUZUMAB OZOGAMICIN		DrugBank	7509291|17139284|17016423
FCGR3A	CYCLOSPORINE		NCI	17852453
FCGR3A	BASILIXIMAB		DrugBank	17139284|17016423
FCGR3A	RITUXIMAB		PharmGKB|DrugBank	17324336|15448014|16609067
FCGR3A	CIMETIDINE		NCI	11556524

Supplementary Table 34. –Continued.

FCGR3A	INDOMETHACIN		NCI	17329922
FCGR3A	ETANERCEPT		DrugBank	15526004|15457442
FCGR3A	CYCLOPHOSPHAMIDE		PharmGKB	
FCGR3A	CYTARABINE		NCI	17852453
FCGR3A	ALEFACEPT		DrugBank	12795239|11970990|17139284|17016423
FCGR3A	LACTULOSE HYDRATE		NCI	1418064
FCGR3A	HEPARIN		NCI	18492254
FCGR3A	RIZATRIPTAN		NCI	10729215
FCGR3A	PHORBOL MYRISTATE ACETATE		NCI	1827816
FCGR3A	THALIDOMIDE		NCI	15457133
FCGR3A	PENICILLIN G SODIUM		NCI	1371977
FCGR3A	SODIUM CHLORIDE		NCI	17187818
FCGR3A	DACLIZUMAB		DrugBank	17139284|17016423
FCGR3A	MAFOSFAMIDE		NCI	1515095
FCGR3A	PALIVIZUMAB		DrugBank	17139284|17016423
FCGR3A	DIMETHYL SULFOXIDE		NCI	16896803
FCGR3A	TESMILIFENE HYDROCHLORIDE		NCI	11556524
FCGR3A	MUROMONAB-CD3		NCI|DrugBank	11599102|17139284|17016423
FCGR3A	GELDANAMYCIN		NCI	7662976
FCGR3A	HYDROGEN PEROXIDE		NCI	2138680
FCGR3A	DOXORUBICIN		NCI	1830717
FCGR3A	PUROMYCIN		NCI	8423352
FCGR3A	ADALIMUMAB		DrugBank	17139284|17016423
FCGR3A	IBRITUMOMAB TIUXETAN		DrugBank	17139284|17016423
FCGR3A	BROMOACETIC ACID		NCI	1832500
GPX2	GLUTATHIONE	cofactor	DrugBank	17510403
GPX4	GLUTATHIONE	cofactor	DrugBank	12751792|17503194|17139284|17016423|14967915

Supplementary Table 34. –Continued.

GSS	ACETYLCYSTEINE	stimulator	DrugBank	2502672
GSS	CYSTEINE		DrugBank	16940754
GSS	CHEMBL460831		DrugBank	10592235|17139284|17016423
GSS	GLUTATHIONE		DrugBank	17401648|17607728|17630655|17452339|17467761
GSS	CHEMBL1230989		DrugBank	10592235|17139284|17016423
GSS	GLYCINE		DrugBank	17401648|16996193|17397529|17452339|17124497
GSTP1	EZATIOSTAT HYDROCHLORIDE	inhibitor	ChemblInteract|DrugBank	10592235
GSTP1	GLYCERIN		DrugBank	17139284|17016423
GSTP1	CIBACRON BLUE		DrugBank	17139284|17016423
GSTP1	IFOSFAMIDE		NCI	16282887
GSTP1	THIOTEPA		PharmGKB	
GSTP1	EZATIOSTAT		TdgClinicalTrial	
GSTP1	CAMPTOTHECIN		NCI	15500952
GSTP1	EPIRUBICIN		PharmGKB	
GSTP1	CHEMBL345292		DrugBank	10592235|17139284|17016423
GSTP1	DAUNORUBICIN		NCI	10050715
GSTP1	PYRIMETHAMINE		PharmGKB	
GSTP1	VERAPAMIL		NCI	3566185
GSTP1	CYTARABINE		NCI	3978635
GSTP1	ALCOHOL		NCI	1302037
GSTP1	ETOPOSIDE		PharmGKB	
GSTP1	BUSULFAN		NCI	15779864
GSTP1	DOCETAXEL		NCI	10639573
GSTP1	MERCAPTOPURINE		PharmGKB	
GSTP1	MIFEPRISTONE		NCI	1302037
GSTP1	OXALIPLATIN		NCI	12072547

Supplementary Table 34. –Continued.

GSTP1	MISONIDAZOLE	NCI	3753520
GSTP1	PACLITAXEL	CIViC	25010864
GSTP1	CARBOPLATIN	NCI|CIViC	25010864|12360105
GSTP1	CANFOSFAMIDE	TdgClinicalTrial|DrugBank	16014111|12738715
GSTP1	MECHLORETHAMINE HYDROCHLORIDE	NCI	2882834
GSTP1	DROLOXIFENE	NCI	11721384
GSTP1	SULFORAPHANE	NCI	1549603
GSTP1	SODIUM BUTYRATE	NCI	12896903
GSTP1	PERFOSFAMIDE	NCI	9382956
GSTP1	LYCOPENE	NCI	10806309
GSTP1	CURCUMIN	NCI	15999103
GSTP1	OMEPRAZOLE	NCI	8529327
GSTP1	CARBOCYSTEINE	DrugBank	10592235|17139284|17016423
GSTP1	CYCLOPHOSPHAMIDE	NCI	9382956
GSTP1	ETHACRYNIC ACID	NCI	10900222
GSTP1	PRIDINOL	NCI	16127053
GSTP1	PREDNISONE	NCI	11186134|10050715
GSTP1	IRINOTECAN	NCI	10639573
GSTP1	RESVERATROL	NCI	11279601
GSTP1	MELPHALAN	NCI	15779864|1988111
GSTP1	GLUTATHIONE	DrugBank	17465221|17517071
GSTP1	GARLIC	NCI	11962257
GSTP1	DECITABINE	NCI	11948118|11960994
GSTP1	VITAMIN E	NCI	17029404
GSTP1	EXATECAN MESYLATE	NCI	10639573
GSTP1	AZACITIDINE	NCI	11696442
GSTP1	SELENOMETHIONINE	NCI	1759407

Supplementary Table 34. –Continued.

GSTP1	DITIOCARB		NCI	2992773
GSTP1	DEXAMETHASONE		NCI	1302037
GSTP1	HYDROQUINONE		NCI	15141365
HSD11B1	PREDNISONE	ligand	DrugBank	20634231
HSD11B1	CARBENOXOLONE	inhibitor	DrugBank	11752352
HSD11B1	CHEMBL222670	inhibitor	GuideToPharmacologyInteract	
HSD11B1	CHEMBL2153191	inhibitor	GuideToPharmacologyInteract	
HSD11B1	CHEMBL2177609	inhibitor	GuideToPharmacologyInteract|TTD	
HSD11B1	PHENYLARSINE OXIDE	inhibitor	TdgClinicalTrial|DrugBank|TTD	
HSD11B1	CHEMBL495597		DrugBank	10592235
HSD11B1	CHEMBL392452		DrugBank	10592235
HSD11B1	CHEMBL427896		DrugBank	10592235
HSD11B1	CHEMBL1161862		DrugBank	17139284|17016423
HSD11B1	CHEMBL460962		DrugBank	10592235
HSD11B1	CORTICOSTERONE		DrugBank	10592235
HSD11B1	CHEMBL455907		DrugBank	10592235
HSD11B1	CHEMBL406572		DrugBank	10592235
HSD11B1	CHEMBL1161866		DrugBank	9141556|17139284|8585102|17016423
HSD11B1	CHEMBL453620		DrugBank	10592235
HSD11B1	CHEMBL218006		DrugBank	10592235
KCNJ3	HALOTHANE	inhibitor	DrugBank	11465552|15175324|11455015
KCNJ3	CHEMBL2409106	activator	GuideToPharmacologyInteract	
KCNJ3	CHEMBL116590	channel blocker	GuideToPharmacologyInteract	
KCNJ3	THYROTROPIN		NCI	10075694
KCNJ3	FLUPIRTINE		TdgClinicalTrial	
KCNJ3	CLOZAPINE		NCI	10780978
NAAA	CARBENOXOLONE	inhibitor	GuideToPharmacologyInteract	

Supplementary Table 34. –Continued.

NAAA	FLUFENAMIC ACID	inhibitor	GuideToPharmacologyInteract	
NADSYN1	L-GLUTAMATE		DrugBank	17139284|17016423
NAMPT	TEGLARINAD CHLORIDE	inhibitor	TdgClinicalTrial|ChemblInteract|DrugBank	
NMNAT1	BETANMN		DrugBank	17139284|17016423
NR1I3	CHEMBL458603	agonist	GuideToPharmacologyInteract	
NR1I3	CLOTRIMAZOLE	antagonist	GuideToPharmacologyInteract	
NR1I3	MECLIZINE	antagonist|modulator	GuideToPharmacologyInteract|TTD	
NR1I3	PRASTERONE	activator	DrugBank	17591676
NR1I3	ANDROSTENOL		DrugBank	10592235
NR1I3	EFAVIRENZ		PharmGKB	
NR1I3	CHEMBL486954		DrugBank	10592235
NR1I3	CARBAMAZEPINE		PharmGKB	
NUDT9	DEXTROSE		DrugBank	17139284|17016423
PROZ	MENADIONE	activator	TEND|DrugBank	17139284|17016423
SIRT1	CHEMBL257991	activator	GuideToPharmacologyInteract	
SIRT1	SODIUM LAURYL SULFATE	inhibitor	GuideToPharmacologyInteract	
SIRT1	CHEMBL420311	inhibitor	TdgClinicalTrial|GuideToPharmacologyInteract	
SIRT1	SPLITOMICIN	inhibitor	GuideToPharmacologyInteract	
SIRT1	RESVERATROL		DrugBank	
SIRT3	SODIUM LAURYL SULFATE	inhibitor	GuideToPharmacologyInteract	
UGT2B15	OXAZEPAM		PharmGKB	
UGT2B15	LORAZEPAM		PharmGKB	

REFERENCES

1. Chun, L. J.; Tong, M. J.; Busuttil, R. W.; Hiatt, J. R., Acetaminophen hepatotoxicity and acute liver failure. *J Clin Gastroenterol* **2009,** *43* (4), 342-9.
2. Lee, W. M., Acetaminophen and the U.S. Acute Liver Failure Study Group: lowering the risks of hepatic failure. *Hepatology (Baltimore, Md.)* **2004,** *40* (1), 6-9.
3. Zhao, P.; Wang, C.; Liu, W.; Chen, G.; Liu, X.; Wang, X.; Wang, B.; Yu, L.; Sun, Y.; Liang, X.; Yang, H.; Zhang, F., Causes and outcomes of acute liver failure in China. *PloS one* **2013,** *8* (11), e80991.
4. Farrell SE; Tarabar A; Burns MJ; Corden TE; Fernandez MC; Tucker JR; VanDeVoort, J.; Windle, M., Acetaminophen Toxicity. *Medscape* **2014**.
5. Lancaster, E. M.; Hiatt, J. R.; Zarrinpar, A., Acetaminophen hepatotoxicity: an updated review. *Arch Toxicol* **2015,** *89* (2), 193-9.
6. Vermeulen, N. P.; Bessems, J. G.; Van de Straat, R., Molecular aspects of paracetamol-induced hepatotoxicity and its mechanism-based prevention. *Drug Metab Rev* **1992,** *24* (3), 367-407.
7. Raheja, K. L.; Linscheer, W. G.; Cho, C., Hepatotoxicity and metabolism of acetaminophen in male and female rats. *J Toxicol Environ Health* **1983,** *12* (1), 143-58.
8. Bajt, M. L.; Knight, T. R.; Lemasters, J. J.; Jaeschke, H., Acetaminophen-induced oxidant stress and cell injury in cultured mouse hepatocytes: protection by N-acetyl cysteine. *Toxicol Sci* **2004,** *80* (2), 343-9.
9. Corcoran, G. B.; Mitchell, J. R.; Vaishnav, Y. N.; Horning, E. C., Evidence that acetaminophen and N-hydroxyacetaminophen form a common arylating intermediate, N-acetyl-p-benzoquinoneimine. *Mol Pharmacol* **1980,** *18* (3), 536-42.
10. Corcoran, G. B.; Racz, W. J.; Smith, C. V.; Mitchell, J. R., Effects of N-acetylcysteine on acetaminophen covalent binding and hepatic necrosis in mice. *J Pharmacol Exp Ther* **1985,** *232* (3), 864-72.
11. Raucy, J. L.; Lasker, J. M.; Lieber, C. S.; Black, M., Acetaminophen activation by human liver cytochromes P450IIE1 and P450IA2. *Arch Biochem Biophys* **1989,** *271* (2), 270-83.
12. Chen, W.; Koenigs, L. L.; Thompson, S. J.; Peter, R. M.; Rettie, A. E.; Trager, W. F.; Nelson, S. D., Oxidation of acetaminophen to its toxic quinone imine and nontoxic catechol metabolites by baculovirus-expressed and purified human cytochromes P450 2E1 and 2A6. *Chem Res Toxicol* **1998,** *11* (4), 295-301.
13. Dong, H.; Haining, R. L.; Thummel, K. E.; Rettie, A. E.; Nelson, S. D., Involvement of human cytochrome P450 2D6 in the bioactivation of acetaminophen. *Drug Metab Dispos* **2000,** *28* (12), 1397-400.
14. Lee, S. S.; Buters, J. T.; Pineau, T.; Fernandez-Salguero, P.; Gonzalez, F. J., Role of CYP2E1 in the hepatotoxicity of acetaminophen. *J Biol Chem* **1996,** *271* (20), 12063-7.
15. Thummel, K. E.; Lee, C. A.; Kunze, K. L.; Nelson, S. D.; Slattery, J. T., Oxidation of acetaminophen to N-acetyl-p-aminobenzoquinone imine by human CYP3A4. *Biochem Pharmacol* **1993,** *45* (8), 1563-9.

16. Laine, J. E.; Auriola, S.; Pasanen, M.; Juvonen, R. O., Acetaminophen bioactivation by human cytochrome P450 enzymes and animal microsomes. *Xenobiotica* **2009,** *39* (1), 11-21.
17. Dahlin, D. C.; Miwa, G. T.; Lu, A. Y.; Nelson, S. D., N-acetyl-p-benzoquinone imine: a cytochrome P-450-mediated oxidation product of acetaminophen. *Proc Natl Acad Sci U S A* **1984,** *81* (5), 1327-31.
18. Leeming, M. G.; Gamon, L. F.; Wille, U.; Donald, W. A.; O'Hair, R. A. J., What Are the Potential Sites of Protein Arylation by N-Acetyl-p-benzoquinone Imine (NAPQI)? *Chem Res Toxicol* **2015,** *28* (11), 2224-33.
19. McGill, M. R.; Lebofsky, M.; Norris, H. R.; Slawson, M. H.; Bajt, M. L.; Xie, Y.; Williams, C. D.; Wilkins, D. G.; Rollins, D. E.; Jaeschke, H., Plasma and liver acetaminophen-protein adduct levels in mice after acetaminophen treatment: dose-response, mechanisms, and clinical implications. *Toxicol Appl Pharmacol* **2013,** *269* (3), 240-9.
20. Ni, H. M.; McGill, M. R.; Chao, X.; Du, K.; Williams, J. A.; Xie, Y.; Jaeschke, H.; Ding, W. X., Removal of acetaminophen protein adducts by autophagy protects against acetaminophen-induced liver injury in mice. *J Hepatol* **2016,** *65* (2), 354-62.
21. Cohen, S. D.; Pumford, N. R.; Khairallah, E. A.; Boekelheide, K.; Pohl, L. R.; Amouzadeh, H. R.; Hinson, J. A., Selective protein covalent binding and target organ toxicity. *Toxicol Appl Pharmacol* **1997,** *143* (1), 1-12.
22. Tirmenstein, M. A.; Nelson, S. D., Subcellular binding and effects on calcium homeostasis produced by acetaminophen and a nonhepatotoxic regioisomer, 3'-hydroxyacetanilide, in mouse liver. *J Biol Chem* **1989,** *264* (17), 9814-9.
23. Ramachandran, A.; Jaeschke, H., Mechanisms of acetaminophen hepatotoxicity and their translation to the human pathophysiology. *J Clin Transl Res* **2017,** *3* (Suppl 1), 157-169.
24. Wang, X.; Wu, Q.; Liu, A.; Anadon, A.; Rodriguez, J. L.; Martinez-Larranaga, M. R.; Yuan, Z.; Martinez, M. A., Paracetamol: overdose-induced oxidative stress toxicity, metabolism, and protective effects of various compounds in vivo and in vitro. *Drug Metab Rev* **2017**, 1-43.
25. Russmann, S.; Kullak-Ublick, G. A.; Grattagliano, I., Current concepts of mechanisms in drug-induced hepatotoxicity. *Curr Med Chem* **2009,** *16* (23), 3041-53.
26. Russmann, S.; Jetter, A.; Kullak-Ublick, G. A., Pharmacogenetics of drug-induced liver injury. *Hepatology (Baltimore, Md.)* **2010,** *52* (2), 748-61.
27. Hinson, J. A.; Roberts, D. W.; James, L. P., Mechanisms of acetaminophen-induced liver necrosis. *Handb Exp Pharmacol* **2010,** (196), 369-405.
28. Fontana, R. J., Pathogenesis of idiosyncratic drug-induced liver injury and clinical perspectives. *Gastroenterology* **2014,** *146* (4), 914-28.
29. Krasniak, A. E.; Knipp, G. T.; Svensson, C. K.; Liu, W., Pharmacogenomics of acetaminophen in pediatric populations: a moving target. *Front Genet* **2014,** *5*, 314.
30. McGill, M. R.; Sharpe, M. R.; Williams, C. D.; Taha, M.; Curry, S. C.; Jaeschke, H., The mechanism underlying acetaminophen-induced hepatotoxicity in humans and mice involves mitochondrial damage and nuclear DNA fragmentation. *J Clin Invest* **2012,** *122* (4), 1574-83.
31. Jiang, J.; Briede, J. J.; Jennen, D. G.; Van Summeren, A.; Saritas-Brauers, K.; Schaart, G.; Kleinjans, J. C.; de Kok, T. M., Increased mitochondrial ROS formation by

acetaminophen in human hepatic cells is associated with gene expression changes suggesting disruption of the mitochondrial electron transport chain. *Toxicol Lett* **2015**.
32. Bourdi, M.; Eiras, D. P.; Holt, M. P.; Webster, M. R.; Reilly, T. P.; Welch, K. D.; Pohl, L. R., Role of IL-6 in an IL-10 and IL-4 double knockout mouse model uniquely susceptible to acetaminophen-induced liver injury. *Chem Res Toxicol* **2007,** *20* (2), 208-16.
33. Wang, X.; Zhang, L.; Jiang, Z., T-helper cell-mediated factors in drug-induced liver injury. *J Appl Toxicol* **2015**.
34. Fannin, R. D.; Gerrish, K.; Sieber, S. O.; Bushel, P. R.; Watkins, P. B.; Paules, R. S., Blood transcript immune signatures distinguish a subset of people with elevated serum ALT from others given acetaminophen. *Clin Pharmacol Ther* **2016,** *99* (4), 432-41.
35. Jiang, J.; Briede, J. J.; Jennen, D. G.; Van Summeren, A.; Saritas-Brauers, K.; Schaart, G.; Kleinjans, J. C.; de Kok, T. M., Increased mitochondrial ROS formation by acetaminophen in human hepatic cells is associated with gene expression changes suggesting disruption of the mitochondrial electron transport chain. *Toxicology letters* **2015,** *234* (2), 139-50.
36. Sjogren, A. K.; Liljevald, M.; Glinghammar, B.; Sagemark, J.; Li, X. Q.; Jonebring, A.; Cotgreave, I.; Brolen, G.; Andersson, T. B., Critical differences in toxicity mechanisms in induced pluripotent stem cell-derived hepatocytes, hepatic cell lines and primary hepatocytes. *Arch Toxicol* **2014,** *88* (7), 1427-37.
37. Watkins, P. B.; Kaplowitz, N.; Slattery, J. T.; Colonese, C. R.; Colucci, S. V.; Stewart, P. W.; Harris, S. C., Aminotransferase elevations in healthy adults receiving 4 grams of acetaminophen daily: a randomized controlled trial. *JAMA* **2006,** *296* (1), 87-93.
38. Harrill, A. H.; Watkins, P. B.; Su, S.; Ross, P. K.; Harbourt, D. E.; Stylianou, I. M.; Boorman, G. A.; Russo, M. W.; Sackler, R. S.; Harris, S. C.; Smith, P. C.; Tennant, R.; Bogue, M.; Paigen, K.; Harris, C.; Contractor, T.; Wiltshire, T.; Rusyn, I.; Threadgill, D. W., Mouse population-guided resequencing reveals that variants in CD44 contribute to acetaminophen-induced liver injury in humans. *Genome Res* **2009,** *19* (9), 1507-15.
39. Kurtovic, J.; Riordan, S. M., Paracetamol-induced hepatotoxicity at recommended dosage. *J Intern Med* **2003,** *253* (2), 240-3.
40. Satirapoj, B.; Lohachit, P.; Ruamvang, T., Therapeutic dose of acetaminophen with fatal hepatic necrosis and acute renal failure. *J Med Assoc Thai* **2007,** *90* (6), 1244-7.
41. Zhao, L.; Pickering, G., Paracetamol metabolism and related genetic differences. *Drug Metab Rev* **2011,** *43* (1), 41-52.
42. Adjei, A. A.; Gaedigk, A.; Simon, S. D.; Weinshilboum, R. M.; Leeder, J. S., Interindividual variability in acetaminophen sulfation by human fetal liver: implications for pharmacogenetic investigations of drug-induced birth defects. *Birth Defects Res A Clin Mol Teratol* **2008,** *82* (3), 155-65.
43. Moyer, A. M.; Fridley, B. L.; Jenkins, G. D.; Batzler, A. J.; Pelleymounter, L. L.; Kalari, K. R.; Ji, Y.; Chai, Y.; Nordgren, K. K.; Weinshilboum, R. M., Acetaminophen-NAPQI hepatotoxicity: a cell line model system genome-wide association study. *Toxicol Sci* **2011,** *120* (1), 33-41.
44. Critchley, J. A.; Critchley, L. A.; Anderson, P. J.; Tomlinson, B., Differences in the single-oral-dose pharmacokinetics and urinary excretion of paracetamol and its

conjugates between Hong Kong Chinese and Caucasian subjects. *J Clin Pharm Ther* **2005,** *30* (2), 179-84.
45. Critchley, J. A.; Nimmo, G. R.; Gregson, C. A.; Woolhouse, N. M.; Prescott, L. F., Inter-subject and ethnic differences in paracetamol metabolism. *Br J Clin Pharmacol* **1986,** *22* (6), 649-57.
46. Chambers, J. C.; Zhang, W.; Sehmi, J.; Li, X.; Wass, M. N.; Van der Harst, P.; Holm, H.; Sanna, S.; Kavousi, M.; Baumeister, S. E.; Coin, L. J.; Deng, G.; Gieger, C.; Heard-Costa, N. L.; Hottenga, J. J.; Kuhnel, B.; Kumar, V.; Lagou, V.; Liang, L.; Luan, J.; Vidal, P. M.; Mateo Leach, I.; O'Reilly, P. F.; Peden, J. F.; Rahmioglu, N.; Soininen, P.; Speliotes, E. K.; Yuan, X.; Thorleifsson, G.; Alizadeh, B. Z.; Atwood, L. D.; Borecki, I. B.; Brown, M. J.; Charoen, P.; Cucca, F.; Das, D.; de Geus, E. J.; Dixon, A. L.; Doring, A.; Ehret, G.; Eyjolfsson, G. I.; Farrall, M.; Forouhi, N. G.; Friedrich, N.; Goessling, W.; Gudbjartsson, D. F.; Harris, T. B.; Hartikainen, A. L.; Heath, S.; Hirschfield, G. M.; Hofman, A.; Homuth, G.; Hypponen, E.; Janssen, H. L.; Johnson, T.; Kangas, A. J.; Kema, I. P.; Kuhn, J. P.; Lai, S.; Lathrop, M.; Lerch, M. M.; Li, Y.; Liang, T. J.; Lin, J. P.; Loos, R. J.; Martin, N. G.; Moffatt, M. F.; Montgomery, G. W.; Munroe, P. B.; Musunuru, K.; Nakamura, Y.; O'Donnell, C. J.; Olafsson, I.; Penninx, B. W.; Pouta, A.; Prins, B. P.; Prokopenko, I.; Puls, R.; Ruokonen, A.; Savolainen, M. J.; Schlessinger, D.; Schouten, J. N.; Seedorf, U.; Sen-Chowdhry, S.; Siminovitch, K. A.; Smit, J. H.; Spector, T. D.; Tan, W.; Teslovich, T. M.; Tukiainen, T.; Uitterlinden, A. G.; Van der Klauw, M. M.; Vasan, R. S.; Wallace, C.; Wallaschofski, H.; Wichmann, H. E.; Willemsen, G.; Wurtz, P.; Xu, C.; Yerges-Armstrong, L. M.; Alcohol Genome-wide Association, C.; Diabetes Genetics, R.; Meta-analyses, S.; Genetic Investigation of Anthropometric Traits, C.; Global Lipids Genetics, C.; Genetics of Liver Disease, C.; International Consortium for Blood, P.; Meta-analyses of, G.; Insulin-Related Traits, C.; Abecasis, G. R.; Ahmadi, K. R.; Boomsma, D. I.; Caulfield, M.; Cookson, W. O.; van Duijn, C. M.; Froguel, P.; Matsuda, K.; McCarthy, M. I.; Meisinger, C.; Mooser, V.; Pietilainen, K. H.; Schumann, G.; Snieder, H.; Sternberg, M. J.; Stolk, R. P.; Thomas, H. C.; Thorsteinsdottir, U.; Uda, M.; Waeber, G.; Wareham, N. J.; Waterworth, D. M.; Watkins, H.; Whitfield, J. B.; Witteman, J. C.; Wolffenbuttel, B. H.; Fox, C. S.; Ala-Korpela, M.; Stefansson, K.; Vollenweider, P.; Volzke, H.; Schadt, E. E.; Scott, J.; Jarvelin, M. R.; Elliott, P.; Kooner, J. S., Genome-wide association study identifies loci influencing concentrations of liver enzymes in plasma. *Nat Genet* **2011,** *43* (11), 1131-8.
47. Urban, T. J.; Shen, Y.; Stolz, A.; Chalasani, N.; Fontana, R. J.; Rochon, J.; Ge, D.; Shianna, K. V.; Daly, A. K.; Lucena, M. I.; Nelson, M. R.; Molokhia, M.; Aithal, G. P.; Floratos, A.; Pe'er, I.; Serrano, J.; Bonkovsky, H.; Davern, T. J.; Lee, W. M.; Navarro, V. J.; Talwalkar, J. A.; Goldstein, D. B.; Watkins, P. B.; Drug-Induced Liver Injury, N.; Diligen; Eudragene; Spanish, D. R.; International Serious Adverse Events, C., Limited contribution of common genetic variants to risk for liver injury due to a variety of drugs. *Pharmacogenet Genomics* **2012,** *22* (11), 784-95.
48. Ueshima, Y.; Tsutsumi, M.; Takase, S.; Matsuda, Y.; Kawahara, H., Acetaminophen metabolism in patients with different cytochrome P-4502E1 genotypes. *Alcohol Clin Exp Res* **1996,** *20* (1 Suppl), 25A-28A.
49. Court, M. H.; Freytsis, M.; Wang, X.; Peter, I.; Guillemette, C.; Hazarika, S.; Duan, S. X.; Greenblatt, D. J.; Lee, W. M., The UDP-glucuronosyltransferase (UGT) 1A polymorphism c.2042C>G (rs8330) is associated with increased human liver

acetaminophen glucuronidation, increased UGT1A exon 5a/5b splice variant mRNA ratio, and decreased risk of unintentional acetaminophen-induced acute liver failure. *J Pharmacol Exp Ther* **2013,** *345* (2), 297-307.
50. Court, M. H.; Peter, I.; Hazarika, S.; Vasiadi, M.; Greenblatt, D. J.; Lee, W. M.; Acute Liver Failure Study, G., Candidate gene polymorphisms in patients with acetaminophen-induced acute liver failure. *Drug Metab Dispos* **2014,** *42* (1), 28-32.
51. Hayashi, S.; Watanabe, J.; Kawajiri, K., Genetic polymorphisms in the 5'-flanking region change transcriptional regulation of the human cytochrome P450IIE1 gene. *J Biochem* **1991,** *110* (4), 559-65.
52. Tsutsumi, M.; Wang, J. S.; Takase, S.; Takada, A., Hepatic messenger RNA contents of cytochrome P4502E1 in patients with different P4502E1 genotypes. *Alcohol Alcohol Suppl* **1994,** *29* (1), 29-32.
53. Kuehl, P.; Zhang, J.; Lin, Y.; Lamba, J.; Assem, M.; Schuetz, J.; Watkins, P. B.; Daly, A.; Wrighton, S. A.; Hall, S. D.; Maurel, P.; Relling, M.; Brimer, C.; Yasuda, K.; Venkataramanan, R.; Strom, S.; Thummel, K.; Boguski, M. S.; Schuetz, E., Sequence diversity in CYP3A promoters and characterization of the genetic basis of polymorphic CYP3A5 expression. *Nat Genet* **2001,** *27* (4), 383-91.
54. Tanaka, K.; Terao, C.; Ohmura, K.; Takahashi, M.; Nakashima, R.; Imura, Y.; Yoshifuji, H.; Yukawa, N.; Usui, T.; Fujii, T.; Mimori, T.; Matsuda, F., Significant association between CYP3A5 polymorphism and blood concentration of tacrolimus in patients with connective tissue diseases. *J Hum Genet* **2014,** *59* (2), 107-9.
55. Birdwell, K. A.; Decker, B.; Barbarino, J. M.; Peterson, J. F.; Stein, C. M.; Sadee, W.; Wang, D.; Vinks, A. A.; He, Y.; Swen, J. J.; Leeder, J. S.; van Schaik, R.; Thummel, K. E.; Klein, T. E.; Caudle, K. E.; MacPhee, I. A., Clinical Pharmacogenetics Implementation Consortium (CPIC) Guidelines for CYP3A5 Genotype and Tacrolimus Dosing. *Clin Pharmacol Ther* **2015,** *98* (1), 19-24.
56. Patel, M.; Tang, B. K.; Kalow, W., Variability of acetaminophen metabolism in Caucasians and Orientals. *Pharmacogenetics* **1992,** *2* (1), 38-45.
57. Russo, M. W.; Galanko, J. A.; Shrestha, R.; Fried, M. W.; Watkins, P., Liver transplantation for acute liver failure from drug induced liver injury in the United States. *Liver Transpl* **2004,** *10* (8), 1018-23.
58. Marzilawati, A. R.; Ngau, Y. Y.; Mahadeva, S., Low rates of hepatotoxicity among Asian patients with paracetamol overdose: a review of 1024 cases. *BMC Pharmacol Toxicol* **2012,** *13*, 8.
59. Kimura, K.; Hayashi, S.; Nagaki, M., Roles of CD44 in chemical-induced liver injury. *Curr Opin Drug Discov Devel* **2010,** *13* (1), 96-103.
60. Consortium, G. P.; Auton, A.; Brooks, L. D.; Durbin, R. M.; Garrison, E. P.; Kang, H. M.; Korbel, J. O.; Marchini, J. L.; McCarthy, S.; McVean, G. A.; Abecasis, G. R., A global reference for human genetic variation. *Nature* **2015,** *526* (7571), 68-74.
61. Navarro, S. L.; Chen, Y.; Li, L.; Li, S. S.; Chang, J. L.; Schwarz, Y.; King, I. B.; Potter, J. D.; Bigler, J.; Lampe, J. W., UGT1A6 and UGT2B15 polymorphisms and acetaminophen conjugation in response to a randomized, controlled diet of select fruits and vegetables. *Drug Metab Dispos* **2011,** *39* (9), 1650-7.
62. Mehboob, H.; Tahir, I. M.; Iqbal, T.; Saleem, S.; Perveen, S.; Farooqi, A., Effect of UDP-Glucuronosyltransferase (UGT) 1A Polymorphism (rs8330 and rs10929303) on

Glucuronidation Status of Acetaminophen. *Dose Response* **2017,** *15* (3), 1559325817723731.
63. Court, M. H.; Zhu, Z.; Masse, G.; Duan, S. X.; James, L. P.; Harmatz, J. S.; Greenblatt, D. J., Race, Gender, and Genetic Polymorphism Contribute to Variability in Acetaminophen Pharmacokinetics, Metabolism, and Protein-Adduct Concentrations in Healthy African-American and European-American Volunteers. *J Pharmacol Exp Ther* **2017,** *362* (3), 431-440.
64. Aleksunes, L. M.; Slitt, A. L.; Maher, J. M.; Augustine, L. M.; Goedken, M. J.; Chan, J. Y.; Cherrington, N. J.; Klaassen, C. D.; Manautou, J. E., Induction of Mrp3 and Mrp4 transporters during acetaminophen hepatotoxicity is dependent on Nrf2. *Toxicol Appl Pharmacol* **2008,** *226* (1), 74-83.
65. Enomoto, A.; Itoh, K.; Nagayoshi, E.; Haruta, J.; Kimura, T.; O'Connor, T.; Harada, T.; Yamamoto, M., High sensitivity of Nrf2 knockout mice to acetaminophen hepatotoxicity associated with decreased expression of ARE-regulated drug metabolizing enzymes and antioxidant genes. *Toxicol Sci* **2001,** *59* (1), 169-77.
66. Harrill, A. H.; Ross, P. K.; Gatti, D. M.; Threadgill, D. W.; Rusyn, I., Population-based discovery of toxicogenomics biomarkers for hepatotoxicity using a laboratory strain diversity panel. *Toxicol Sci* **2009,** *110* (1), 235-43.
67. Bushel, P. R.; Fannin, R. D.; Gerrish, K.; Watkins, P. B.; Paules, R. S., Blood gene expression profiling of an early acetaminophen response. *Pharmacogenomics J* **2016**.
68. Ruepp, S. U.; Tonge, R. P.; Shaw, J.; Wallis, N.; Pognan, F., Genomics and proteomics analysis of acetaminophen toxicity in mouse liver. *Toxicol Sci* **2002,** *65* (1), 135-50.
69. Reilly, T. P.; Bourdi, M.; Brady, J. N.; Pise-Masison, C. A.; Radonovich, M. F.; George, J. W.; Pohl, L. R., Expression profiling of acetaminophen liver toxicity in mice using microarray technology. *Biochem Biophys Res Commun* **2001,** *282* (1), 321-8.
70. Fukushima, T.; Hamada, Y.; Yamada, H.; Horii, I., Changes of micro-RNA expression in rat liver treated by acetaminophen or carbon tetrachloride--regulating role of micro-RNA for RNA expression. *J Toxicol Sci* **2007,** *32* (4), 401-9.
71. Fannin, R. D.; Russo, M.; O'Connell, T. M.; Gerrish, K.; Winnike, J. H.; Macdonald, J.; Newton, J.; Malik, S.; Sieber, S. O.; Parker, J.; Shah, R.; Zhou, T.; Watkins, P. B.; Paules, R. S., Acetaminophen dosing of humans results in blood transcriptome and metabolome changes consistent with impaired oxidative phosphorylation. *Hepatology (Baltimore, Md.)* **2010,** *51* (1), 227-36.
72. Paddison, P. J.; Silva, J. M.; Conklin, D. S.; Schlabach, M.; Li, M.; Aruleba, S.; Balija, V.; O'Shaughnessy, A.; Gnoj, L.; Scobie, K.; Chang, K.; Westbrook, T.; Cleary, M.; Sachidanandam, R.; McCombie, W. R.; Elledge, S. J.; Hannon, G. J., A resource for large-scale RNA-interference-based screens in mammals. *Nature* **2004,** *428* (6981), 427-31.
73. Deans, R. M.; Morgens, D. W.; Okesli, A.; Pillay, S.; Horlbeck, M. A.; Kampmann, M.; Gilbert, L. A.; Li, A.; Mateo, R.; Smith, M.; Glenn, J. S.; Carette, J. E.; Khosla, C.; Bassik, M. C., Parallel shRNA and CRISPR/Cas9 screens enable antiviral drug target identification. *Nat Chem Biol* **2016,** *12* (5), 361-6.
74. Morgens, D. W.; Deans, R. M.; Li, A.; Bassik, M. C., Systematic comparison of CRISPR/Cas9 and RNAi screens for essential genes. *Nat Biotechnol* **2016,** *34* (6), 634-6.

75. Carette, J. E.; Guimaraes, C. P.; Wuethrich, I.; Blomen, V. A.; Varadarajan, M.; Sun, C.; Bell, G.; Yuan, B.; Muellner, M. K.; Nijman, S. M.; Ploegh, H. L.; Brummelkamp, T. R., Global gene disruption in human cells to assign genes to phenotypes by deep sequencing. *Nat Biotechnol* **2011,** *29* (6), 542-6.
76. Bibikova, M.; Carroll, D.; Segal, D. J.; Trautman, J. K.; Smith, J.; Kim, Y. G.; Chandrasegaran, S., Stimulation of homologous recombination through targeted cleavage by chimeric nucleases. *Mol Cell Biol* **2001,** *21* (1), 289-97.
77. Urnov, F. D.; Miller, J. C.; Lee, Y. L.; Beausejour, C. M.; Rock, J. M.; Augustus, S.; Jamieson, A. C.; Porteus, M. H.; Gregory, P. D.; Holmes, M. C., Highly efficient endogenous human gene correction using designed zinc-finger nucleases. *Nature* **2005,** *435* (7042), 646-51.
78. Boch, J.; Scholze, H.; Schornack, S.; Landgraf, A.; Hahn, S.; Kay, S.; Lahaye, T.; Nickstadt, A.; Bonas, U., Breaking the code of DNA binding specificity of TAL-type III effectors. *Science (New York, N.Y.)* **2009,** *326* (5959), 1509-12.
79. Christian, M.; Cermak, T.; Doyle, E. L.; Schmidt, C.; Zhang, F.; Hummel, A.; Bogdanove, A. J.; Voytas, D. F., Targeting DNA double-strand breaks with TAL effector nucleases. *Genetics* **2010,** *186* (2), 757-61.
80. Riordan, S. M.; Heruth, D. P.; Zhang, L. Q.; Ye, S. Q., Application of CRISPR/Cas9 for biomedical discoveries. *Cell Biosci* **2015,** *5*, 33.
81. Xue, H. Y.; Ji, L. J.; Gao, A. M.; Liu, P.; He, J. D.; Lu, X. J., CRISPR/Cas9 for medical genetic screens: applications and future perspectives. *J Med Genet* **2016,** *53* (2), 91-7.
82. Shalem, O.; Sanjana, N. E.; Hartenian, E.; Shi, X.; Scott, D. A.; Mikkelsen, T. S.; Heckl, D.; Ebert, B. L.; Root, D. E.; Doench, J. G.; Zhang, F., Genome-scale CRISPR/Cas9 knockout screening in human cells. *Science (New York, N.Y.)* **2014,** *343* (6166), 84-7.
83. Gilbert, L. A.; Horlbeck, M. A.; Adamson, B.; Villalta, J. E.; Chen, Y.; Whitehead, E. H.; Guimaraes, C.; Panning, B.; Ploegh, H. L.; Bassik, M. C.; Qi, L. S.; Kampmann, M.; Weissman, J. S., Genome-Scale CRISPR-Mediated Control of Gene Repression and Activation. *Cell* **2014,** *159* (3), 647-61.
84. Konermann, S.; Brigham, M. D.; Trevino, A. E.; Joung, J.; Abudayyeh, O. O.; Barcena, C.; Hsu, P. D.; Habib, N.; Gootenberg, J. S.; Nishimasu, H.; Nureki, O.; Zhang, F., Genome-scale transcriptional activation by an engineered CRISPR/Cas9 complex. *Nature* **2015,** *517* (7536), 583-8.
85. Chen, S.; Sanjana, N. E.; Zheng, K.; Shalem, O.; Lee, K.; Shi, X.; Scott, D. A.; Song, J.; Pan, J. Q.; Weissleder, R.; Lee, H.; Zhang, F.; Sharp, P. A., Genome-wide CRISPR screen in a mouse model of tumor growth and metastasis. *Cell* **2015,** *160* (6), 1246-60.
86. Wang, T.; Wei, J. J.; Sabatini, D. M.; Lander, E. S., Genetic screens in human cells using the CRISPR/Cas9 system. *Science (New York, N.Y.)* **2014,** *343* (6166), 80-4.
87. Wang, T.; Birsoy, K.; Hughes, N. W.; Krupczak, K. M.; Post, Y.; Wei, J. J.; Lander, E. S.; Sabatini, D. M., Identification and characterization of essential genes in the human genome. *Science (New York, N.Y.)* **2015,** *350* (6264), 1096-101.
88. Shalem, O.; Sanjana, N. E.; Zhang, F., High-throughput functional genomics using CRISPR/Cas9. *Nat Rev Genet* **2015,** *16* (5), 299-311.

89. Sanjana, N. E.; Shalem, O.; Zhang, F., Improved vectors and genome-wide libraries for CRISPR screening. *Nat Methods* **2014,** *11* (8), 783-4.
90. Joung, J.; Konermann, S.; Gootenberg, J. S.; Abudayyeh, O. O.; Platt, R. J.; Brigham, M. D.; Sanjana, N. E.; Zhang, F., Genome-scale CRISPR/Cas9 knockout and transcriptional activation screening. *Nat Protoc* **2017,** *12* (4), 828-863.
91. Nakabayashi, H.; Taketa, K.; Miyano, K.; Yamane, T.; Sato, J., Growth of human hepatoma cells lines with differentiated functions in chemically defined medium. *Cancer Res* **1982,** *42* (9), 3858-63.
92. Scheiermann, P.; Bachmann, M.; Hardle, L.; Pleli, T.; Piiper, A.; Zwissler, B.; Pfeilschifter, J.; Muhl, H., Application of IL-36 receptor antagonist weakens CCL20 expression and impairs recovery in the late phase of murine acetaminophen-induced liver injury. *Sci Rep* **2015,** *5*, 8521.
93. Mobasher, M. A.; de Toro-Martin, J.; Gonzalez-Rodriguez, A.; Ramos, S.; Letzig, L. G.; James, L. P.; Muntane, J.; Alvarez, C.; Valverde, A. M., Essential role of protein-tyrosine phosphatase 1B in the modulation of insulin signaling by acetaminophen in hepatocytes. *J Biol Chem* **2014,** *289* (42), 29406-19.
94. Macanas-Pirard, P.; Yaacob, N. S.; Lee, P. C.; Holder, J. C.; Hinton, R. H.; Kass, G. E., Glycogen synthase kinase-3 mediates acetaminophen-induced apoptosis in human hepatoma cells. *J Pharmacol Exp Ther* **2005,** *313* (2), 780-9.
95. Choi, S.; Sainz, B.; Corcoran, P.; Uprichard, S.; Jeong, H., Characterization of increased drug metabolism activity in dimethyl sulfoxide (DMSO)-treated Huh7 hepatoma cells. *Xenobiotica* **2009,** *39* (3), 205-17.
96. Olsavsky, K. M.; Page, J. L.; Johnson, M. C.; Zarbl, H.; Strom, S. C.; Omiecinski, C. J., Gene expression profiling and differentiation assessment in primary human hepatocyte cultures, established hepatoma cell lines, and human liver tissues. *Toxicol Appl Pharmacol* **2007,** *222* (1), 42-56.
97. Blight, K. J.; McKeating, J. A.; Rice, C. M., Highly permissive cell lines for subgenomic and genomic hepatitis C virus RNA replication. *J Virol* **2002,** *76* (24), 13001-14.
98. Martin, M., Cutadapt removes adapter sequences from high-throughput sequencing reads. *2011* **2011,** *17* (1).
99. Langmead, B.; Salzberg, S. L., Fast gapped-read alignment with Bowtie 2. *Nat Methods* **2012,** *9* (4), 357-9.
100. Li, W.; Xu, H.; Xiao, T.; Cong, L.; Love, M. I.; Zhang, F.; Irizarry, R. A.; Liu, J. S.; Brown, M.; Liu, X. S., MAGeCK enables robust identification of essential genes from genome-scale CRISPR/Cas9 knockout screens. *Genome Biol* **2014,** *15* (12), 554.
101. Subramanian, A.; Tamayo, P.; Mootha, V. K.; Mukherjee, S.; Ebert, B. L.; Gillette, M. A.; Paulovich, A.; Pomeroy, S. L.; Golub, T. R.; Lander, E. S.; Mesirov, J. P., Gene set enrichment analysis: a knowledge-based approach for interpreting genome-wide expression profiles. *Proc Natl Acad Sci U S A* **2005,** *102* (43), 15545-50.
102. Rodrigues, R. M.; Heymans, A.; De Boe, V.; Sachinidis, A.; Chaudhari, U.; Govaere, O.; Roskams, T.; Vanhaecke, T.; Rogiers, V.; De Kock, J., Toxicogenomics-based prediction of acetaminophen-induced liver injury using human hepatic cell systems. *Toxicol Lett* **2016,** *240* (1), 50-9.
103. Trapnell, C.; Pachter, L.; Salzberg, S. L., TopHat: discovering splice junctions with RNA-Seq. *Bioinformatics* **2009,** *25* (9), 1105-11.

104. Trapnell, C.; Roberts, A.; Goff, L.; Pertea, G.; Kim, D.; Kelley, D. R.; Pimentel, H.; Salzberg, S. L.; Rinn, J. L.; Pachter, L., Differential gene and transcript expression analysis of RNA-seq experiments with TopHat and Cufflinks. *Nat Protoc* **2012,** *7* (3), 562-78.
105. Zhang, L. N., M; Huang, P; Heruth, DP; Riordan, SM; Shortt, K; Zhang, N; Grigoryev, DN; Li, DY; Friesen, CA; Haandel, LV; Leeder, JS; Olson, J; Ye, SQ, Novel Protective Role of Nicotinamide Phosphoribosyltransferase in Acetaminophen-induced Acute Liver Injury in Mice. *Am J Pathol* **2018**.
106. O'Leary, N. A.; Wright, M. W.; Brister, J. R.; Ciufo, S.; Haddad, D.; McVeigh, R.; Rajput, B.; Robbertse, B.; Smith-White, B.; Ako-Adjei, D.; Astashyn, A.; Badretdin, A.; Bao, Y.; Blinkova, O.; Brover, V.; Chetvernin, V.; Choi, J.; Cox, E.; Ermolaeva, O.; Farrell, C. M.; Goldfarb, T.; Gupta, T.; Haft, D.; Hatcher, E.; Hlavina, W.; Joardar, V. S.; Kodali, V. K.; Li, W.; Maglott, D.; Masterson, P.; McGarvey, K. M.; Murphy, M. R.; O'Neill, K.; Pujar, S.; Rangwala, S. H.; Rausch, D.; Riddick, L. D.; Schoch, C.; Shkeda, A.; Storz, S. S.; Sun, H.; Thibaud-Nissen, F.; Tolstoy, I.; Tully, R. E.; Vatsan, A. R.; Wallin, C.; Webb, D.; Wu, W.; Landrum, M. J.; Kimchi, A.; Tatusova, T.; DiCuccio, M.; Kitts, P.; Murphy, T. D.; Pruitt, K. D., Reference sequence (RefSeq) database at NCBI: current status, taxonomic expansion, and functional annotation. *Nucleic Acids Res* **2016,** *44* (D1), D733-45.
107. Harrow, J.; Frankish, A.; Gonzalez, J. M.; Tapanari, E.; Diekhans, M.; Kokocinski, F.; Aken, B. L.; Barrell, D.; Zadissa, A.; Searle, S.; Barnes, I.; Bignell, A.; Boychenko, V.; Hunt, T.; Kay, M.; Mukherjee, G.; Rajan, J.; Despacio-Reyes, G.; Saunders, G.; Steward, C.; Harte, R.; Lin, M.; Howald, C.; Tanzer, A.; Derrien, T.; Chrast, J.; Walters, N.; Balasubramanian, S.; Pei, B.; Tress, M.; Rodriguez, J. M.; Ezkurdia, I.; van Baren, J.; Brent, M.; Haussler, D.; Kellis, M.; Valencia, A.; Reymond, A.; Gerstein, M.; Guigo, R.; Hubbard, T. J., GENCODE: the reference human genome annotation for The ENCODE Project. *Genome Res* **2012,** *22* (9), 1760-74.
108. Zerbino, D. R.; Achuthan, P.; Akanni, W.; Amode, M. R.; Barrell, D.; Bhai, J.; Billis, K.; Cummins, C.; Gall, A.; Giron, C. G.; Gil, L.; Gordon, L.; Haggerty, L.; Haskell, E.; Hourlier, T.; Izuogu, O. G.; Janacek, S. H.; Juettemann, T.; To, J. K.; Laird, M. R.; Lavidas, I.; Liu, Z.; Loveland, J. E.; Maurel, T.; McLaren, W.; Moore, B.; Mudge, J.; Murphy, D. N.; Newman, V.; Nuhn, M.; Ogeh, D.; Ong, C. K.; Parker, A.; Patricio, M.; Riat, H. S.; Schuilenburg, H.; Sheppard, D.; Sparrow, H.; Taylor, K.; Thormann, A.; Vullo, A.; Walts, B.; Zadissa, A.; Frankish, A.; Hunt, S. E.; Kostadima, M.; Langridge, N.; Martin, F. J.; Muffato, M.; Perry, E.; Ruffier, M.; Staines, D. M.; Trevanion, S. J.; Aken, B. L.; Cunningham, F.; Yates, A.; Flicek, P., Ensembl 2018. *Nucleic Acids Res* **2018,** *46* (D1), D754-d761.
109. Ward, L. D.; Kellis, M., HaploReg: a resource for exploring chromatin states, conservation, and regulatory motif alterations within sets of genetically linked variants. *Nucleic Acids Res* **2012,** *40* (Database issue), D930-4.
110. Becker, K. G.; Hosack, D. A.; Dennis, G., Jr.; Lempicki, R. A.; Bright, T. J.; Cheadle, C.; Engel, J., PubMatrix: a tool for multiplex literature mining. *BMC Bioinformatics* **2003,** *4*, 61.
111. Ritchie, G. R.; Dunham, I.; Zeginni, E.; Flicek, P., Functional annotation of noncoding sequence variants. *Nat Methods* **2014,** *11* (3), 294-6.

112. Cotto, K. C.; Wagner, A. H.; Feng, Y. Y.; Kiwala, S.; Coffman, A. C.; Spies, G.; Wollam, A.; Spies, N. C.; Griffith, O. L.; Griffith, M., DGIdb 3.0: a redesign and expansion of the drug-gene interaction database. *Nucleic Acids Res* **2017**.
113. Stewart, S. A.; Dykxhoorn, D. M.; Palliser, D.; Mizuno, H.; Yu, E. Y.; An, D. S.; Sabatini, D. M.; Chen, I. S.; Hahn, W. C.; Sharp, P. A.; Weinberg, R. A.; Novina, C. D., Lentivirus-delivered stable gene silencing by RNAi in primary cells. *RNA (New York, N.Y.)* **2003,** *9* (4), 493-501.
114. Sancak, Y.; Peterson, T. R.; Shaul, Y. D.; Lindquist, R. A.; Thoreen, C. C.; Bar-Peled, L.; Sabatini, D. M., The Rag GTPases bind raptor and mediate amino acid signaling to mTORC1. *Science (New York, N.Y.)* **2008,** *320* (5882), 1496-501.
115. Banerjee, S.; Melnyk, S. B.; Krager, K. J.; Aykin-Burns, N.; McCullough, S. S.; James, L. P.; Hinson, J. A., Trifluoperazine inhibits acetaminophen-induced hepatotoxicity and hepatic reactive nitrogen formation in mice and in freshly isolated hepatocytes. *Toxicol Rep* **2017,** *4*, 134-142.
116. Holownia, A.; Menez, J. F.; Braszko, J. J., The role of calcium in paracetamol (acetaminophen) cytotoxicity in PC12 cells transfected with CYP4502E1. *Inflammopharmacology* **1998,** *6* (2), 133-42.
117. Li, W.; Koster, J.; Xu, H.; Chen, C. H.; Xiao, T.; Liu, J. S.; Brown, M.; Liu, X. S., Quality control, modeling, and visualization of CRISPR screens with MAGeCK-VISPR. *Genome Biol* **2015,** *16*, 281.
118. Nikiforov, A.; Kulikova, V.; Ziegler, M., The human NAD metabolome: Functions, metabolism and compartmentalization. *Crit Rev Biochem Mol Biol* **2015,** *50* (4), 284-97.
119. Lin, J.; Schyschka, L.; Mühl-Benninghaus, R.; Neumann, J.; Hao, L.; Nussler, N.; Dooley, S.; Liu, L.; Stöckle, U.; Nussler, A. K.; Ehnert, S., Comparative analysis of phase I and II enzyme activities in 5 hepatic cell lines identifies Huh-7 and HCC-T cells with the highest potential to study drug metabolism. *Arch Toxicol* **2012,** *86* (1), 87-95.
120. Jiang, L.; Ke, M.; Yue, S.; Xiao, W.; Yan, Y.; Deng, X.; Ying, Q. L.; Li, J.; Ke, B., Blockade of Notch signaling promotes acetaminophen-induced liver injury. *Immunol Res* **2017,** *65* (3), 739-749.
121. Lehne, B.; Lewis, C. M.; Schlitt, T., From SNPs to genes: disease association at the gene level. *PloS one* **2011,** *6* (6), e20133.
122. Mesbah-Uddin, M.; Elango, R.; Banaganapalli, B.; Shaik, N. A.; Al-Abbasi, F. A., In-silico analysis of inflammatory bowel disease (IBD) GWAS loci to novel connections. *PloS one* **2015,** *10* (3), e0119420.
123. Kramer, A.; Green, J.; Pollard, J., Jr.; Tugendreich, S., Causal analysis approaches in Ingenuity Pathway Analysis. *Bioinformatics* **2014,** *30* (4), 523-30.
124. Zhang, F.; Lupski, J. R., Non-coding genetic variants in human disease. *Hum Mol Genet* **2015,** *24* (R1), R102-10.
125. Cech, T. R.; Steitz, J. A., The noncoding RNA revolution-trashing old rules to forge new ones. *Cell* **2014,** *157* (1), 77-94.
126. Siemionow, K.; Teul, J.; Dragowski, P.; Palka, J.; Miltyk, W., New potential biomarkers of acetaminophen-induced hepatotoxicity. *Adv Med Sci* **2016,** *61* (2), 325-330.
127. Wei, R.; Yang, F.; Urban, T. J.; Li, L.; Chalasani, N.; Flockhart, D. A.; Liu, W., Impact of the Interaction between 3'-UTR SNPs and microRNA on the Expression of

Human Xenobiotic Metabolism Enzyme and Transporter Genes. *Front Genet* **2012,** *3*, 248.
128. Zhang, J.; Huang, W.; Chua, S. S.; Wei, P.; Moore, D. D., Modulation of acetaminophen-induced hepatotoxicity by the xenobiotic receptor CAR. *Science (New York, N.Y.)* **2002,** *298* (5592), 422-4.
129. Lu, Z.; Bourdi, M.; Li, J. H.; Aponte, A. M.; Chen, Y.; Lombard, D. B.; Gucek, M.; Pohl, L. R.; Sack, M. N., SIRT3-dependent deacetylation exacerbates acetaminophen hepatotoxicity. *EMBO Rep* **2011,** *12* (8), 840-6.
130. Henderson, C. J.; Wolf, C. R.; Kitteringham, N.; Powell, H.; Otto, D.; Park, B. K., Increased resistance to acetaminophen hepatotoxicity in mice lacking glutathione S-transferase Pi. *Proc Natl Acad Sci U S A* **2000,** *97* (23), 12741-5.
131. Rada, P.; Pardo, V.; Mobasher, M. A.; Garcia-Martinez, I.; Ruiz, L.; Gonzalez-Rodriguez, A.; Sanchez-Ramos, C.; Muntane, J.; Alemany, S.; James, L. P.; Simpson, K. J.; Monsalve, M.; Valdecantos, M. P.; Valverde, A. M., SIRT1 Controls Acetaminophen Hepatotoxicity by Modulating Inflammation and Oxidative Stress. *Antioxid Redox Signal* **2017**.
132. Lorincz, T.; Jemnitz, K.; Kardon, T.; Mandl, J.; Szarka, A., Ferroptosis is Involved in Acetaminophen Induced Cell Death. *Pathol Oncol Res* **2015,** *21* (4), 1115-21.
133. Chan, K.; Han, X. D.; Kan, Y. W., An important function of Nrf2 in combating oxidative stress: detoxification of acetaminophen. *Proc Natl Acad Sci U S A* **2001,** *98* (8), 4611-6.
134. Nacak, T. G.; Leptien, K.; Fellner, D.; Augustin, H. G.; Kroll, J., The BTB-kelch protein LZTR-1 is a novel Golgi protein that is degraded upon induction of apoptosis. *J Biol Chem* **2006,** *281* (8), 5065-71.
135. Yamamoto, G. L.; Aguena, M.; Gos, M.; Hung, C.; Pilch, J.; Fahiminiya, S.; Abramowicz, A.; Cristian, I.; Buscarilli, M.; Naslavsky, M. S.; Malaquias, A. C.; Zatz, M.; Bodamer, O.; Majewski, J.; Jorge, A. A.; Pereira, A. C.; Kim, C. A.; Passos-Bueno, M. R.; Bertola, D. R., Rare variants in SOS2 and LZTR1 are associated with Noonan syndrome. *J Med Genet* **2015,** *52* (6), 413-21.
136. Piotrowski, A.; Xie, J.; Liu, Y. F.; Poplawski, A. B.; Gomes, A. R.; Madanecki, P.; Fu, C.; Crowley, M. R.; Crossman, D. K.; Armstrong, L.; Babovic-Vuksanovic, D.; Bergner, A.; Blakeley, J. O.; Blumenthal, A. L.; Daniels, M. S.; Feit, H.; Gardner, K.; Hurst, S.; Kobelka, C.; Lee, C.; Nagy, R.; Rauen, K. A.; Slopis, J. M.; Suwannarat, P.; Westman, J. A.; Zanko, A.; Korf, B. R.; Messiaen, L. M., Germline loss-of-function mutations in LZTR1 predispose to an inherited disorder of multiple schwannomas. *Nat Genet* **2014,** *46* (2), 182-7.
137. Fu, F.; Deng, Q.; Lei, T. Y.; Li, R.; Jing, X. Y.; Yang, X.; Liao, C., Clinical application of SNP array analysis in fetuses with ventricular septal defects and normal karyotypes. *Arch Gynecol Obstet* **2017,** *296* (5), 929-940.
138. Bauer, L.; Hapfelmeier, A.; Blank, S.; Reiche, M.; Slotta-Huspenina, J.; Jesinghaus, M.; Novotny, A.; Schmidt, T.; Grosser, B.; Kohlruss, M.; Weichert, W.; Ott, K.; Keller, G., A novel pretherapeutic gene expression based risk score for treatment guidance in gastric cancer. *Ann Oncol* **2017**.
139. Garten, A.; Schuster, S.; Penke, M.; Gorski, T.; de Giorgis, T.; Kiess, W., Physiological and pathophysiological roles of NAMPT and NAD metabolism. *Nat Rev Endocrinol* **2015,** *11* (9), 535-46.

140. Zhang, M.; Ying, W., NAD+ deficiency is a common central pathological factor of a number of diseases and aging: Mechanisms and therapeutic implications. *Antioxid Redox Signal* **2018**.
141. Blakemore, A. I.; Meyre, D.; Delplanque, J.; Vatin, V.; Lecoeur, C.; Marre, M.; Tichet, J.; Balkau, B.; Froguel, P.; Walley, A. J., A rare variant in the visfatin gene (NAMPT/PBEF1) is associated with protection from obesity. *Obesity (Silver Spring, Md.)* **2009,** *17* (8), 1549-53.
142. Saddi-Rosa, P.; Oliveira, C.; Crispim, F.; Giuffrida, F. M.; de Lima, V.; Vieira, J.; Doria, A.; Velho, G.; Reis, A., Association of circulating levels of nicotinamide phosphoribosyltransferase (NAMPT/Visfatin) and of a frequent polymorphism in the promoter of the NAMPT gene with coronary artery disease in diabetic and non-diabetic subjects. *Cardiovasc Diabetol* **2013,** *12*, 119.
143. Aller, R.; de Luis, D. A.; Izaola, O.; Sagrado, M. G.; Conde, R.; Velasco, M. C.; Alvarez, T.; Pacheco, D.; Gonzalez, J. M., Influence of visfatin on histopathological changes of non-alcoholic fatty liver disease. *Dig Dis Sci* **2009,** *54* (8), 1772-7.
144. Revollo, J. R.; Korner, A.; Mills, K. F.; Satoh, A.; Wang, T.; Garten, A.; Dasgupta, B.; Sasaki, Y.; Wolberger, C.; Townsend, R. R.; Milbrandt, J.; Kiess, W.; Imai, S., Nampt/PBEF/Visfatin regulates insulin secretion in beta cells as a systemic NAD biosynthetic enzyme. *Cell Metab* **2007,** *6* (5), 363-75.
145. van der Veer, E.; Ho, C.; O'Neil, C.; Barbosa, N.; Scott, R.; Cregan, S. P.; Pickering, J. G., Extension of human cell lifespan by nicotinamide phosphoribosyltransferase. *J Biol Chem* **2007,** *282* (15), 10841-5.
146. Hasmann, M.; Schemainda, I., FK866, a highly specific noncompetitive inhibitor of nicotinamide phosphoribosyltransferase, represents a novel mechanism for induction of tumor cell apoptosis. *Cancer Res* **2003,** *63* (21), 7436-42.
147. Wakayama, Y.; Inoue, M.; Kojima, H.; Murahashi, M.; Shibuya, S.; Yamashita, S.; Oniki, H., Aciculin and its relation to dystrophin: immunocytochemical studies in human normal and Duchenne dystrophy quadriceps muscles. *Acta Neuropathol* **2000,** *99* (6), 654-62.
148. Uzozie, A. C.; Selevsek, N.; Wahlander, A.; Nanni, P.; Grossmann, J.; Weber, A.; Buffoli, F.; Marra, G., Targeted Proteomics for Multiplexed Verification of Markers of Colorectal Tumorigenesis. *Mol Cell Proteomics* **2017,** *16* (3), 407-427.

VITA

Katherine is an interdisciplinary Ph.D degree candidate for Cell Biology and Biophysics and Bioinformatics in the Department of Cell Biology and Biophysics, University of Missouri Kansas City School of Biological Sciences and Department of Biomedical and Health Informatics, University of Missouri Kansas City School of Medicine, Missouri. She was born in St. Charles, Missouri. She began assisting with biotechnology research at age 15 and graduated from Indiana University, Bloomington in 2011 with a bachelor's of science in Biology with a minor in French and a minor equivalent in chemistry. She earned a M.S in Bioinformatics from UMKC in 2014. She published her MS thesis work on ARDS in Plos One (2014) and has published and presented numerous conference abstracts and posters since 2011, including an oral presentation of her work on acetaminophen-induced hepatotoxicity at the 2017 Midwest Bioinformatics Conference (Kansas City, MO). She has earned several funding awards, including a Sara Morrison Student Research Award of the UMKC School of Medicine (2013), a Research Grant of the UMKC School of Graduate Studies (2017), and five Graduate Assistance Fund awards of the UMKC Women's Council (2014-2018), including an award with outstanding merit in 2018. After graduation, she plans to pursue a career in bioinformatics research.